

DYNAMIC MORPHOLOGY OF THE SITTAUNG ESTUARY, MYANMAR

A DETAILED INVESTIGATION AND MODELLING
OF RAPID BANK EROSION

HUCKLEBERRY DE HAAS



TU Delft



ARCADIS

Dynamic morphology of the Sittaung estuary, Myanmar

A detailed investigation and modelling of rapid
bank erosion.

by

Huckleberry de Haas

to obtain the degree of Master of Science
at Delft University of Technology,
to be defended publicly on January 29, 2021

Thesis committee: Prof. dr. ir. Z. B. Wang, TU Delft, Chair
Dr. T. A. Bogaard, TU Delft
Dr. ir. E. Mosselman, TU Delft
Dr. Ir. J. Cleveringa, Arcadis Nederland B.V.
Student number: 4216415
Project duration: February 20, 2020 - January 29, 2021

Cover picture: Sittaung river by Eric Winny, cc by-sa 4.0

An electronic version of this thesis is available at <https://repository.tudelft.nl>.

Preface

This research is conducted in the context of a master's thesis of Water Resources Engineering at the Technical University of Delft. In this research a detailed investigation and modeling of rapid bank erosion in the dynamic morphology of the Sittaung estuary is performed. It is carried out in cooperation with the TU Delft and Arcadis, a renowned Dutch engineering firm.

While participating in different projects along the Myanmar coast and Ayeyarwady delta i came into contact with the extreme dynamics of the Sittaung estuary erosion, it left me intrigued. Being able to do this research on the Sittaung estuary is possible because of the fruitful partnership between Myanmar, the TU Delft and the Dutch water sector. With this thesis I hope to have contributed positively to this partnership and to have helped Myanmar forward in their continuous efforts to improve water security. I am grateful to have had the opportunity to work in such an exciting and stimulating domain. It has been a successful venture and certainly a joyous personal experience.

The academic supervising committee has played a large role in this research and i would like to thank them sincerely. Their guidance and expertise were indispensable throughout the entire process. The committee comprised a perfect mix of expertise and experience. From fundamental system related knowledge and computational capabilities to real life boots on the ground insights and overarching process dynamics. Zheng Bing Wang, Thom Bogaard, Erik Mosselman and Jelmer Cleveringa. I am grateful for your enthusiasm and knowledgeable contributions. You have put me on the right track and were also able to pull me back to the surface when i was too immersed in a particular sub-process.

I am also thankful to the Arcadis colleagues who contributed. Jos van der Baan, as expert in Delft3-D, who could make the complex seem somewhat simple. Tanya Huizer and Rob Steijn who were involved in the initiation and entrancement of the project, as well as the Yangon team. I enjoyed your collegiality. Also the students and TU Delft staff who were ready to assist whenever requested.

Due to the continuing and escalating circumstances related to the current coronavirus pandemic there have been some challenges in the execution of the research. An initial research proposal was completed in the end of February. Consisting of an extensive fieldwork and a measurement campaign. After careful consideration the proposal was altered to accommodate the new paradigm. Moving towards a more desk orientated study. This has been accomplished by virtue of the resourceful attitude of the supervising committee. A field measurement campaign instigated from the Netherlands could eventually also not be executed. Furthermore, all the work on this project has been performed from the confines of home offices. Imposing a noticeable hindrance to the workflow. In-person contact with colleagues, supervisors and fellow students would have certainly been a welcome.

Nevertheless, i am glad to have been able to continue the research in an appropriate fashion. The corona induced inconveniences related to this research are less than minor when compared to the situation at large. The Lamminga and FAST funds of the TU Delft were prepared to support the envisioned field work with resources. For which i am nonetheless grateful.

Additionally i would like to address and thank Helvetas, the Yangon Technical University and DWIR. all filled with talented staff and engineers. Hopefully i have contributed to the cause with the results and during this thesis. I wish you all well with your endeavours and am sure a lot will be accomplished in the future.

Lastly, I would like to thank my mom, dad and brother for their unrelenting support through my student years. Your support has made the whole process fun and exciting. I also was very fortunate to have had my friends from: Centrum, Water Gang, Hokje, Ski Cafe and IJsbeer. There was enough room for serious conversations but also for banter and laughter. Stay safe and stay wave everybody!

*Huckleberry de Haas
Delft, January 2021*

Abstract

The Gulf of Mottama, located in the southwest of Myanmar, is home to morphologically interesting processes. An entrance of around 100 *km* wide narrows into a funnel-shaped bay towards the Sittaung River in the north. The entire estuary region is subject to strong dynamic morphological activity which is alleged to be driven by the large tidal energy and sediment inputs. The dynamics of the tidal channels in the Sittaung estuary have resulted in rapid bank erosion of up to 3 *km/y*. The estuary inherently experiences cyclic processes that are generated through interactions between different forcing types. Under certain conditions a tidal bore forms in the Sittaung estuary which has a visible impact on the bank. Previous research has indicated that river discharge influences channel dimensions and the planform of estuaries in general. Growing tidal bars can affect large-scale estuary planform through bar push or bank pull processes.

The Sittaung estuary harbours a unique set of characteristics as has been explained. This has made the question of which processes and mechanisms cause the bank erosion a complex one for which no clear cut answer is currently available. The knowledge of the main processes and mechanisms is valuable to improve the understanding of morphological functioning in dynamic estuaries. The understanding is also required when determining suitable and sustainable solutions to reduce the erosion problems. There has not been a comprehensive study looking into the possibilities of combining morphodynamic development of tidal channels and cross section bank erosion in a numerical simulation for such a dynamic environment. The main research question has thus been formulated as:

- **What is the effect of the large incoming tide and storm events on the bank erosion of the Sittaung estuary and to what extent can this erosion be simulated with a numerical model?**

The purpose of this study has been to improve the understanding of the aforementioned hydrodynamic and morphological processes in regards to the dynamic morphology. Following the main research question, the following sub-questions have been addressed. In what regards can the Sittaung estuary erosion situation be called unique? What are the triggers for the reversal of the channel migration direction? What does the large-scale sediment transport of the estuary indicate? In order to address the research questions three distinct hypotheses have been formed and have been tested which are presented in the introduction.

The research objectives have been achieved through a literature analysis, system analysis, satellite analysis and modelling simulations. The literature analysis has positioned the current study in the active academic discussion. It also provided the information necessary for a constructive research setup through examining the previous research.

The goal of the system analysis has been to retrieve and analyse the relevant recent data on the Sittaung estuary from previous field measurements, satellite analyses and studies. The focus regions have been determined based on the extrapolation and system understanding based on this data.

The satellite analysis has build on the available information and provided data about the process specific developments that were needed to perform accurate analysis. The activities were aimed at the processes of the main hypotheses. Such processes were the influence of the incoming tide on the erosion, the influence of river discharge and that of large storms on the morphodynamics. Also the development of new tidal channels in previous cycles has been examined.

A depth-averaged 2-dimensional morphodynamic model has been used to investigate the hypotheses on the bank erosion against he data from the satellite analysis. Multiple cases have been evaluated with an elaboration on the case specific physical and numerical parameters in the respective sections. The effects of the incoming tide, the large storm have been simulated here. To investigate the different orientations the velocity and the transport have been used as indicators. A large-scale sediment transport analysis of the estuary has been performed through analyzing the residual transport. The capabilities of the numerical model to simulate long term bank erosion have been examined. This has been done by analysing to what extent the approach was successful and where it seems to be lacking technically. Looking at the applicability of the process based modeling it has been important to be conscious of the goal that the modelling endeavours were supposed to serve.

Results

The satellite analysis has shown little to no correlation between the wet season and the bank erosion rates. The resulting heavy increase in discharge due to the monsoon is a factor that would have been suspected to be inducive to an increase in erosion. There has been examined a large difference between the erosion of the upper cross section of the estuary and the middle cross section of the estuary. The large incidental storm events contribution to the dynamic behaviour of the estuary is found to be limited. Analysis of the recent cyclone arrival shows no additional implications.

The examination of the velocity and transport profiles of different modelling configurations indicate a strong effect of the incoming tidal bore on the erosion. In the upper cross section there were high flow velocities for almost the entire time of the simulated cycle. Only when the tide arrived did the velocity decrease. The flows were much higher for a longer period of time than in the middle of the estuary. This was the case for all configurations. There has been an observed difference in relative importance between geomorphic processes. Modelling results indicate a prominent role but cannot substantiate a quantitative impact of the tidal forcing and associated tidal bore. Model simulations substantiated the satellite analysis that showed the large storm events have a limited effect on the the dynamic morphology of the system. Model simulations showed that there was little increased erosive force resulting from the storm configuration.

The large scale sediment analysis indicate a flood dominant system. The calculated residual transports point to large-scale and local redistribution of sediments. The presence of adjacent upstream and downstream directed zones in the estuary indicates sediment circulation at the scale of the entire estuary. The two-dimensional model setup was unable to simulate baroclinic sediment transports. Fine sediments are transported out of the estuary according to the model simulations. But field observations clearly indicate the presence and even import of fine sediments into the estuary. It has been investigated how the model could be used to simulate long term bank erosion. Initial model simulations showed a slight move of the channel boundaries in the correct direction. But the qualitative representations were not near the correct values. Long-term simulations with respect to the bank erosion resulted in several hindrances. Heightened levels of channel incision occurred through a fault in the numerical schematization. The wrong upwind direction could be chosen for the bed celerity and the system would than become unstable. The model also did not ascribe the erosion to the bank (dry) cells correctly, even with the drycell feature of Delft3D enabled. This caused stalling of the supposedly eroding bank. Applying the numerical modelling approaches to a longitudinal stretch of estuary bank which resides on the wet/dry interface will eventually further modelling potency but has currently not been applicable.

Key findings

- **The satellite analysis has shown little to no correlation between the wet season discharge increase and the bank erosion rates. It also showed large differences between erosion rates at different heights of the estuary.**
- **Tidal forcing results in critically different erosive patterns in the region where erosion is most potent. Modelling results indicate a prominent role but cannot substantiate a quantitative impact of the tidal forcing and associated tidal bore. River discharge fluctuations were shown to have little effect on the bank erosion.**
- **The results of both the satellite and numerical modelling analysis have shown no additional implications on the dynamic morphology caused by large incidental storm events.**
- **The estuary wide sediment transport analysis has shown the estuary to be flood dominated with a net import of sediment. It also showed a discrepancy between the observed import of fines and the simulated export. Owing to the 2-dimensional aspect of the model which understates certain 3-dimensional aspects.**
- **Long-term simulations with respect to the bank erosion resulted in several hindrances. Heightened levels of channel incision occurred through a fault in the numerical schematization. The representation of bank erosion in the model has also been subject to stalling.**

Contents

Preface	i
Abstract	ii
1 Introduction and research setup	1
1.1 Background of the Sittaung estuary morphodynamics	1
1.2 Problem statement	2
1.3 Research objective	2
1.4 Report setup	3
1.5 Social domain of the erosion problems	4
1.6 Examination of relevant literature review	5
2 Methodology	13
2.1 Previous studies of the Sittaung estuary	13
2.2 Satellite analysis	13
2.3 Modeling simulations	14
2.4 Modelling tool and model set-up	15
3 Previous studies of the Sittaung estuary	23
3.1 Introduction and historical evolution the the estuary	23
3.2 Morphodynamic activity of the estuary	24
3.3 Hydrodynamics of the Sittaung estuary	25
3.4 Sediment availability & distribution	26
3.5 Resulting intended field measurement campaign	28
4 Satellite analysis of morphological trends in the Sittaung estuary	31
4.1 Bank erosion trends at multiple positions	31
4.2 Tidal channel formation	33
4.3 Incidental large storm effects	36
4.4 Recap of the results from the satellite analysis	37
5 Modelling simulations of the physical system	39
5.1 Simulations of hydrodynamic differences	39
5.2 Simulations of incidental large storm events	41
5.3 Simulations of large-scale sediment transport	43
6 Modelling capabilities and limitations	47
6.1 Simulations of cross section development	47
6.2 Chanel incision depth and transverse bed slope factor	48
6.3 Limitations of accurate model representation	50
7 Discussion	53
7.1 Discussion of the preceding state of research	53
7.2 Discussion of the satellite analysis	53
7.3 Discussion of the numerical modelling simulations	54
7.4 Discussion of the modelling capabilities and limitations	55
8 Conclusions and Recommendations	57
8.1 Conclusions	57
8.2 Recommendations	58

Bibliography	61
List of Figures	65
List of Tables	69
Appendices	71
A Research context	73
B Processing of satellite data	75
C Delft3D general	81
D System analysis and data	85
E Numerical modelling simulations	91
F Designed field measurement campaign	97

Introduction and research setup

1.1. Background of the Sittaung estuary morphodynamics

The Gulf of Mottama, located in the southwest of Myanmar, is home to morphologically interesting processes. An entrance of around 100 *km* wide narrows into a funnel-shaped bay towards the Sittaung River in the north, see figure 1.1. The entire estuary region is subject to strong dynamic morphological activity which is alleged to be driven by the large tidal energy and sediment inputs. The clip at figure A.2 provides a quick introduction. The dynamics of the tidal channels in the Sittaung estuary have resulted in rapid bank erosion of up to 3 *km/y*, as can be seen in figure 1.2. Estuaries are dynamic environments where ocean and riverine processes interact to form complex and changing morphology. The hydrodynamic and morphological properties of the tidal channels are interdependent. The Sittaung estuary harbours a unique set of characteristics which have made the question of which processes and mechanisms cause the bank erosion a complex one.

The estuary inherently experiences cyclic processes that are generated through interactions between different forcing types. Constant evolution and new configurations can alter the dynamic behaviour in original ways. Previous research has indicated that river discharge influences channel dimensions and the planform of estuaries. Growing tidal bars can affect large-scale estuary planform. Diversion of flow around bars contributes to bank erosion through bar push or bank pull processes (Leuven et al., 2018). Under certain conditions a tidal bore forms which has a visible impact on the bank (de Ridder, 2017). Anthropogenic factors have shown to be limited (Steijn et al., 2019).

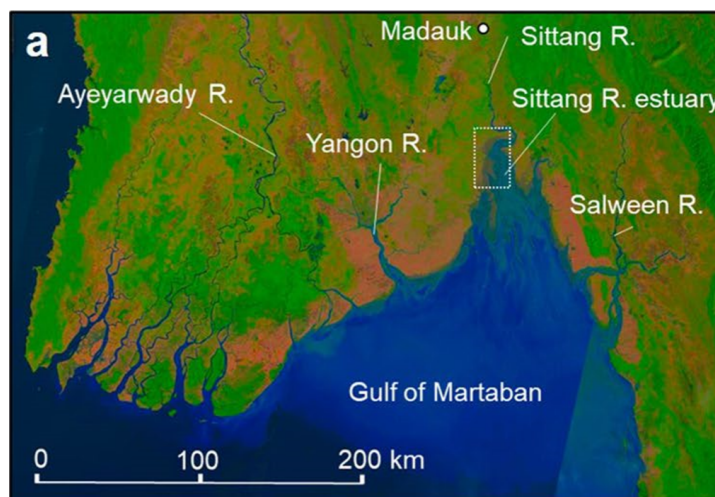


Figure 1.1: Overview of the region of the gulf of Mottoma and Sittaung estuary system from (Shimozono et al., 2019).

1.2. Problem statement

At the basis of the dynamic behaviour are naturally occurring morphological processes. How the different processes contribute to the bank erosion is not completely known. The knowledge of these main processes and mechanisms is valuable to improve the understanding of morphological functioning in dynamic estuaries. The understanding is also required when determining suitable and sustainable solutions to reduce the erosion problems. Key components of the dynamic morphology in the estuary are the estuary bank erosion and the migration of the tidal channel. The tidal bore and channel migration are alleged to be a result of and contributing to the dynamic behaviour (Ahmed et al., 2019; Shimozono et al., 2019). To what extent these contribute to the bank erosion is as of yet uncertain. Studies have been performed where morphodynamic numerical models have been applied to study the development of tidal channels (Xie et al., 2009). Also, studies have been done to research the simulation of cross section bank erosion with numerical models (Stecca et al., 2017). There has not been a comprehensive study looking into the possibilities of combining these modelling aspects for such a dynamic environment. The main research question has thus been formulated as:

- **What is the effect of the large incoming tide and storm events on the bank erosion of the Sittang estuary and to what extent can this erosion be simulated with a numerical model?**

1.3. Research objective

The purpose of this study has been to improve the understanding of the contribution of the aforementioned hydrodynamic and morphological processes and mechanisms to the dynamic morphology. The Sittang estuary has shown to be interesting from a scholarly point of view, it is unique and important in itself. Correct information on the possible future behaviour of the estuary has proven to be vital for inhabitants of the region and essential for the governance of the changes in bank position (SDC, 2016).

Following the main research question, the following sub-questions have been addressed. In what regards can the Sittang estuary erosion situation be called unique? What are the triggers for the reversal of the channel migration direction? What does the large-scale sediment transport of the estuary indicate? From examining the system there have been some aspects in particular that required consideration. These were the tidal bore related phenomena and channel migration characteristics. These have been investigated in their relation to the dynamic morphological activity. In order to address the research questions three distinct hypotheses have been formed and have been tested:

Hypotheses

1. **The incoming tide and tidal bore have a large effect on the bank erosion in the estuary.**
2. **The arrival of a storm event influences the development and migration of the tidal channel.**
3. **Numerical modelling with Delft3D is suitable to simulate the rapid bank erosion of the estuary.**

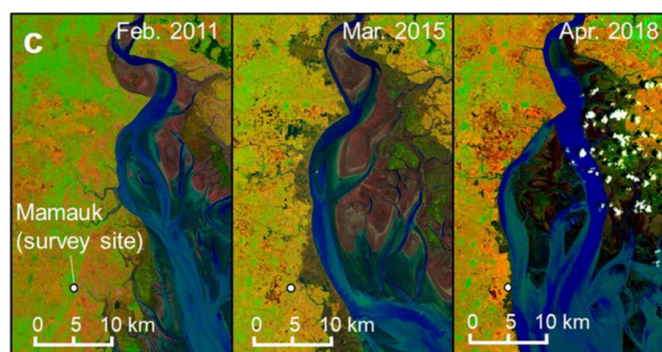


Figure 1.2: Rapid bank erosion and tidal channel formation of the Sittang estuary in the last decade (Shimozono et al., 2019).

1.4. Report setup

The analysis has been performed in four steps. The first step, presented at the end of this chapter, is a literature review on the main processes active in the development of the estuary. This section has outlined the relevant processes, the current state of research and the kind of formulations that are used in numerical modelling. In the next chapter the methodology is presented along with the model setup. Subsequently a system analysis has been performed. Here the characteristics of the system have been examined through evaluating previous studies of the region. This has been presented in chapter 3. Occurrences such as erosion trends and channel migration have proven to be interesting to the research. The research area has been analysed in more detail. Observations from satellite imagery are analysed and the valuable notions have been extracted. In chapter 5, the Delft3D model analyses of different situations and configurations have been performed to explore the hydro-morphodynamic relations. In the next chapter the possibilities and limitations of numerical simulation have been considered. The combined discussion and synopsis of the results is presented in chapter 7. The report finishes with the conclusions and recommendations in chapter 8. The overview of the research buildup and workflow can be seen in the box chart in figure 1.3.

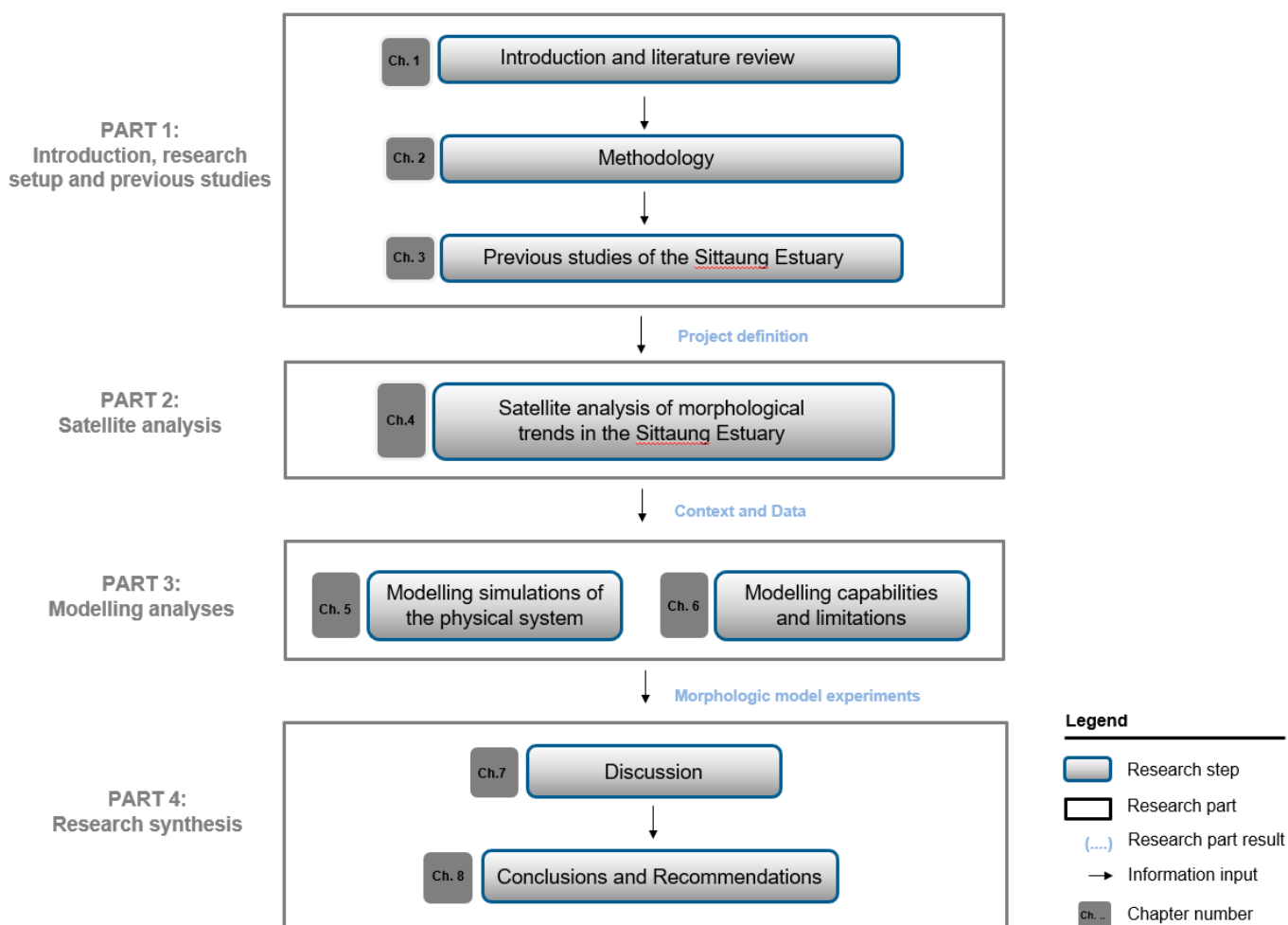


Figure 1.3: Flow chart of the grouped report and research structure with indicated steps and parts.

1.5. Social domain of the erosion problems

The perils of the affected communities and the dire need for assistance in the mitigation of the problem have long been recognized (SDC,2016). Still, adaption to the bank erosion has proven to be challenging. In any well regulated environment the rapid loss of land in populated areas will pose problems. In addition, the Sittaung estuary region suffers from a lack of awareness, expertise and governmental inadequacy.

Stakeholder engagement has been considered an essential part of sustainable coastal management. In this process there are several important aspects: sharing of information and transparent communication are the main aspects. There is a knowledge gap, this was visible in the fact that there lives quite a persistent sentiment that the erosion is caused by sand mining. While in fact an overload of sediment has been one of the mechanisms behind the erosion. This study has contributed to the clarify of the complexity of the situation and the actual causes of the erosive problems. This has been achieved by considering the following questions:

- **How is the mitigation of the problems arranged and envisioned?**
- **How can the current research contribute practically to envisioned mitigation activities?**

Hard measures to protect vulnerable areas are not economically viable, see table 1.1. The focus has thus been set on active monitoring and managed retreat solutions. Essential for the management of the extreme changes on the Bago and Mon shorelines has proven to be the monitoring of bank erosion developments. In order to maximize the effectiveness, expertise and resources, the monitoring would benefit from a unified structure. The availability of recent satellite images in the public domain allowed for actualization of the developments of the shorelines and the tidal channels. Ideally the analysis and reporting would be supervised or reviewed by an expert panel. Such an approach would benefit all the involved parties, see figure A.3. Eventually enabling responsible authorities to perform a yearly shoreline maps containing useful information for affected communities.

There remained a challenge of suitable dissemination of the information once obtained. In order to perform the monitoring at any level the use of technical computer programs has proven to increase the impact significantly. An excerpt of the research has serve to quickly gain a working insight into the occurring erosion phenomena in the Sittaung estuary. A compact document that outlines the major trends and important insights to potential future staff that will need to perform technical judgement. Besides this the satellite analyses and geographical maps of the research functioned as a basis on which to continue the monitoring endeavours.

Table 1.1: Tabular overview of the costs and benefits of the several avenues of mitigation of the problem. The hard engineering solutions are opposed to the more softer managerial solutions.

Measure	Effectiveness	Local capacity	Costs	Benefits	Expertise
Status quo	-	+	0	-	-
Hard engineering solutions					
Slope protection	+/-	+	\$\$	+	+++
Dredging channels	-	-	\$\$\$	-	++++
Soft engineering solutions					
Mangroves	-	+/-	\$\$	-	++
Vegetated flats	+	+	\$\$	+/-	++
Data supported governance					
Managed retreat	++	+/-	\$	++	++
Bank position monitoring	+	+/-	\$	+	+
Information dissemination	++	+	\$	++	+

1.6. Examination of relevant literature review

1.6.1. Introduction

In hydrological and morphological analyses of a particular water body, it is necessary to examine all its constituents, the hydrodynamics as well as the solid ingredients. Both in the theory of the process and in the methodology of modelling simulations of events a balance should be found between the contributing liquid and solid ingredients (Klaven, 1997). This literature review section will try to position the current study in the active discussion in the relative research fields. As well as determining the gaps in current understanding and how the research can contribute in an academic way.

1.6.2. Estuary morphology

Based on the to the definition of Dalrymple (Dalrymple et al., 1992; Dalrymple, 2006). By tide-dominated estuaries are meant those estuaries in which the sediment dynamics are dominated by tidal currents at the entrance. Estuary and tidal systems are complex with various scales active at the same time. The system acts on different time- and spatial scales than the morphological elements and morphological features (Eelkema et al., 2009), see figure 1.4.

Most estuaries evolve towards an equilibrium and studies are aimed at investigating this state. The morphology in an estuary can deviate from its equilibrium because of sediment differences in a seasonal timescale. But taken over a year the two opposite processes can also be balanced, giving rise to a dynamic equilibrium (Xie et al., 2018).

Forcing and planform effects

Research has been done on the idea of river discharge influencing channel dimensions and planform of estuaries (Savenije and Veling, 2005; Davies and Woodroffe, 2010). The river can have effect on other large-scale dimensions as well. Higher estuary convergence will result in larger channel width, assuming an equal length of the estuary, on all locations (Davies and Woodroffe, 2010). In natural sinuous estuaries there often arises bank erosion and point bar deposition (Xie et al., 2018). "Growing tidal bars can effect large-scale estuary planform, causing deviations from the ideal planform in natural estuaries" (Leuven et al., 2018). The diverted flow around forced mid channel bars causes bank erosion, see figure 1.5. This can happen in several distinct fashions. A channel will naturally approach an equilibrium state after some time. Before the equilibrium attained the river follows a phase-plane trajectory of which the two last processes of Eke are interesting to note (Eke et al., 2014). If both banks migrate outward, but the depositing bank moves faster the process is called bar push. If instead the eroding bank moves faster the process is called bank pull.

A concise view on the factors that are actively determining the estuary dimensions is given by Leuven (Leuven, 2014). Channel convergence and bottom friction are generally the control parameters for tidal amplitude, phase speed and relative phase difference between tidal velocity and elevation (Friedrichs, 2010). Convergence tends to increase the tidal amplitude, friction causes decay. A balance can be derived between friction and convergence of equilibrium estuaries. (Friedrichs, 2010). River discharge can affect water depth and flow velocity, which determine the friction factor.

Large storm effects

The effects of large incidental storms can be quite severe, causing direct impact on coastal geomorphology and other functions integral to estuarine functioning (Dame et al., 2000). The frequency and intensity of storms remains are highly unpredictable, as do their impacts on coastal marine environments. They can be considered as expressions of climate change. The impact on the estuary that a certain storm has will depend on size, location, speed, the state of the tide, shoreline configuration, and slope of the adjacent continental shelf (Hayes, 1978). Storm related processes affecting coastal sedimentation include strong currents and suspended and bedload sediments driven by storm surges and flooding resulting from heavy rainfall (Hayes, 1978).

Channel migration

The evolution of channels and bars in estuaries has high socio-economic relevance, with strong implications for navigation, dredging and ecology. However, the spatial and temporal evolution of channels and bars in estuaries is poorly understood. Channel migration is mostly a discontinuous process within

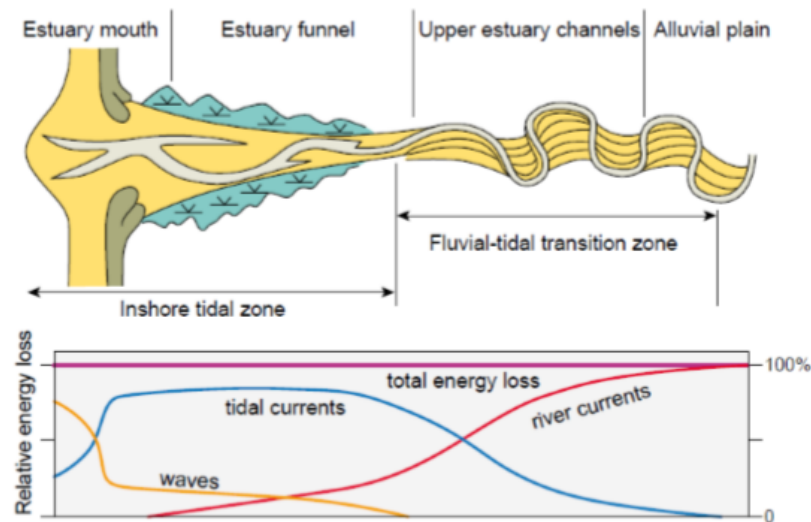


Figure 1.4: Classification of morphological components in a filled estuary. As presented in (Leuven, 2014) from (Martinius and Van den Berg, 2011). Because energy dissipation plays an important role in sediment dynamics, the morphology can be related to the loss of hydraulic energy.

bends. These variations in migration rate are likely a response to channel width fluctuations because of a short-term imbalance between the rate of bank erosion and the rate of point-bar sediment accumulation (Nanson and Hickin, 1983). The rate of channel-bend migration peaks when the ratio radius of channel curvature to stream width (r_m/w_m) is around 3.0. The rate of channel migration rapidly declines when values for r_m/w_m are greater or less than 3.0 (Hickin and Nanson, 1975).

Sediment transport

With the arrival of the tidal wave into the estuary there is strong deformation. The bed topography and other properties influence the way in which the wave propagates into the estuary. Tidal asymmetry is a distortion of the tidal wave created by bathymetry, geometry, friction and tide-tide interaction. Sediment transport capabilities are affected by these changes in the tidal wave propagation and stand to increase under certain conditions (Bosboom and Stive, 2013).

With a shorter flood period, mean flood velocities are higher than the mean ebb velocities. This is how flood dominance is enabled. With a shorter ebb period it is the other way around and the system is ebb dominant. Coarse sediments are mostly transported as bed load and fines in suspension. Large intertidal areas can slow down the flood propagation into the system, enhancing ebb dominance. The wet surface area at high water over the wet surface area at low water can be used as an indicator (S_{hw}/S_{lw}). The hypsometric curve can show this relation by expressing the bed level over the basin area, see figure D.1.

If the channels become deeper it will affect the ebb duration and shorten it. Enhancing ebb dominance and sediment export (Dronkers et al., 1998). Opposite, flood dominance is enhanced when channels are shallow, wide, or when the the intertidal storage area decreases and tidal amplitude increases (Bosboom and Stive, 2013).

Sediment characteristics and available flux

Erosion behaviour of soft cohesive sediment deposits has been investigated in laboratory experiments. Such deposits are representative of the top, active layer of estuarial beds. In general, the bed shear strength increased with depth and was also influenced by the type of sediment, bed consolidation period and salinity. The rate of erosion was found to vary exponentially when the stress exceeds the strength. In modelling estuarial bed erosion, it is important to take these characteristics of the bed shear stress and the rate of erosion into account (Parchure and Mehta, 1985). Cohesive sediment fractions experience cohesive behaviour caused mainly by physico-chemical forces between the clay particles. This cohesive behaviour causes complex processes that influence the erosion and deposition of sediments (Braat et al., 2017).

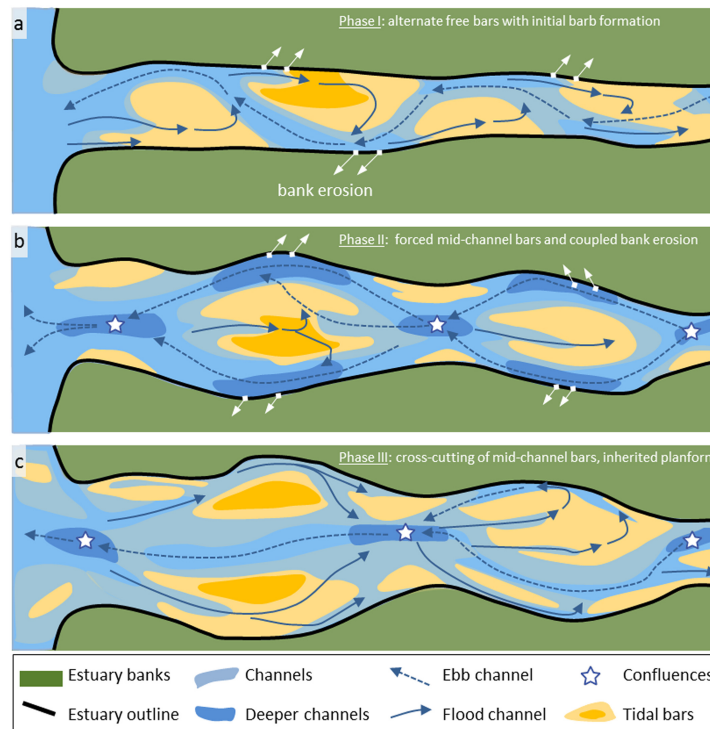


Figure 1.5: "Conceptual model for the development of self-formed estuaries. Interesting is phase II, where flow is diverted around the mid channel bar, causing high flow rates and extra bank erosion". From (Leuven et al., 2018).

Mud supply has an effect on the large-scale estuary morphology and development. Coastal waves excite settled mud and reduce the tendency to form muddy coastlines and the formation of mudflats in the downstream part of the estuary. However, when mud concentrations rise, higher discharge and low tidal amplitude, the estuary tends to narrow and fill up (Braat et al., 2017). Sediment that is more recently deposited has a different erosion capacity than sediments which have been compounding over a longer period. In the field of soil mechanics consolidation refers to the reduction of volume of a sediment under imposed loads. Erosion capability often decreases with sediment age, leading to a storage time distribution that is not exponential (Bradley and Tucker, 2013).

Recent studies have shown that the contribution of bank-derived sediments to catchment sediment budgets may be higher than previously thought (Simon and Darby, 2002; Rinaldi and Darby, 2007). Particularly in annual sediment yields and suspended sediment yield in some highly unstable systems. With the fractions of material within the alluvial sediment system derived from banks rising. It becomes more important to have a view on the rates of bank-erosion events for a complete understanding of the transport regime. A floodplain constructed by lateral accretion will contain sediment with a range of depositional ages. The age of sediment in the flux is determined by the available sediment that the flow erodes.

Numerical morphological modelling

In recent studies a wide range of morphological processes in estuaries is examined with the help of modelling. Morphodynamic models have revealed that an equilibrium state of morphology can be reached asymptotically under conditions where erosion and accretion balance (Xie et al., 2018). Sandbars are important sedimentary systems within estuaries and can form depending on sediment availability (Xie et al., 2018). As is the formation and development of tidal channels which can be simulated in detail by process based morphodynamic models (Xie et al., 2009; Xie et al., 2013). Simulations of hydrodynamic and sediment transport reveal the specific zone where a sandbar might develop, taking into account the interactions between river discharge and tidal currents (Yu et al., 2012).

1.6.3. Tidal bore

A tidal bore is the natural occurrence of a hydraulic jump effect. It can form at the transition front between two streams with different flow depths, see figure 1.6. large-scale mechanisms determining tidal bore formation in convergent estuaries are still not completely understood. Key relevant features of a tidal bore are the high turbulence and turbulent mixing that occur during the bore propagation. Since a tidal bore is an impressive phenomenon, certain causal relations as to experienced erosion problems are quick to be assigned to it. The formation and dynamics of tidal bores in estuaries are highly complex phenomena dependent on nonlinear interactions between different spatio-temporal scales (Bonneton et al., 2015). Factors of influence in the formation of a tidal bore are the tidal range, river discharge, estuary geometry (see figure 1.6) and the channel bed topography (Chanson, 2011; Savenije et al., 2008). Undular bores occur when the Froude number is below 1.7 generally. This kind of tidal bore is characterised by a large front wave followed by a array of secondary waves (Chanson, 2010).

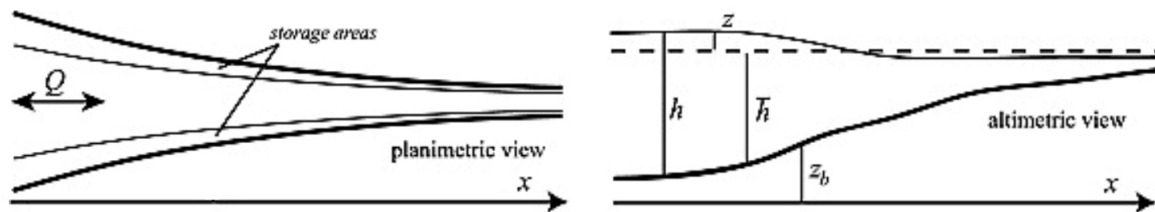


Figure 1.6: Schematic representation of the funnel mechanism contribution to the tidal bore formation from (Savenije et al., 2008)

For the case specific Sittang estuary tidal bore phenomenon a recent study has been conducted into its formation and contributing factors (de Ridder, 2017). It outlines the particular characteristics of the effective tidal bore and other insights into local channel flow and bank erosion. There is not a lot of exact knowledge about the relations between the forcing, bed topography and geometry of the estuary for the formation of a tidal bore. Difficulties in determining the relations arise because formation of a tidal bore depends on processes on different scales.

Two dimensionless parameters are proposed as classification (Lanzoni and Seminara, 1998). The dissipative parameter: dissipative properties causes the propagation to become non-linear, resulting in deformation of the tidal wave (Bonneton et al., 2015). The convergence parameter: as channel convergence increases, the distortion of the tidal wave is enhanced and both tidal wave speed and wave length increase. Strongly convergent and moderately dissipative estuaries enhance wave peaking as the effect of local inertia is increased (Lanzoni and Seminara, 1998). The funnel shape of estuary's will amplify the amplitude. This becomes evident when examining the energy balance for waves. From this energy balance, given by the following equation assuming no friction, an interesting relation can be derived, see D.

The wave celerity, see D.3, and the tidal damping both depend on the balance between friction and convergence. (Savenije and Veling, 2005). Studies refer to the effect of the tidal bore and the turbulence generated by it on the sedimentation process (Chanson, 2011; Simpson et al., 2004). A recent study into the Qiantang estuary has examined the contribution of the tidal bore phenomenon to certain morphodynamic processes (Xie et al., 2018). It found that the landward sediment transport is not effected significantly by the tidal bore for it to differ from flood dominance in other estuaries. The capacity of sediment transport does see an increase as to estuaries without a tidal bore. Flow velocities during spring tides can increase immensely as opposed to ebb tides maximums. "Furthermore, when the bore arrives, SSC also increases drastically because of the fine sediment that can be easily resuspend and, therefore, the sediment flux during flood tides is very large." (Xie et al., 2018, p.30). The presence of a tidal bore will notably increase the sediment availability and fluxes in the estuary.

1.6.4. Bank erosion

Bank erosion is a key process that can contribute extensively to the dynamics of an aquatic system, causing a variety of problems. It contributes to channel morphology changes and is a significant source of sediment. Fluvial erosion is defined as the removal of bank sediments by the direct action of hydraulic flow forces, though it generally occurs in combination with enabling processes (Hooke, 1980). Most studies recognise bank erosion as a combined product of three interacting processes (weathering and weakening, fluvial erosion, and mass failure) (Rinaldi and Darby, 2007). It is recognised that certain soil properties contribute to the stability of the bank, such as near-bank flow intensity, sediment transport, channel geometry and bed topography, vegetation, ground water level land bank material properties (Islam et al., 2008). All active till a certain extent but outside the scope of the current research and thus assumptions and simplifications will be necessary.

Bank erosion is a complex phenomenon, in research the emphasis is usually on sedimentary controls of bank erosion (Nanson and Hickin, 1983). However, these simple conceptualisations hold fast complexity, coming from the inherent variance of controlling parameters. Resulting observed rates of fluvial-erosion exist over several orders of magnitude and are predictable only to the extent that the underlying parameters can be determined accurately (Rinaldi and Darby, 2007; Hooke, 1980).

Shear stress forces exerted on the bank are highly variable, as it is dependent on factors like the geometry, cross-subsection size and shape, channel curvature, and flow stage. Which are themselves all very variable factors in space and time. It is generally accepted that fluvial bank erosion rates can be quantified using an excess shear stress formula such as presented by Partheniades (Partheniades et al., 1965).

$$\epsilon = \kappa_d (\tau - \tau_c)^a \quad (1.1)$$

Here $\epsilon(m/s)$ is the fluvial bank-erosion rate per unit time and unit bank area, $\tau(Pa)$ is the boundary shear stress applied by the flow, $\kappa_d(m^2s/kg)$ and $\tau_c(Pa)$ are erodibility parameters (erodibility coefficient, κ_d , and critical shear stress, τ_c), and a (dimensionless) is an empirically derived exponent. Thus some uncertainty remains over the value of the exponent a (Partheniades et al., 1965).

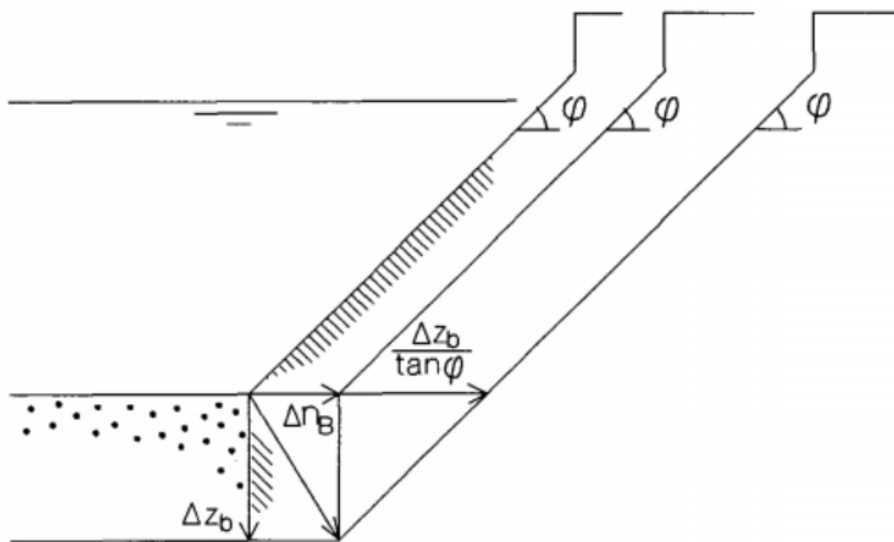


Figure 1.7: "Erosion of a cohesive river bank by lateral fluvial entrainment, Δn_s , and near-bank bed degradation, Δz_b , both inducing mass failure". A schematic representation from (Mosselman, 1993, p38).

Modelling approach

Bank erosion is a complicated process, methods have been created to predict the bank erosion rates. One of these compares bank erosion on the basis of local geometry, flow and sediment processes

Mosselman, 1993). For non-cohesive banks the erosion can be represented in a simpler way than for cohesive banks. For non-cohesive sediments, bank erodibility parameters are modelled based on the same methods that are used to predict the entrainment of bed sediments. Bank consisting of cohesive material require extra soil mechanic considerations. Determination of critical shear stress for cohesive materials is more complex, given that it is widely recognised that fluvial entrainment for cohesive sediments depends on several factors, for example clay and organic content. The soil's resistance to concentrated flow erosion is an important factor for predicting erosion rates (Knapen et al., 2007). The lower bank is eroded by hydraulic forces but the upper bank is less affected by flow forces but still erodes due to an undercutting process, see figure 1.7. Modelling bank retreat as a sequence of mass failures by toe erosion and subsequent sediment adaption into the flow. The erosion at the bottom of the bank or the sandy layer will eventually result in the upper part being in a suspended state. When the erosion grows and the momentum of suspended block is greater than the resistance, failure occurs. This view is at the basis of several mathematical models of bank erosion in where the rate of bank erosion is assumed to be related to near-bank flow velocity and shear stress. (Darby and Thorne, 1996).

Numerical erosion representation

With the recent progress in computational techniques, two-dimensional numerical models have become valuable tools for investigating flow and sediment transport in open channels at large temporal and spatial scales. Despite the computational power the implementation of mass failure processes in numerical models remains a difficult task (Die Moran et al., 2014). Slope instability effects can be integrated at sediment transport steps. Adding the bed evolution due that has been computed as a factor in determining the erosion (Die Moran et al., 2014). This is a rather sensitive way of approaching the bank erosion modelling question.

It is stated by Hickin (Hickin and Nanson, 1984) that the bank erosion rate is likely to depend on many variables as stream power, resistance to lateral migration, bank height, bend radius and channel width. The lateral migration coefficient in turn is shown to be a function of the texture of the outer bank materials, with a complex form similar to that of the Shields sediment entrainment function. The task of specifying the channel migration rate appears to be essentially a sediment transport problem (Islam et al., 2008). An example of expressing the lateral erosion of cohesive riverbanks is presented by Thome (Thome and Osman, 1988) D.4.

The time-average representation determines the bank erosion by looking at the fluvial transport of material at the toe. Circumventing the more intricate bank stability mechanism inducing mass failure. When the cohesive properties of material at the toe are canceled out in the averaging, the bank erosion mechanism reduces to a sediment transport approach (Mosselman, 1993). The distance between phenomena and the processes actually modelled is quite severe. Keeping this in mind is important when assessing the the possibilities of such an approach. As the computational time span increases round of errors and discretisations can generate truncation errors. Frameworks can be applied to avoid the complexity of analyzing model results. A differentiation is made by Stecca (Stecca et al., 2017) between three modelling steps: identification of the bank, computation of sediment fluxes due to bank erosion, and bank updating.

1.6.5. Transverse bed slope effects & spiral flow

Sediment transport is affected by bed level gradients. Two bed slope directions are distinguished: the slope in the initial direction of the transport (longitudinal bed slope) and the slope in the direction perpendicular to that (transverse bed slope) (Deltares, 2014).

In a normal river subsection with a level cross subsection sediment particles are directed downstream by the drag of the flow. The gravity also directs the particles along the incline of the bed. Which is the same direction in the case of a system without tidal influence. In cross subsection with a transverse gradient like bends the gravity pulls the sediment particle down slope in a direction divergent from the flow. Close to the bed the flow pattern is altered by secondary flow (spiral flow), also affecting the shear stress. Direction the bed shear stress towards to inner bend and slightly up the slope. The downslope gravitational pull on the sediment particles is counteracted by the secondary flow. An equilibrium between these forces determines the configuration of the transverse slope (Struiksmas et al., 1985). Besides the balance between the upslope drag force induced by spiral flow and the downslope gravitational force. An additional contribution of non-local effects from the redistribution of flow can increase the lateral bed slope (Struiksmas et al., 1985). Large-scale morphology like bar dimensions, meander dynamics, depth in bends and scours are greatly affected by the deflection of sediment transport on transverse bed slopes due to these mechanisms. The bed slope effect determines a range of geometric characteristics of banks and bars in different morphologically active systems (Baar et al., 2018).

When the flow velocity increases enough and other conditions are right, sediment can be transported in a suspended state moving above the bed (Van Rijn, 1984). If particles are in contact with the slope only momentarily, their movement direction is determined by the flow and not continuously affected by gravity. The less a particle is in contact with the ground the less it will be forced downslope by a gravitational pull. Though it seems that sediment in suspension is not entirely unaffected the the downslope gradient (Talmon, 1992). With particles in suspension, the downslope sediment transport decreases significantly as opposed to bed load conditions with similar flow conditions (Talmon et al., 1995). The choice of a particular transport mode will therefore lead to a different transverse slope evolution. The transport relation of 'Van Rijn' for instance differentiates between bed load and suspended sediment. In this case just the bed load fraction is subjected to downslope sediment transport. The 'Engelund-Hansen' (1967) is a total load transport relation. Resulting in the transverse bed slope effect acting on both the suspended load and bed load, the complete fraction of the sediment in transport (Baar, 2019). Different equations to simulate the transverse bed slope factor are the Koch-Flokstra D.8 and the Ikeda D.9. Koch-Flokstra shows an adaption of the direction of the sediment movement due to the transverse effects according to the Koch-Flokstra relation (Flokstra and Koch, 1980). While equation D.9 follows the relation according to the Ikeda (Ikeda, 1984).

Transverse effects representation in modelling

The application mode of the main effect of the transverse bed slope, a change in transport downslope, depends on the applied method. It may be accomplished by a rotation of the transport vector or by adding a transverse transport component (Deltares, 2014). Downslope sediment transport is calculated by a transverse slope predictor that deflects the streamwise sediment transport vector as a result of the local bed slope. There are several options for transverse slope predictors in Delft3D to implement a change in direction. The two most commonly used methods are the one by Ikeda (1984) D.9 and by Koch and Flokstra (1981) D.8. These methods differ in the way the the alterations are calculated and added to the sediment transport vector.

2

Methodology

2.1. Previous studies of the Sittaung estuary

This chapter has analysed the previous studies into the Sittaung estuary system and the problems connected to the bank erosion. Previous studies into the region and situation have been discussed and the important findings were extracted. The results have been presented along with the main implications. Findings of this analysis have functioned as a basis for the further research and model simulation experiments. The goal has been to retrieve and analyse the relevant recent data on the Sittaung estuary from satellite analysis and recent studies. For instance, data on the tidal channel evolution and erosion rates at several locations along the estuary banks. Data about the site specific developments were needed to perform accurate analyses. Research to contribute to the understanding of the system had to be focused on specific effects and regions. This was determined based on extrapolation of data and system understanding from the data analyses.

The morphodynamics of the Gulf of Mottama had been assessed by means of satellite imagery in several studies. To contribute to the understanding of the system it was productive to determine indicative effects of regions and possible erosion trends.

2.2. Satellite analysis

The satellite analysis chapter has build on the progress made in the preceding chapter where the system and its properties were analysed. The goal was to retrieve the relevant and necessary recent data on the Sittaung estuary from satellite analysis and recent studies and supplement the information of the previous chapter for the focus regions. This in order to better understand the dynamic behaviour of the system and test the hypotheses. Data about the site specific developments have been needed to perform accurate analysis. The activities were aimed at the main hypotheses presented in the research objective section 1.3. This way the hypotheses have been provided with the necessary information. Processes concerning the hypotheses have been the influence of the tidal bore on the erosion, the entry direction of the river discharge and the influence of a large storm on the morphodynamics. To substantiate these hypotheses the following characteristics of the estuary have been focused on:

- The difference between erosion rates at different locations in the estuary.
- The effect of changes in the river discharge and tidal range on the erosion rates.
- Channel migration tipping point behaviour.
- The development of new tidal channels in previous cycles.

2.3. Modeling simulations

To examine the effect of a particular process a model situation has been created where this process is examined in different states. Comparisons between the results of the different modeled situations served to determine the relative effect of the process focused on. The threshold of erosion of cohesive banks might be modified by complex interaction of multiple factors.

Hypotheses have been formed at the start of the research which evolved through the initial analyses and have been subject to slight alterations. The previous analyses showed where the crucial points lie for the numerical analysis.

Determining the contribution to erosion has been quite specific as this was dependent on a range of factors and requires an accurate representation in order to produce meaning full results. To investigate the different orientations the velocity and the transport have been used as indicators. As these were the main factors of the erosion and the sediment transport at the toe has been used to determine bank erosion (Stecca et al., 2017; Nicholas, 2013).

The satellite observations showed that there is no clear increase in erosion rates from dry season to monsoon season. It became interesting to see the differences in simulated orientations. Two hypotheses have been handled in a more straightforwards manner. The complexity and application of processes based morphological modelling has been used for studies in different context (Lesser et al., 2004; Xie et al., 2009). The question of the long term possibilities of bank erosion has proven to be open to interpretation. A large-scale sediment transport analysis of the estuary has also been performed through analyzing the residual transport. The research objective has been achieved by the analysis of a process based numerical modelling of different situations. Formation of a tidal channel has been investigated in a likewise manner in this study of the Hangzhou Bay (Xie et al., 2009). The differing characteristics of high river flow and flood tides and the tidal bore have been assessed in this research. With the results of the modelling efforts the performance has been assessed against surveyed bank erosion. A comprehensive framework to asses the performance of erosion modelling has been created by Stecca et al. (Stecca et al.,2017). The division of three modelling steps proposed by that framework has been used as guidance to asses the results in this study.

Engineering approach

Looking at the applicability and functioning of the process based modeling when examining morphological evolution, a distance arises between reality and the approached model situation, certainly in a data scarce system. It was important to be conscious of the goal that the modelling endeavours were supposed to serve. There was a culprit of diving into to much details of the physical processes modeling activities. If the modeled situation was applied to investigate certain hypotheses or calibrated against a certain feature, discrepancy's might unfortunately develop. Keeping these developments in consideration called for an added level of caution when interpreting the results and stating the competencies of the model. In a sense, the model has been applied with an engineering approach and to serve a prospective goal. The following research activities have been pursued:

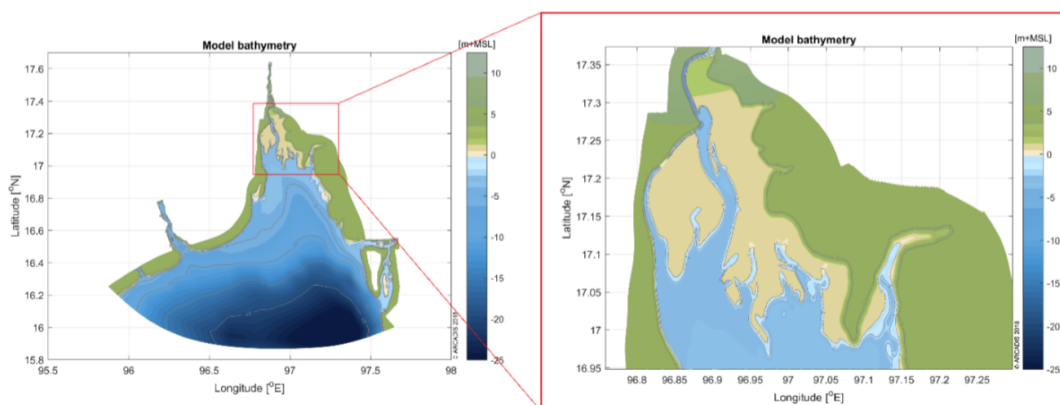


Figure 2.1: Current bathymetric profile of the created Gulf of Mottoma model. Main channel in the middle of the estuary (Arcadis,2018).

2.3.1. Methods for data acquisition

1. A literature study into the Sittang estuary, bank erosion and application of numerical modelling; *Positioning of the current study in the active discussion in the research field. As well as determining the available and current modelling methods.*
2. Gathering field measurement and satellite imagery data. *Data to analyse the hypotheses and to create the conditions for the numerical model. Using GIS solutions to determine rates, specific event locations and bed topography for model purposes.*
3. Contact with stakeholders and experts *Verification of the assumptions in line with the observed situation.*

2.3.2. Methods for analysis

1. Initial prediction of the effect of different factors and parameters on the erosion; *Hypotheses have been formed based on the encountered literature and previous studies in section 1.3*
2. Analysis on the basis of satellite data. *Determining the interest area to simulate erosion effects. Relating satellite data to use full model input. Hind-cast to analyse the past trends.*
3. Numerical modelling of conditions in different system configurations. *An estuary wide Delft3D morphodynamic model has been used to simulate different configurations. The model has been updated from the initial hydrodynamic model of the estuary, see figure 2.1.*
4. Model analysis in which individual variables have been changed to study the erosion effects. *Insight into the effect of specific parameters on the erosion process.*
5. Relating the system processes to the numerical morphodynamic activity. *Examination of the numerical descriptions and determining suitable configurations.*
6. Examining the capabilities of the numerical model to simulate long term bank erosion. *Analysing the areas where this approach seems to be technically hindered.*

2.4. Modelling tool and model set-up

2.4.1. General model characteristics

This section discusses the properties and application of the modelling tool. Some important points of awareness have been raised with respect to the capabilities of the model and the application of the results. The setup of the main model has been outlined and a detailed explanation of the chosen characteristics has been presented.

With the developments in computational capabilities and the continuing development of modelling tools it becomes possible to evaluate ever more complex problems and broader time scales. The complexity and application of process based morphological modelling can be used for studies in different contexts (Lesser et al., 2004; Xie et al., 2009). The findings of the previous studies have also been relevant for the model set-up and simulations of this thesis. As were modeling studies that might have focused on different aspects but in the same region of interest (de Ridder, 2017; Ahmed et al., 2018).

A distance arises between the theory and the reality approached model situation, certainly in a data scarce system. It is important to be conscious of the goal that modelling endeavours are supposed to serve. There is a culprit of diving into too much details of the physical processes modeling activities. If the modeled situation is applied to investigate certain hypotheses or calibrated against a certain feature, discrepancy's might unfortunately develop. Keeping these developments in consideration will call for an added level of caution when interpreting the results and stating the competencies of the model. In a sense, the model has been applied with an engineering approach to serve a prospective goal. Parametrisation and supportive features can enable an application to the desired specific problems and processes.

2.4.2. Model setup

In this thesis multiple cases have been evaluated with elaborations on the case specific physical and numerical parameters in the respective sections. However, there are generally corresponding overall parameter values and settings of the model. A previous study into the estuary by Arcadis has yielded a hydrodynamic numerical model which has been used to elaborate on for the purposes of the current thesis research (Arcadis, 2018). The relevant features of the existing model for the estuary have been expounded here along with relevant design and validation steps.

Delft3D is capable of flow, sediment transport and morphological development simulations. It consists of several modules that are capable of interacting with one another. The main module is the D-Flow, while engaging the D-Morphology for the morphological capabilities. Sediment transport is a large part of the current study, so it was relevant to examine the way transport processes are handled by Delft3D. The hydrodynamics have been simulated in a 2DH manner (depth averaged). A priority has been given to extra detail in the horizontal domain, to be able to distinguish the tidal channel system within the bed topography. This made it possible to simulate the tidal propagation and the interaction with upstream river discharge in the Gulf of Mottama as accurately as possible. A more detailed description of the computational properties of the software are available in the appendix C.

The default transport relation has been set to "van Rijn 93". The sediment fractions have been set to represent the sediment distribution in the system. The transverse bed slope has been given a value which results in a decent representation of channel formation and the hydrodynamic boundary forcing has been set to the desired run time.

2.4.3. Model domain

Grid generation was at the basis of numerical computations to the equations that describe the physical processes. The result of the numerical solutions of a model depend upon the quality of the constructed grid. The computational northern boundary rested in the Sittaung river from 25km south of Madauk to the river mouth. The southern boundary has been located in the Andaman Sea, see figure 2.2. The lateral boundaries were defined in such a way, that the computational domain covered the current hydrodynamically active region and allows for coastal erosion. The computational domain has been comprised of 600 by 1080 grid cells in a curvi-linear fashion. This allowed the grid to follow the local direction of the flow and is numerically effective (Arcadis, 2018).

The resolution of the grid varied from more detailed along the Sittaung river region and northern part of the estuary to a gradually coarser grid in the southern part of the domain. Furthermore, the grid was made slightly more detailed in the interest area's, resulting in a higher degree of model and computational detail. Up the Sittaung River the grid has been 15x40m, in the area of interest estuary 60x200m and in the southern part of the model 400x500m. The omittance of smaller channels has been of no significant effect to the large-scale accuracy because the impact on the large-scale tidal propagation in the estuary was negligible (Arcadis, 2018). To ensure an accurate computation and minimize the truncation error guidelines have been applied to certain aspects: The grid orthogonality, the grid smoothness and the grid aspect ratio (Deltares, 2014).

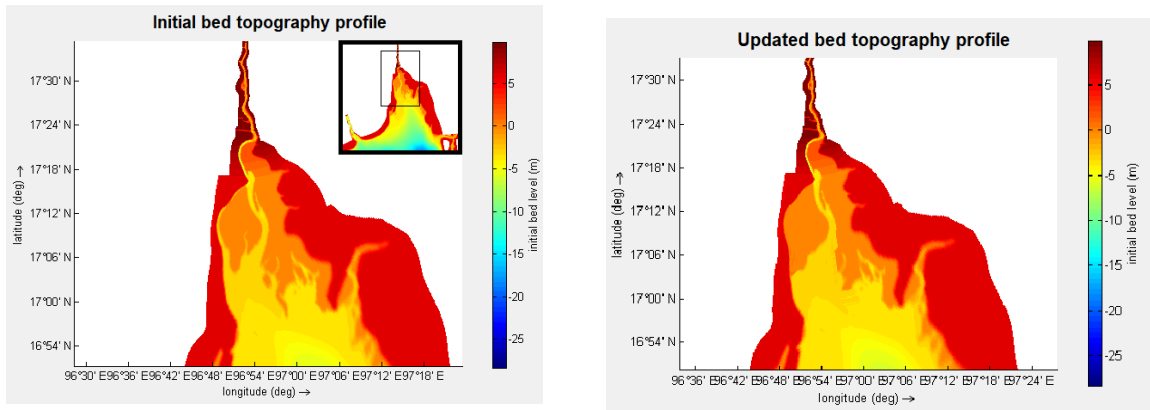


Figure 2.2: "Visualization of the computational grid (blue) (Source background imagery: Google Earth)" from (Arcadis,2018) Appendix C, p2.

2.4.4. Bed topography

The bed topography was one of the leading characteristics of the model simulations. Morphological development has been analysed by examining, among other things, the evolution of the bed topography. A combination of different sources has been used in the generation of the initial 2018 profile, see figure 2.3a. For deviating configurations based on this situation the accuracy decreases. The river bed topography upstream of the river mouth has been relatively stable in time. Downstream the bed topography in the start of the estuary remains highly dynamic. That is why this part has been considered the interesting area to investigate. But it also means that the exact bed topography was only portrayed for a short period of time.

Satellite data at low tide has been used to determine the geometry of the deeper channels and tidal flats within the morphologically active regions. Data from field measurements, figure D.8, provided depth measurements of transects along the main channels in the estuary. From these inputs the updated bed topography of the 2020 situation has been determined, see 2.3b. This new bed level profile has been used in the main model simulations investigating the tidal influence on the erosive properties. The resulting bed topography remained highly schematic. Possible new field measurement campaigns can provide the research with new and accurate data on the bed topography and cross section profile of tidal channels. However these would have to be updated systematically in order to have continuous worth. This would have an instrumental added value for the model, understanding and research as a whole.



(a) Initial bed topography as was generated for the July 2018 situation. Initial bed level values of the entire domain, focused on the area of interest. (b) Updated bed level profile of the estuary. Notice the secondary channel bordering the west bank and the entry to the new main channel.

Figure 2.3: Overview of the of bed level profiles of the estuary with 2018 configuration (a) and updated 2020 configuration (b).

2.4.5. Boundary conditions

Time varying boundary conditions have been used as forcing to the open boundaries of the model. A discharge boundary in m^3/s in the north represented the Sittoung rivers discharge. A spatially varying water level boundary along the southern boundary represented the tide in the Andaman sea. Both boundaries were located sufficiently far away from the area of interest to avoid any boundary effects in this area. Discharges along both lateral sides of the estuary, like the Yangon and Salween Rivers, do not have a significant impact on the tidal propagation and have not been assigned a value.

Depending on the required goal of the simulation, dry- wet season and annual discharge scenario's have been determined from the discharge data examined in the system analysis. For the dry season scenario for instance, a representative, constant discharge of $400 m^3/s$ has been used. For the wet season scenario a representative constant discharge of $4000 m^3/s$ has been used. Which has been determined from 3.4 in the system analysis chapter.

The model for the Gulf of Mottama has been nested in large-scale model, covering the Bay of Bengal and the Andaman sea. A spatially varying tidal signal was determined using the large Bay of Bengal model. The tidal range varied between almost 3m at neap tide and just over 5.5m at spring tide at the interest area and had an amplitude of 6m at the south boundary, see figure 2.4. The water levels for the south boundary have been created for a 6 month period.

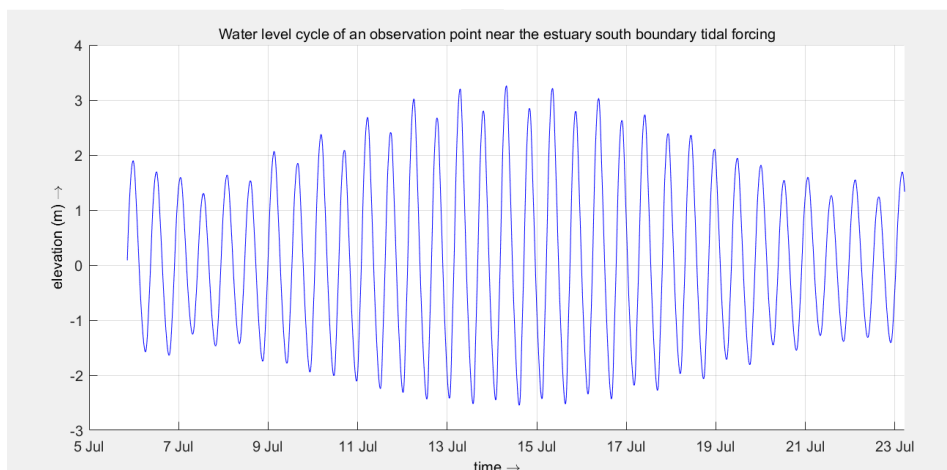


Figure 2.4: Water level cycle of an observation point near the estuary south boundary tidal forcing. With a visible amplitude of nearly 6 meters at the maximum moment just after full and new moons.

2.4.6. Time frame

The tidal forcing water levels from the embedded Andaman sea model were available for a period of 6 months. This has also been the longest time a single simulation has run. With the morphological scaling factor this has been extended when necessary to a period of 5 to 10 years depending on the stability. The exact timescale and duration depended on the goal of the simulation. Using the morphological scaling factor in a situation with tidal forcing and river discharge required extra attention to the way the discharge boundary was enforced.

the Alternate Direction Implicit difference scheme (ADI) was used, it basically divides one time step in two stages, during the first stage all equations are solved implicitly in one direction and during the second stage equations are solved explicitly in the other horizontal direction (see Appendix-C for further explanation). In theory the ADI method is an unconditionally stable integration method. However, in real-world applications with irregular coastlines, this is not automatically the case. For accuracy reasons it was still wise to limit the maximum used time step. The maximum has been determined by a limit on the Courant number (Deltares, 2008). The Courant number can be calculated with the following formula:

$$C = a \frac{\Delta t}{\Delta x} \quad (2.1)$$

Here a is the velocity magnitude. With ADI for barotropic mode in complex geometries the accuracy need limited the Courant number in the following way (Deltares, 2008):

$$C_f = 2\Delta t \sqrt{gH \left(\frac{1}{\Delta x^2} + \frac{1}{\Delta y^2} \right)} < 4\sqrt{2} \quad (2.2)$$

In general practical situations a time step equivalent to a Courant number up to 10 generally still gives accurate solutions (Deltares, 2008). Looking at the grid cell size in the area of interest, the maximum timestep can be calculated. With the size of the grid in the area 60x200m but 15x40m up the river, a general time step of about 24 seconds has been applied as maximum. This can be modified based on the time span and area of interest of a specific simulation.

2.4.7. Validation and verification

Model validation has been achieved by comparing model results with measurements at the interest area, which gives a measure of the quality of the model. Accurate representation of the water levels at these locations by the model provided confidence in the simulation of the tidal propagation. Even if data within the area was scarce (Arcadis, 2018). The tidal range has been predicted reasonably well, but the lower water levels during ebb tide were slightly under estimated during the spring tidal part of this time series, see figure D.3a. Sut Pa Nu is a town located at the mouth of the Sittaung river at a large distance from where the tidal signal was forced. An accurate representation of the tidal signal at this location provided much confidence in the model bed topography from the southern boundary up to this location. From figure 2.5 it can be observed that the representation of the water levels at this location with the updated bed topography were very similar to the original, which is related to field measurements in D.3b. The simulated phase was in agreement with the measurement with both the aggressive flood tide and elongated ebb tide occurring within the measured time frame. The tidal range was accurately predicted, showing a local tidal range of about 0.75m at this location. This accurate representation of the hydrodynamic tidal characteristics brought confidence to the application of the model in morphodynamic investigations. Flow velocity measurements would have presented more challenges when used to validate the model output.

2.4.8. Factor for erosion of adjacent dry cells

In the case of erosion near a dry bank, the standard scheme does not include erosion of the dry cells. Therefore a scheme has been implemented that allows the (partial) redistribution of an erosion flux from a wet cell to the adjacent dry cell. The distribution is directed by a factor "ThetSD" which determines the fraction of the erosion to be assign to the adjacent cells. The 'wet' and 'dry' cells have been defined

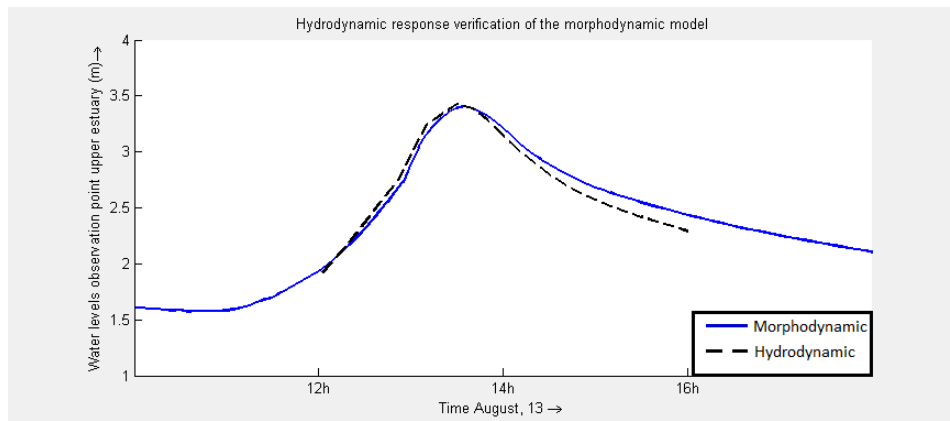


Figure 2.5: Hydrodynamic verification of the morphodynamic model after altering boundary conditions. Water level responses of the observation point at Sat Pu Na in the upper estuary.

as cells at which the water depth is above or below the threshold depth $SedThr$ for computing sediment transport. By specifying a parameter $HMaxTH$ larger than the threshold depth $SedThr$ for computing sediment transport this method can be altered slightly. The factor has been set to 1 for the initial modeling simulations. The actual factor to be redistributed for erosion in such cases has been computed as:

$$Thet = \frac{(h_1 - SedThr)}{(HMaxTH - SedThr)} * ThetSD \quad (2.3)$$

Here $Thet = \min(Thet, ThetSD)$ and h_1 is the local water depth. The purpose of this formulation is to allow erosion of parts that are inactive in terms of transport but still wet, while limiting the erosion of the dry beach.

Table 2.1: Physical parameters Delft3D

Parameter	Subject	Setting
Constants	Gravity	9.81 m/s ²
	Water density	1025 kg/m ³
Roughness	Bottom roughness formula	Chézy
	Bottom roughness value	65 m ^{1/2} /s
	Slip condition (wall roughness)	Free
Viscosity	Background horizontal viscosity/diffusivity	Uniform
	Horizontal eddy viscosity	1 m/s ²
	Horizontal eddy diffusivity	0.5 m/s ²
Sediment	Reference density for hindered settling	1600 kg/m ³
	Specific density	2650 kg/m ³
	Dry bed density	1600 kg/m ³
	Median sediment diameter	Fractions / 200 μm
	Initial sediment layer thickness at bed	8 m
Morphology	Update bathymetry during FLOW simulation	True
	Include effect of sediment on fluid density	False
	Equilibrium sand concentration profile at inflow boundaries	True
	Morphological scale factor	20
	Spin-up interval before morphological changes	2160 min
	Minimum depth for sediment calculation	0.1 m
	Van Rijn's height factor	1
	Threshold sediment thickness	0.05
	Factor for erosion of adjacent dry cells	1
	Current-related reference concentration factor	1
	Current-related transport vector magnitude factor	1

Table 2.2: Numerical parameters Delft3D

Subject	Parameter	Setting
Numerical parameters	Drying and flooding check	Grid cell centres and faces
	Depth at grid cell faces	Mor
	Threshold depth	0.1 m
	Marginal depth	-999 m
	Smoothing time	180 min
	Advection scheme for momentum	Cyclic
	Advection scheme for transport	Cyclic
	Forester filter horizontal	False

Previous studies of the Sittaung estuary

3.1. Introduction and historical evolution the the estuary

The Sittaung River is a river in the Bago Division of south central Myanmar, see figure 1.1 for an overview of the greater system. The Bago Range separates its basin from that of the Irrawaddy. It has a length of 420 km and has a mean annual discharge of around 50 km³ (May Thu Kyaw and Oo, 2019). Over longer time spans a significantly larger area is exposed to erosion by the migration of the channels. Given the extreme erosion rates, the evidence for large-scale dynamics and the lack of natural obstacles in a flat and low-lying region, the entire coastal plain could be subject to erosion (Arcadis, 2018). It seems as if the flow channels cannot reach much deeper, probably because of the presence of any kind of flow-resistant layer in the subsoil or an overload of sediment choking the channels. This may explain the speed of the horizontal channel movement in this part of the estuary. Figure 3.1 shows the position of the estuary in the past. In the map in figure B.1 the region that is potentially prone to erosion has been indicated. This has been determined by examining historic charts of the region and the current system characteristics. It indicates the dynamic activity and illustrates the need for awareness of this activity.

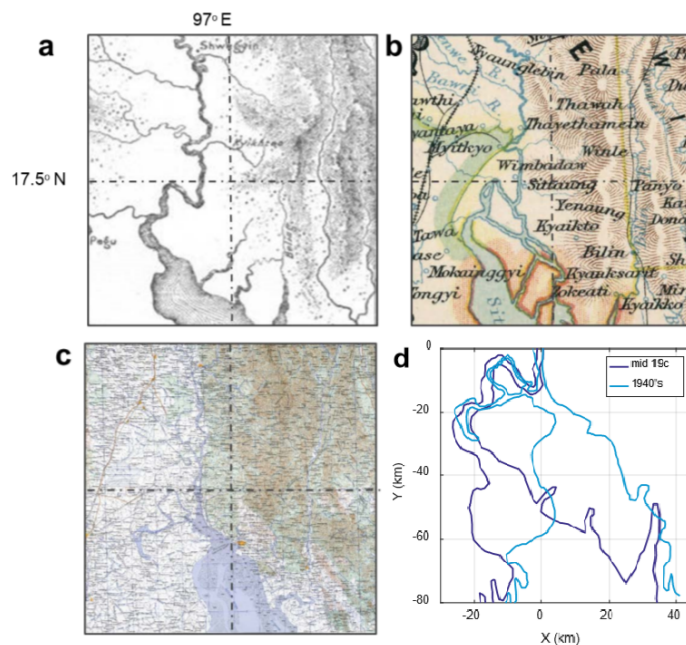


Figure 3.1: Historic estuary locations extracted from old maps of the region (a,b,c) and the mapped outline superpositions of the estuary around 100 years apart (d). Supplementary figures from (Shimozono et al., 2019).

3.2. Morphodynamic activity of the estuary

The morphodynamics of the Gulf of Mottama has been assessed previously by means of satellite imagery in several studies. The important conclusions from these studies have been used to determine the research direction. The position of the banks of the tidal channel at the limits of the estuary has been mapped, seen in figure B.2. This resulted in channel migration rates and an estimation of the periodicity in channel migration. Based on the results two areas have been distinguished with markedly different behaviour:

- Area 1: Unidirectional migration of the channel
- Area 2: Channel migrates in both directions

In area 1 of figure 3.2, a unidirectional meander migration has been taking place over the past 40 years. The location of the channel along the western shoreline, for the period from 1984 to 2012, was depicted in 4.1. The position of the west bank has shifted towards the west.

In area 2 of figure 3.2, the main channels are not able to develop more depth because either the presence of a flow-resistant layer in the subsoil or a sediment overload. This may explain why the speed of the horizontal channel movement in this part of the estuary has been so rapid. Less unconfined land has to be removed with shallower channels compared to deeper channels. The cross-sectional areas of the flow are considered small compared to similar type of channels in other estuaries, in turn increasing flow velocities (Arcadis, 2018). The direction of the migration and the erosion changes in periods of 10 to 15 years in the southern part of the estuary. The change in direction has shown to be repetitive.



Figure 3.2: Overview of the Sittaung estuary. The circles indicate the areas with differing levels of dynamic activity (Arcadis, 2018).

The migration cycle can also be seen as an deposition-erosion cycle of the estuary's evolution. Both the upper channel and the central basin are filled with a tight meander. The estuary evolution likely happens with the changing of the transitional region through the destruction and creation of bends (Shimozono et al., 2019). Other estuaries in similar tidal settings, such as Qiantang estuary in China, do not exhibit such an obvious cycle. There is a distinct difference in the path of the flood and ebb flow, see figure B.3.

System characteristics

The coastal erosion of the shorelines of Bago Region and Mon State result from the natural migratory dynamics of the flow channels of the Sittaung estuary. There is no human forcing behind it nor any human control on the observed dynamics (Arcadis, 2018). Wave forcing contributes little to the erosion and to the transport. Erosion from wave forcing would be localized at the top of the bank. While erosion from flow at the toe would render this contribution negligible. The effects of accelerated sea-level rise will be limited for the Sittaung estuary and its shorelines. There is an abundance of sediment available in the system that allows for buildup of the coastal plain and estuary at rates way above the water level rise.

Meander amplitude could indicate the maximum extent of erosion by outer bend erosion. Based on a typical channel width of 3 km (Arcadis, 2018), it is expected that meander amplitude is about 17 km (Leuven et al., 2018), see figure 3.3. This can serve as an indication a possible active erosion zone within which the erosion might occur.

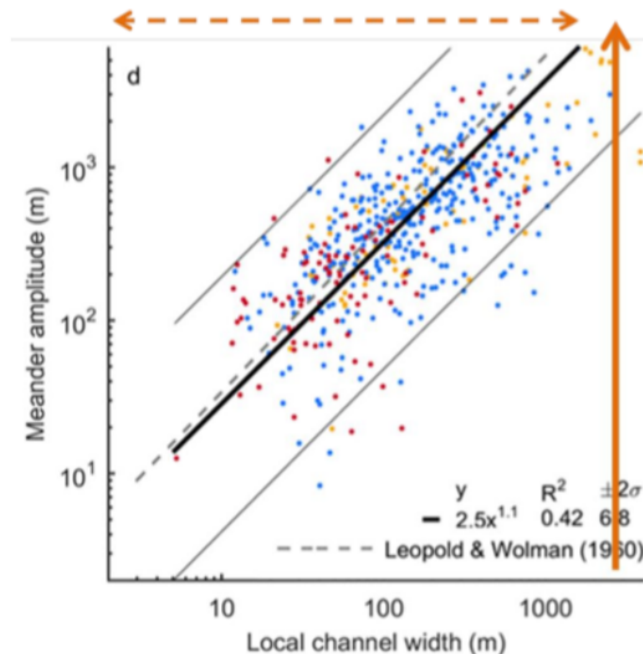


Figure 3.3: "Relationship between the local channel width and the meander amplitude from (Leuven et al., 2018)". From the study of Arcadis (Arcadis, 2018) based on fluvial-tidal meanders worldwide.

3.3. Hydrodynamics of the Sittaung estuary

The current estuary bed profile shows a single, relatively wide but shallow tidal channel that is responsible for the conveyance of the main tidal flow, figure 3.2. The remnants of the earlier main channel at the west side have been still visible as a smaller channel. In the north the river mouth is located past a relatively sharp bend on the western bank. The mouth consists of a tidal flat and a relatively narrow but deep channel along the western bank. At the south side boundary the estuary is forced by an incoming tide from the gulf of Mottoma.

3.3.1. The Sittaung river

The Sittaung River is highly volatile on account of the monsoon climate. Asian summer monsoon is the predominant climate system in Myanmar and nearly 90 % of total rainfalls result from the summer monsoon. Figure 3.4 shows the observed river discharge at Madauk station from a recent study. A yearly pattern for the river discharge is observed where there is a relatively low discharge during the 'dry season' in the first half of every year and a high discharge during the 'wet season'. During the dry

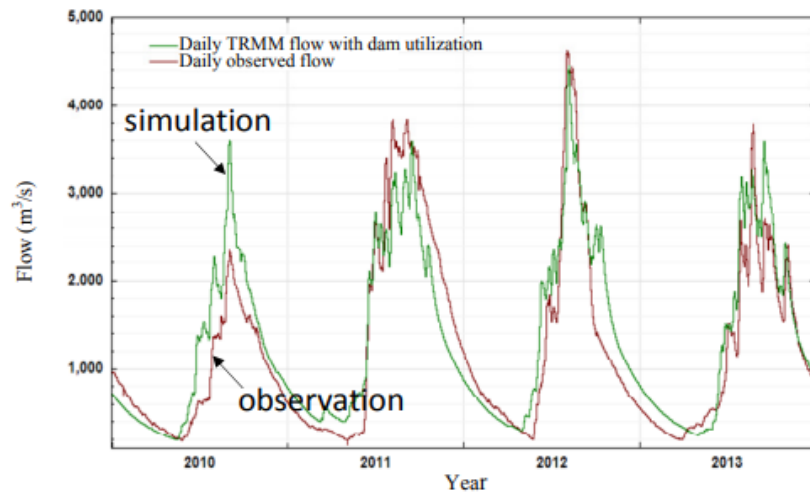


Figure 3.4: Daily discharge comparison between observations and simulations upstream in the Sittaung river. (Yamashita and Aung, 2016)

season, the discharge systematically drops below $400 \text{ m}^3/\text{s}$. During the wet season the river discharge can rise to $4000 \text{ m}^3/\text{s}$, with peaks of up to $4500 \text{ m}^3/\text{s}$. Dry-wet season and annual discharge scenario's can be determined from this data depending on the required goal of the simulation. For the dry season scenario a representative constant discharge of $400 \text{ m}^3/\text{s}$ has been used. While for the wet season scenario a representative constant discharge of $4000 \text{ m}^3/\text{s}$ has been used. Analysis of historical data has shown that the increase in discharge has been severe during the raining season (Yamashita and Aung, 2016). The cause of these unceasing discharges is unclear, deforestation is mentioned (May Thu Kyaw and Oo, 2019). The effects of climate change can cause the discharge to be more peaked.

3.3.2. Incoming tide of the Sittaung estuary

The water levels in the estuary vary heavily due to the semi-diurnal tide in the Gulf of Mottoma. The tidal range varies between almost 3m at neap tide and just over 5.5m at spring tide. The southern boundary located in the Andaman sea is still relatively shallow at a depth of 15m to 25m below mean sea level. The tide consists of a short flood period, where the water level rises quickly and a long ebbing period, where the water level drops slowly. Tide gauges within the estuary are absent.

Tidal bore

A special feature of the Sittaung estuary is the occurrence of a tidal bore in the central part of the estuary. Under spring tide conditions, this bore can reach spectacular heights (more than 2 m). Bank erosion of estuary is said to be driven by strong tidal currents following the passage of a bore head (Ahmed et al., 2018). The height of the bore increases when it reaches shallower areas such as the tidal flats due to shoaling effects (Arcadis, 2018; de Ridder, 2017). The tidal bore is more severe at the downstream area of the estuary occurring here 5 till 7 days after full and new moon. It induces a strong turbulent mixing in the estuarine zone and the effects may be noticeable along considerable distances. Eroded sediment at the foot of the bank prevents lower bank erosion, a large bank retreat can occur every two tidal cycles, see figure E.7. Erosion rates suggest that bank erosion intensely progressed due to flood flows of the high tides (Shimozono et al., 2019). Satellite observation of annual coastline changes shows that the bank erosion has a seemingly constant rate over dry and rainy seasons, see figure B.6.

3.4. Sediment availability & distribution

An interesting aspect of this estuary is presence of large sediment sources on the sea side. The continuous sediment supply is likely to support the fast bank accretion on the opposite side of the bank erosion (Shimozono et al., 2019). Sediment composed of bed material in the lower areas of the Sittaung river compare well with the material in the upstream river. Indicating that the estuary sediments are supplied by the same source (Ahmed et al., 2018). Sediment studies where the concentration

is measured over time show that the computed suspended sediment concentration shows changes corresponding to strength of tidal currents. Indicating that the tidal bore and associated strong current provides a sediment flux towards the estuary (Ahmed et al., 2019).

A study by Ramaswamy (Ramaswamy et al., 2004) looked at the factors influencing suspended sediment concentrations (SSC) and dispersal in the northern Andaman Sea and Gulf of Martaban, one of the largest highly turbid areas of the world's oceans, see figure 3.5. Sediment discharged by the Ayeyarwady River is transported mainly eastward towards the entry of the Gulf of Mottoma. Perennial high SSC in the Gulf of Mottoma are caused by a combination of factors including resuspension of sediments by strong tidal currents, shallow bed topography (see figure 3.6a) and seasonal sediment influx from the Ayeyarwady Delta.

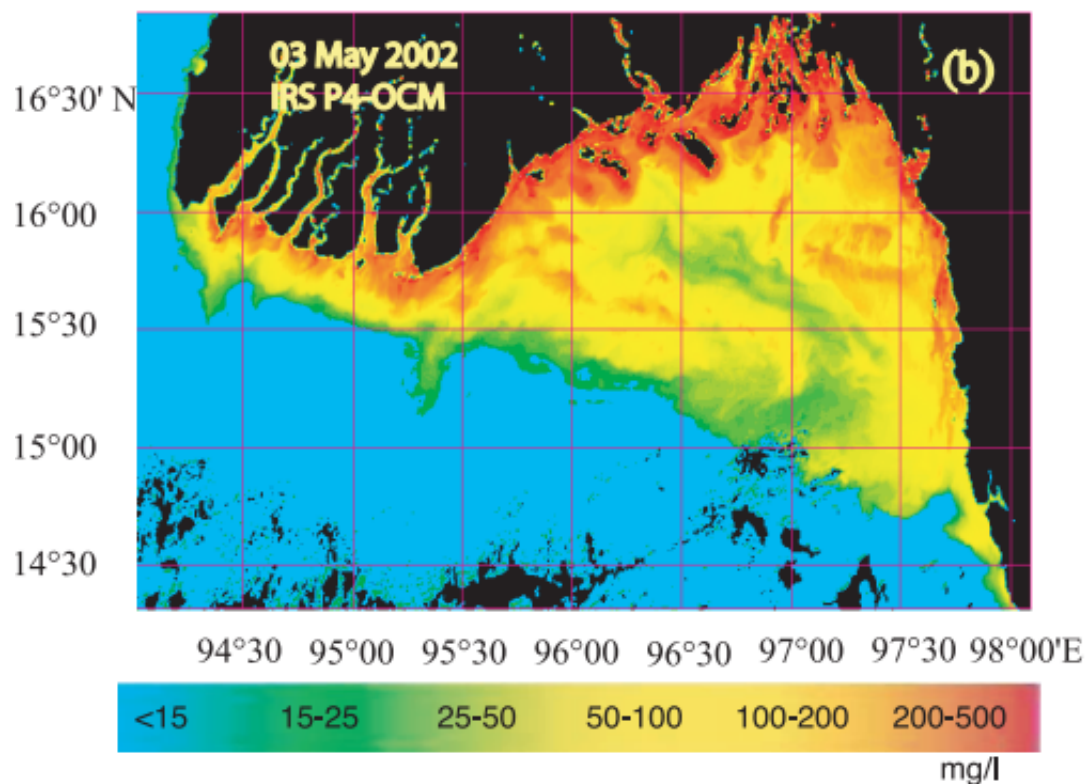


Figure 3.5: Suspended sediment concentrations data by satellite analysis from (Ramaswamy et al., 2004). Showing the eastward transport toward the gulf of Mottoma.

Figure D.5 shows the grain size distribution curves of bank materials obtained from a field survey conducted on February, 2019. The number 1 to number 4 samples were collected from locations near Mamauk and number 40 and number 41 samples were collected from the river course upstream of Sittaung Bridge and downstream of the artificial shortcut. It was seen from the particle size distribution analysis that bank materials at Mamauk are of the same size as material found along the lower reach of Sittaung river. Another investigation into the particle distribution curves was performed by Ahmed et al. (Ahmed et al., Ahmed et al.), see figure 3.7. Here the difference between the bed materials and bank materials was visualized. Which of itself showed not that great of a difference. What did strike as an interesting result was the difference between the particle size of the lower and upper part of the bank. The upper part of the banks have a constant composition of smaller particles. Even up to levels of more than 50% mud concentrations. It could further be deduced from the available particle size data that the average size was around 200 μm and that there was at least a partial fraction of cohesive sediments ranging up to a significant fraction.

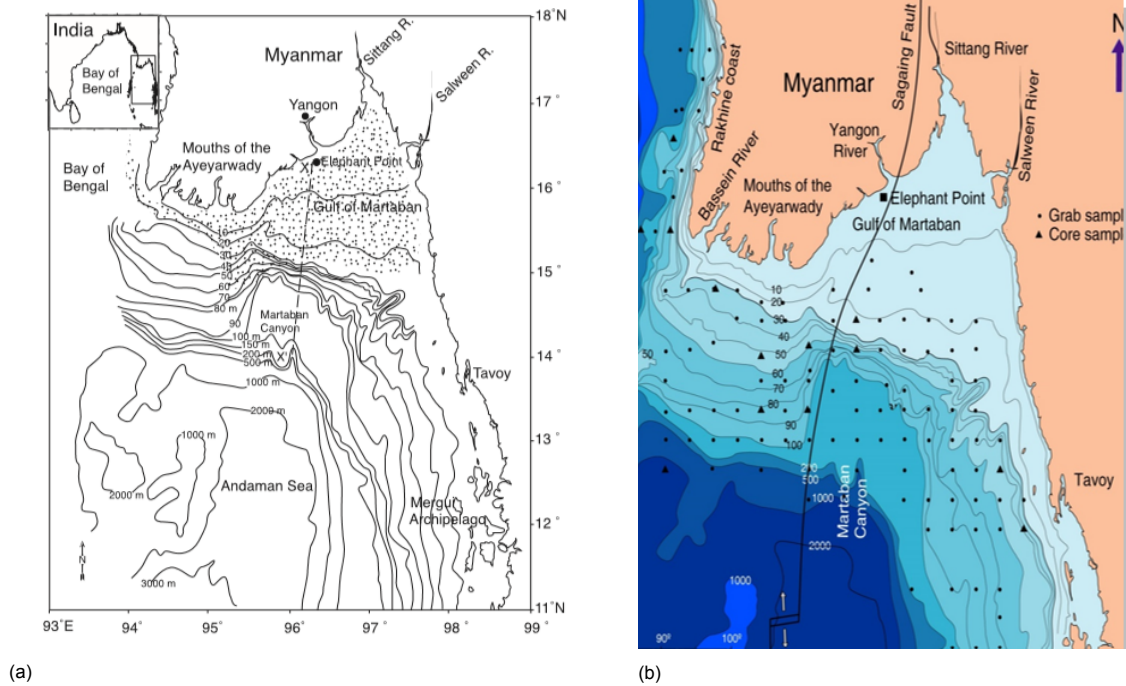


Figure 3.6: "Bathymetric map of the northern Andaman Sea and Gulf of Martaban. Contour values are in meters. Stippled area (a) denotes area occupied by modern mud's (sand <20%)." (Ramaswamy et al., 2004)

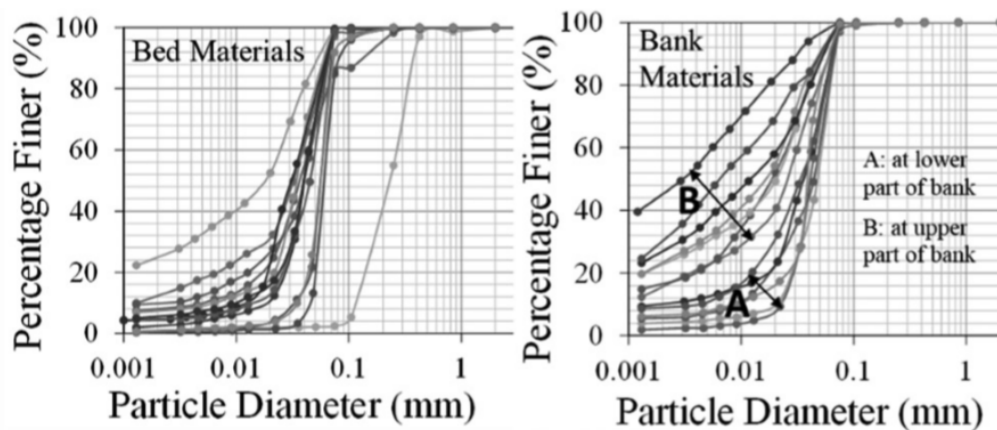


Figure 3.7: Particle diameter distribution for bed and bank samples in the estuary. From a field survey by (Ahmed et al., 2018). It shows the particle size distributions of sediment collected in beds and banks, in which sediment sizes of the estuary's sediment are shown. Silt and clay particles are dominant in the upper bank material according to the results illustrated

3.5. Resulting intended field measurement campaign

A key element in the understanding of the coastal dynamics, through the analysis of existing data sets, is the use of numerical modeling and by performing field measurements. The field measurements would have been used to test hypotheses and to gain extra qualitative information to potentially calibrate the model. They were created to focus on the key parameters for the understanding and modelling of the estuary and encompasses sediment-bed composition and incoming tide characteristics. See the outtake of the original plan in the appendix F, also the locations where measurements would have taken place are visible in figure F.1. In an abbreviated form the measurement intent is here presented.

Unfortunately there were developments concerning the current global pandemic in Myanmar impeding the save and responsible execution of the field measurements. The sudden surge in the number of infections resulted in a strict new resolution of lockdown and travel restrictions. These were announced just as the planning and preparations had come to fruition. All involved found the well being of the

researchers and staff most important and were convinced that it would be responsible to postpone the field measurements. Not being possible to execute within the range of the current research the field measurements can be submitted as recommendations and if there remains an interest even be performed when conditions allow. The campaign, partly or in its entire proposed form, can be carried out as part of a new research or as part of the Yangon Technical University research activity.

Wavedroid and hand drill measurements

Because of the dynamic position of the tidal channel and force of the incoming tidal wave. The options to measure the wave profile or water level are limited. The Wavedroid offers a very apt solution. Originally data collection on waves is often expensive, difficult and laboursome. WaveDroid offers an accurate, lightweight and low-cost solution: with a small motion sensor it measures wave speed, height and frequency. It is easy to install, provides real-time data and has GPS tracking to limit the risk of theft.

The relatively shallow channels in the Gulf of Mottama can either result from an overload in sediment caused by constant reworking of soil stored temporarily in land, or from the presence of erosion-resistant layers in the subsurface (like clay). The latter hypothesis can be investigated with a geological investigation of the top 10 meters of sediments by use of hand coring. The cores can be collected from land-sites (or the tidal flats) where in the recent past a tidal channel was located. The analysis of the cores should focus on the presence of erosion resistant materials in the deeper segments

Hypotheses concerned with the field measurement campaign

Hypotheses connected to the proposed and prepared measurement campaign concerned with the wave profile and soil sediment distributions

1. **The contribution of the wave profile to the bank erosion is insubstantial;**
 - *Test: Examine the wave profile with the help of the WaveDroid.*
 - *Expected: Wind driven wave profile is low and has no influence on the erosion.*
2. **In the wake of the tidal wave arrival the wave profile will increase for a limited time ;**
 - Test: Examine the wave profile with the help of the WaveDroid around the tidal wave arrival.*
 - *Expected: The waves will increase substantially for a short period.*
3. **The subsoil of estuary is comprised of an erosion resistant layer ;**
 - *Test: Examine the subsoil of the abandoned bank to see if there is an erosion resistant layer. Sediment samples and core drilling into the subsoil.*
 - *Expected: Around and below 8 meters an erosion resistant layer is expected / sediment with a lot of clay.*
4. **Sediment distribution of the newly deposited material ;**
 - *Test: Gather sediment samples and analyze the composition of the sediment that is actively accretion in the estuary.*
 - *Expected: Sediment distribution is in the range of the previously gathered sediment samples with small difference. Newly gained information on the distribution will be used to validate the model choices.*

4

Satellite analysis of morphological trends in the Sittaung estuary

This chapter presents the satellite analyses that have been performed on the system. From the information that is gathered several maps have been created to give an accessible view of the developments. Images clearly display the position and development of the tidal channels, the tidal flats and bank erosion. Relevant data from existing satellite analysis has also been reported here. First the historic evolution of the system is presented. After which the general implications of the previous studies are evaluated. After this the analyses aimed to investigating the hypotheses are elaborated on. This chapter has build on the progress made in the previous chapter where the system and its previous studies have been analysed.

4.1. Bank erosion trends at multiple positions

Flow velocities will increase at distinct locations which aggravates the erosion. A funnel effect resulting from gulf geometry and the cross section gradients directs the tidal bore and increases flow velocity. The rates of shoreline erosion in the northern part of estuary, see figure 4.1 and B.7, have been less severe than the changes in the south, see figure 4.3. The rates have been calculated and presented in table 4.1. But because the direction of the erosion has been the same for the pas 40 years, changes of the trend in this region may come as a bigger surprise than the changes in the south.

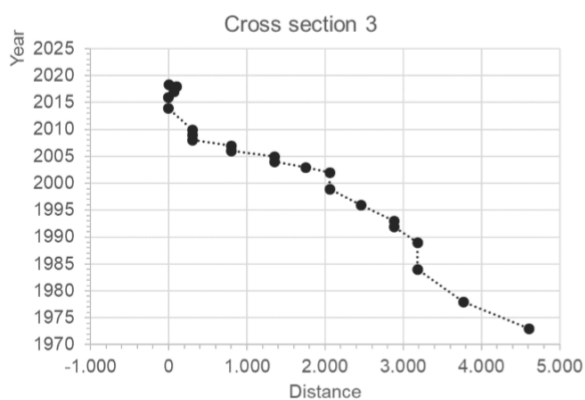
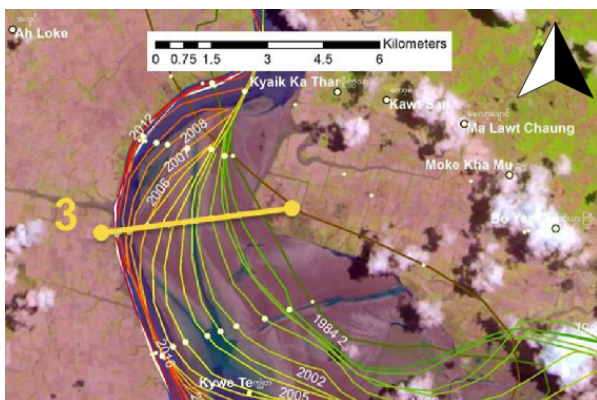


Figure 4.1: Bank position lines over the past years indicating a gradual erosion trend towards the west, gathered from (Arcadis, 2018)
Figure 4.2: Cross section erosion data of the bank position lines through the years. Cross section 3 indicated at 4.1, gathered from (Arcadis, 2018)

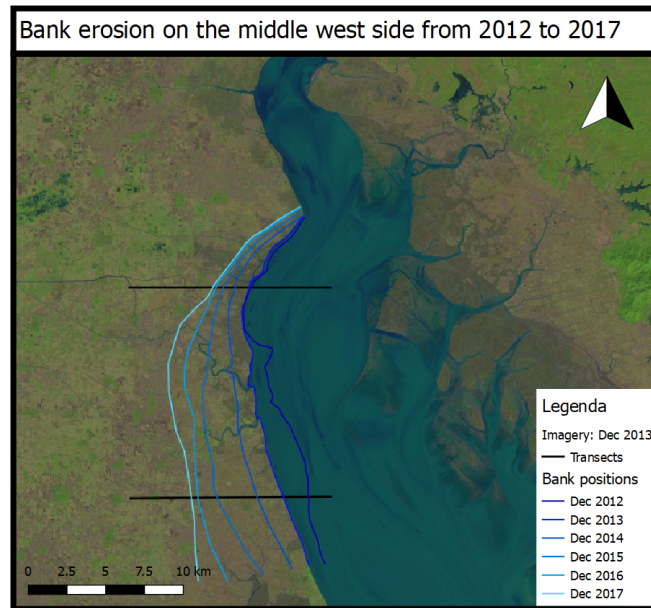


Figure 4.3: Map of the Sittaung estuary showing the erosion of the middle west bank. The lines indicate the position of the channel bank from 2012 till 2017. A clear erosion trend can be discerned. The upper transect showed a lot less erosion than the lower transect. The rates have been calculated and presented in table 4.1.

Period	'12 - '13	'13 - '14	'14 - '15	'15 - '16	'16 - '17
Upper transect bank erosion (m)	100	900	750	500	200
Lower transect bank erosion (m)	1600	1700	2600	1200	400

Table 4.1: Erosion rates of the middle west side of the estuary from 2012 to 2017 for two transects. The lower transect has seen considerably more erosion than the upper transect.

4.1.1. Erosion in area 1

The observed rates of coastal erosion have been derived from the position of the channel bank on a transect perpendicular to the shoreline and the direction of the migration. Observed rates of erosion can be used as an indicator to the speed at which bank erosion might occur in the future, but should not be regarded as a forecast. Transect 3 in figure 4.1 showed a steady, almost continuous, retreat of the shoreline. The last four years the position of the shoreline has been stable (Arcadis, 2018). The most extreme part of that development has been the cut-off and avulsion of the channel meanders in 2002, which can be seen in figure B.9.

4.1.2. Erosion in area 2

Characteristic for area 2 has been that the erosion position shifts more rapidly. The direction relates to the evolution of the meander bend and the direction of the flow entry. Why exactly this direction has been changing so frequently is difficult to answer. It is related to the rate at which the banks erode in this area. The evolution during the last decade showed that the area where most of the migration occurs can shift and this determines where exactly the erosion will be most intense. The cyclic trend has an observed phase of around 15 years. Recently the direction of migration has shifted towards the east and this is expected to continue in the coming years, see figure 4.4.

4.1.3. Erosion rates

The recent west bank erosion rates have been high and consistent. Up until the forming of the new main tidal channel the bank has eroded here steadily towards the west. The map in figure 4.3 shows the bank lines for the years from 2012 up until 2017. The distances between the lines have been measured at the transect and can be read in table 4.1. What is striking is the large difference of erosion distances between the upper and lower transect.

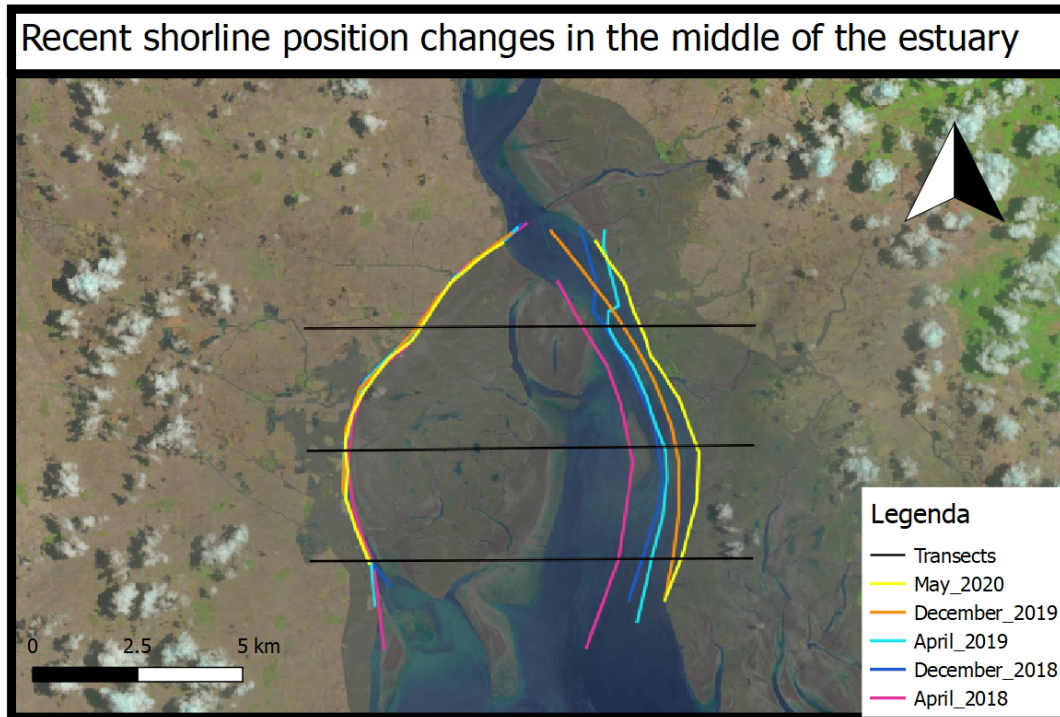


Figure 4.4: Map of the recent shoreline position changes and transect erosion rates in the region of the estuary indicated as area 2. The distances between the lines that have been measured at the transects can be read in table 4.2 and B.1.

After the new main channel has formed, a rapid change in the location where the bank erosion takes place has taken place. The map in figure 4.4 shows the most recent shoreline position changes in the middle of the estuary. Here it is clearly visible that the erosion at the west bank has halted and the estuary has started eroding at the east side. Three transects have been analysed and they all show heavy erosion at the east bank, both at the upper transects and lower transects. The remaining dissimilarity with the recent west bank erosion could be because of the difference in shape and position of the bends. The table of B.1 shows the values that have resulted from analyzing the transect erosion rates. It shows that there has been but very little correlation between the wet season and the bank erosion rate. The heavy increase in discharge due to the monsoon season has been a factor that was expected to cause a stronger correlation.

Figure 4.2 shows a graph of the bank erosion at the upper west side of the estuary from 1973 to 2018. An average retreat of 120 meter per year has taken place over this period. Figure B.4 and the accompanying chart B.5 show the same data for the transect a bit more downstream. Here the bank erosion has happened at the outer bend of the channel initially. The erosion rate has been larger with an average of around 200 meter per year. But the bank has been almost stagnant for the last decade. Erosive flow is directed to the outside lower bends of the estuary making these locations more prone to rapid bank erosion.

Figure B.6 shows the bank erosion rates at the middle west side of the estuary for the year 2016 and a part of 2017. Erosion rates have been extracted from radar imagery in a study by Shimozono (Shimozono et al., 2019). It shows the highest erosion rates for this period near the village of Mamauk at the lower part of the bend. Incidental erosion rates have been observed here of up to 3300 meter in a year.

4.2. Tidal channel formation

Recent developments in the southern part of the estuary have shown the formation of a tidal channel located towards the center of the estuary. This channel has rapidly taken over the role of the main and migrating channel previously located along the western bank. Figure 4.5 shows the most recent

Period	4 - '18 / 12 - '18	12 - '18 / 2 - '19	4 - '19 / 12 - '19	12 - '19 / 5 - '20
Upper transect eastern bank erosion (m)	1000	150	750	800
Middle transect eastern bank erosion (m)	1350	300	550	1000
Lower transect eastern bank erosion (m)	1100	500	1000	400

Table 4.2: Erosion rates of the middle of the estuary east bank after the formation of the new middle tidal channel from 2018 to the start of 2020 for three transects. The west bank of the estuary clearly shows a stop in the erosion trend. The erosive behaviour has been transferred to the east bank.

incident of such formation of a new tidal channel over a period of almost 2 years. Most satellite images have been selected for a situation where the estuary is under ebb flow. This way the water indicates the locations and distribution of the channels better. The location of the channels has been the point of interest in this analysis. Because in the flood flow situation the mudflats were covered with water as well which makes it more difficult to distinguish the channels.

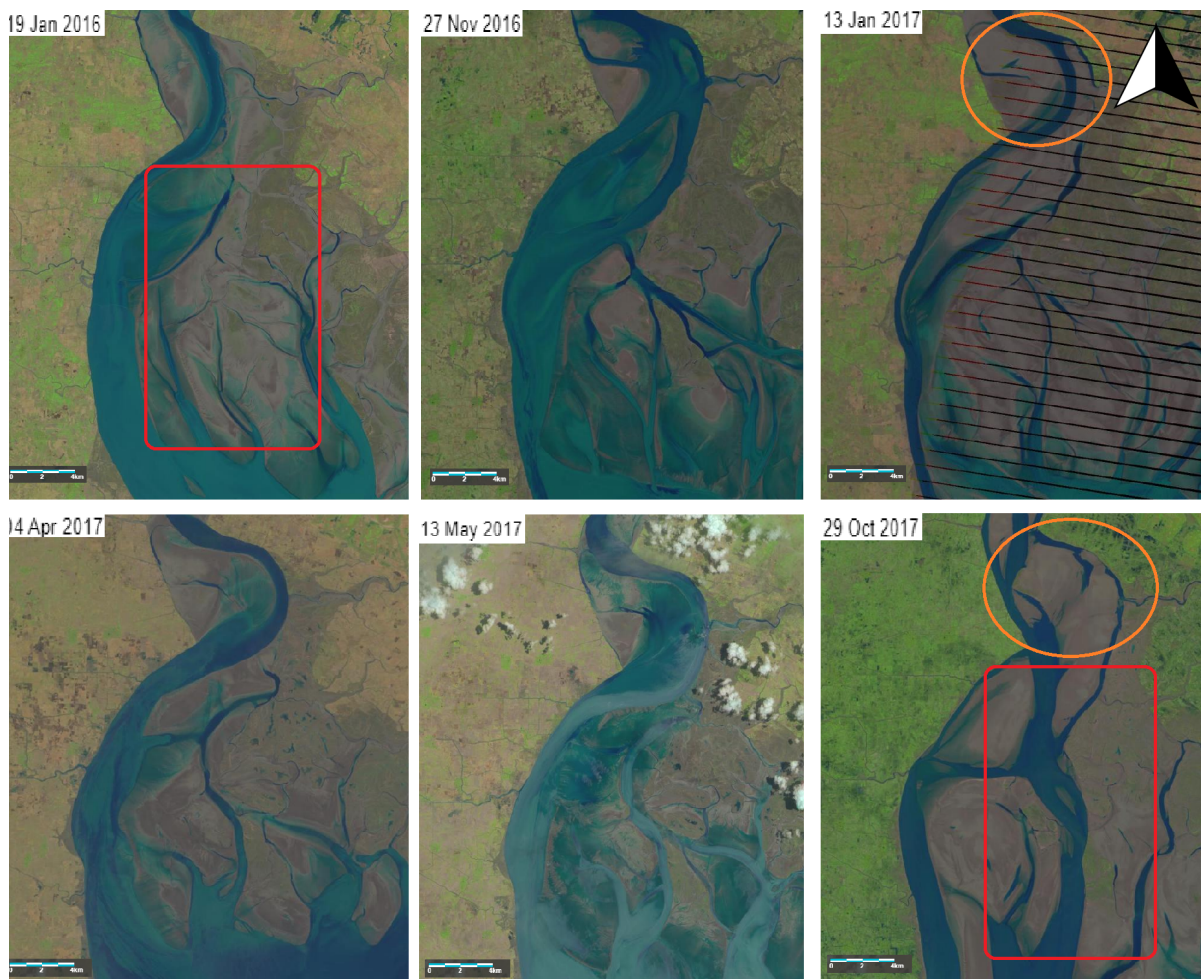


Figure 4.5: Formation of the tidal channel overview. Sequential satellite imagery showing the emergence and evolution of the tidal channel in the new middle main tidal channel in the upper part of the estuary. Red area indicating the channel position and the orange area is the upstream region of influence on the direction of the flow

In the summer monsoon around 80% of the annual rainfall precipitates. It starts at the end of May and ceases in October. The data from January 2017 shows that the ebb discharge of the river flows along the meander outer band and streams towards the west bank. In January the river discharge is low and cannot surpass the threshold necessary to propagate into the mud flat. River discharge has had a strong impact on the formation of the channel. This has been validated by the configuration of the tidal channel after the monsoon, when satellite data yield a sufficient view again. On the mudflats there have emerged flow paths and small channels because of the water that flows there during flood flows.

During flood flow the river discharge flowed along an altered path positioned more over the mud flat. In the image of April 2017 this is clearly visible, the flow was directed with a meander towards the west. After the high river discharges of the monsoon season this bend has been abandoned and the main stream flows straight into the downstream estuary. This entry connected well with the main tidal channel of the rest of the estuary.

4.2.1. River entry configuration effects

The characteristics of the riverine discharge entry into the estuary were likely to have an effect on the tidal channel development, orange area in figure 4.5. Downstream of this point the dynamic activity increases rapidly. Development of the tidal channels, the direction and duration of the migration and the associated bank erosion are dependent on the configuration of this point. The location just before this point has been deemed to function as a hinge point. Migration direction and boundary situations have been relatively stable for around 40 years 4.1. Recently the situation has been changing atypically 4.6. The direction that the discharge flow is guided on and the flow velocity at this location, close to the actual river mouth, influence the development of the rest of the estuary. Just as it determines where the new tidal channel forms. Over the period of channel migration cycle this also influences the duration of the cycle.

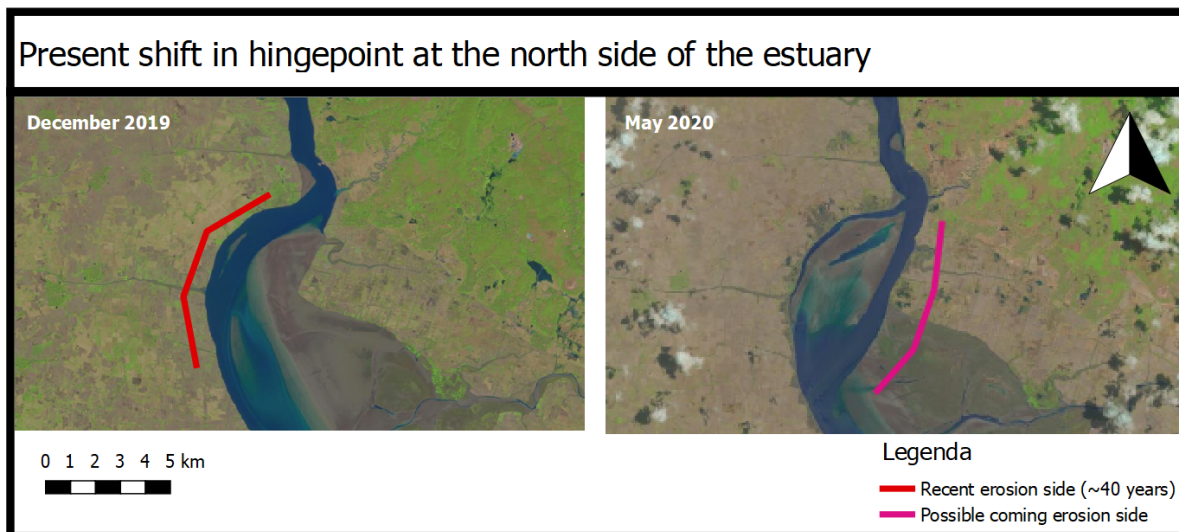


Figure 4.6: A map indicating the present changes that have happened at the upper part of the estuary. In previous years the outer bend was directed to the west. Recent development has seen the main flow direction shift to the east. This has possible implications for the erosion of the bank and subsequently the tidal channel further downstream of the estuary.

The present developments at the upstream part of the estuary have been interpreted as a break in the trend. The position of the channel curves seem to have shifted to the south, see the map in figure 4.6. Those positions have been relatively stable in the north for the last 40 years, figure 4.1, and are considered as hinge point. Currently in the north the sandbar only pushes the remnant of the channel close to the west bank.

Figure B.9 shows satellite imagery with the location of the meander cut-off indicated with arrows as presented in (Arcadis, 2018). It indicates the volatile and dynamic behaviour starting downstream of the estuary entry point. This showed that the configuration of this area can be subject to large and fast changes. During the wet season of 2002, over a period of 6 months the two meanders have connected through the land mass that separated the two. The entire area then turned in a west facing meander. The area indicated in orange in figure 4.5 has shown that alterations of this area are linked to the way in which the tidal channel evolves.

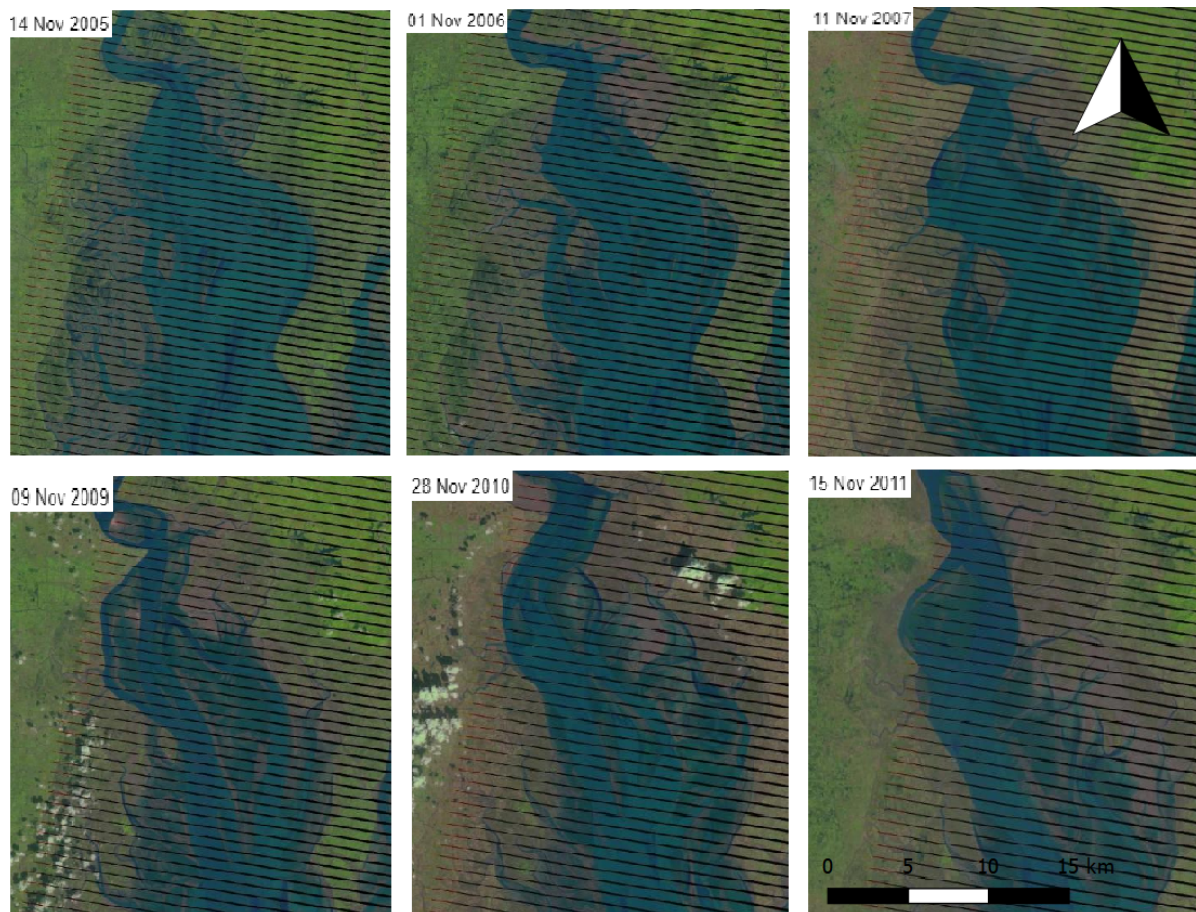


Figure 4.7: Overview of the estuary and development trends in the years before cyclone Nargis and the years after. There has been no obvious change visible in the direction of the migration or the location of the erosion. Trends that have been initiated before the storm remain present after.

4.3. Incidental large storm effects

From the literature there came forth a possible effect of cyclones on the morphology of the estuary. Through the force and water levels that have been connected to the arrival of a large storm on the tidal migration direction. The phenomenon has been active on an event scale. But the possible effects should have influenced trends spanning several years. Cyclone Nargis made landfall with sustained winds of 130 mph and gusts of 150-160 mph, which is the equivalent of a strong Category 3 or minimal Category 4 hurricane. It was an extremely destructive tropical storm, that send a surge 40 kilometres up the densely populated Irrawaddy delta, see figure B.8. The cyclone made landfall in Myanmar on Friday, 2 May 2008.

4.3.1. Pre & post storm channel migration trend

Satellite imagery has shown that from 1995 onward the channel has migrated to the east side of the estuary. This migration halted in 2007, see figure 4.7. From this time the direction of the channel migration would turn to the west. In 2008 the area was hit by cyclone Nargis. Next migration cycle continues in 2008 and seems to hit an end at 2018. The cyclone hit the system right after the turning point in the cycle for this segment of the estuary. The duration of the migration cycle in which the storm was active can be considered as below average. Continuation of the trends and location of the erosion have continued despite the storm, seen in figure 4.7. It might be that the trend has been slightly aggravated because of the storm. But the configuration and location of the tidal channels and erosion positions has evolved in the same before the storm and after. This indicates no significant contribution of the storm event to the dynamic behaviour of the estuary.

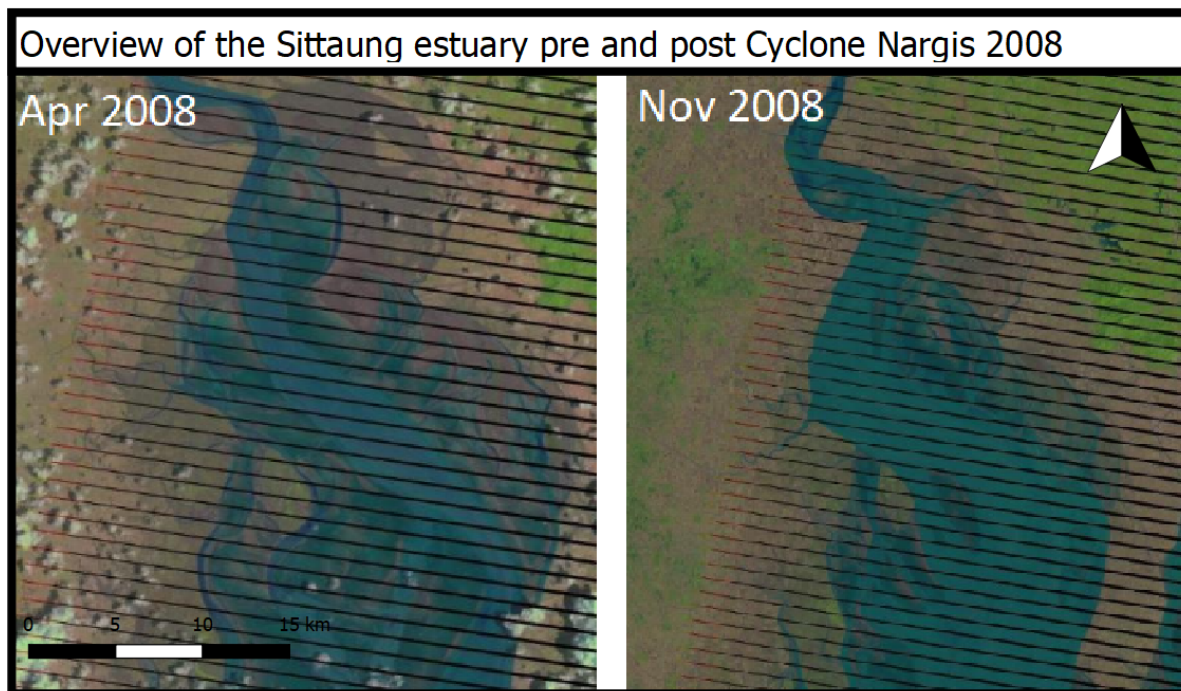


Figure 4.8: Map of the Sittaung estuary situation pre and post the cyclone Nargis Event in 2008. The imagery of April 2008 is from a low tide, this makes the channel positions well visible. The November imagery is during high tide. There is no large redistribution of channels or bank positions. But the migration trend present at the time is continued.

4.4. Recap of the results from the satellite analysis

Specific rates of erosion and values for the latest bank line retreat have been recovered in the satellite analysis. In the conclusions the important findings and observations are presented. Implications and further inquiry which these conclusions might yield are covered in the following part of the research. The discussion will touch upon the agreement of the analysis with the hypotheses and preconceived notions. It will also discuss the expectations for the near future and the interesting points to consider.

Bank erosion

- High rates of bank erosion in the middle of the estuary where the migration of the tidal channel is active.
- Bank erosion at the middle of the estuary has been much more rapid than erosion at the upper part of the estuary.
- Erosion of the channel bank has been considerably higher in the lower outer bends. This has been the case in both the upstream and downstream positions.
- Erosion of the west bank has halted soon after the new main tidal channel has formed.
- Current migration cycle has moved towards the east with erosion rates similar to the recent west bank observed erosion.
- Erosion has happened more at the locations where there are mudflats and larger visible difference in water area between ebb and flood.

Tidal channel formation

- The monsoon period brings forth high river discharge and has had a sizeable effect on the formation of the tidal channel.
- Upstream configuration of the entry location has been connected to the direction of the stream flow and formation of the channel.

- Small channels have emerged and evolved on the mudflat. Seemingly contributing to the channel formation.
- Flood river discharge under certain conditions flowed along a different path and eroded parts of the mudflat.
- A formerly stable point upstream of the river entry location has recently been changing.

Large storm

- Cyclone Nargis arrived at the estuary shortly after a change in the direction of the tidal channel migration cycle.
- There have been no distinct changes in the configuration of channels and banks after the storms arrival.
- Channel migration cycle has not been obstructed by the storm. The cycle continued with a pace near average for the channel migration.

5

Modelling simulations of the physical system

5.1. Simulations of hydrodynamic differences

This chapter presents the results of model simulations of the physical system with current and altered configurations. Two hypotheses have been handled in a more straightforward manner. Supplemented by the analysis of the large-scale sediment transport of the estuary.

There has been an observed difference in relative importance between geomorphic processes. Extreme events or more frequent events with a smaller magnitude are assessed by the amount of bank deformation they effectuate (Wolman and Miller, 1960). In most rivers the bankfull stage seems to have most effect on the channel shape and dimensions. This stage occurs generally more often. The relative importance of flows can be evaluated based on the quantity of sediment transported by each flow. When the quantity of sediment and frequency of flow are known, the percentage of total transported material for the significant flows is known (Wolman and Miller, 1960). A lot of the time it is not the more catastrophic or large storm events that have a critical impact but rather the more frequent reasonably high water levels which have more geomorphic effect. This has also come forth clearly in the simulations and satellite analysis.

5.1.1. Tidal forcing and river discharge

Simulations have been created and performed in this section to investigate the relation between flow velocity and erosion at different cross sections and orientations. The erosion of the upper estuary banks, as indicated in figure B.4, in relation to the erosion of the banks in the middle of the estuary. The values of which were calculated and shown in figure 4.4. The cross sections have been positioned in such a way that there is a continuous and representative flow pattern, see figure 5.1. The difference of these positions has been examined to study the difference between erosion due to discharge forcing and due to tidal forcing. In the upper area the tidal forcing is less intense and the discharge is more heavily present. As can be seen in the difference between the water level amplitudes in these positions, see figure 5.2. The expectations were for the tidal forcing to play a stronger role in the erosion process. Interesting has been to see to what degree the tidal flows increased intensity can account for the difference in erosion. What was expected was that it would not be responsible for the complete erosion difference. What is still unaccounted for is how much this will influence the erosion is still to be investigated. The lack of evidence or results indicated the workings of unrepresented mechanisms. Model simulations have been performed to specifically outline the connection between these mechanisms and the erosive capacity.

Monsoon season high river discharges

With high river discharge the continuous flow velocity becomes larger throughout the estuary. This is in line with what the amplitude and bore arrival showed in figure 5.2. The velocity profiles of the simulations for the wet season at the upper cross section can be seen in figures 5.3 and 5.4. In the

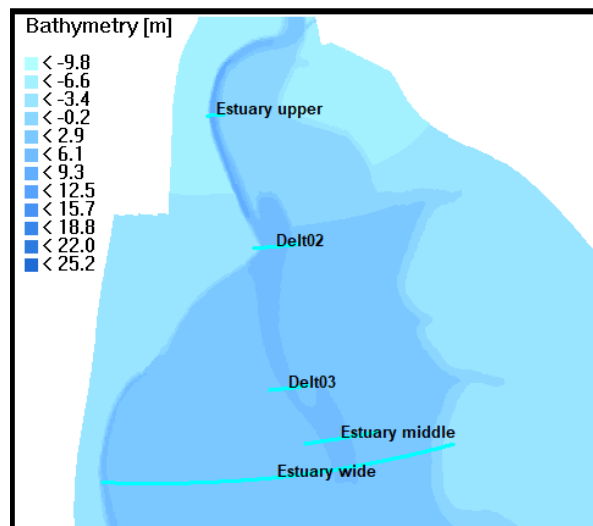


Figure 5.1: Observation cross sections for erosion capability analysis of different hydrodynamic modifications.

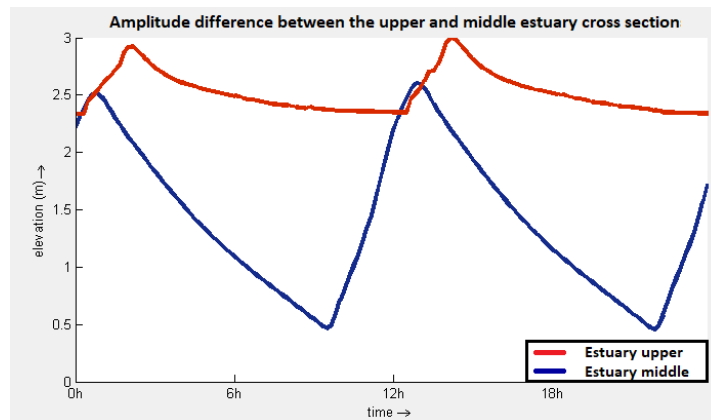


Figure 5.2: Amplitude difference between the cross section in the middle of the estuary and higher up towards the river. The figure has been created from the 29th of August of the model simulation where the largest amplitude of the tidal signal is active.

upper estuary the simulations showed a southward directed flow for almost the entire time between the high tide arrivals, which was around noon and midnight. The flow velocities were high in this case of up to 2 m/s . Which can be related partly to the narrow width of the cross section. In the right plot of figure 5.3 the accompanying bed load transport is shown. This correlated well with the flow velocity profile. Bed load transport has been almost continuous throughout the day except for the time of the tidal water arrival. Following the flow direction, the transport was directed here towards the south. Except for the times of high tide at which time there was little to no transport. This was for short periods around noon and midnight.

Comparing this with the results of the middle estuary cross section an entirely different, almost opposite, picture arises. Figure 5.4 shows the velocity and bed load transport profiles for the middle estuary cross section during a wet season simulation. Here the majority of the time the flow was directed southward but at a relatively low speed. Which can be ascribed again to the channel geometries. It become interesting during the arrival of the tidal high water. Here the flow direction reversed and the velocity increased significantly. Looking at the bed load transport profile this induced transport only at a short period during the tidal cycle. This is very a distinct difference between the two cross sections which was driven by the incoming tide and the increases of flow intensity. The erosion at these cross sections would influenced accordingly. For the middle cross section a short period but with much more intense efforts.

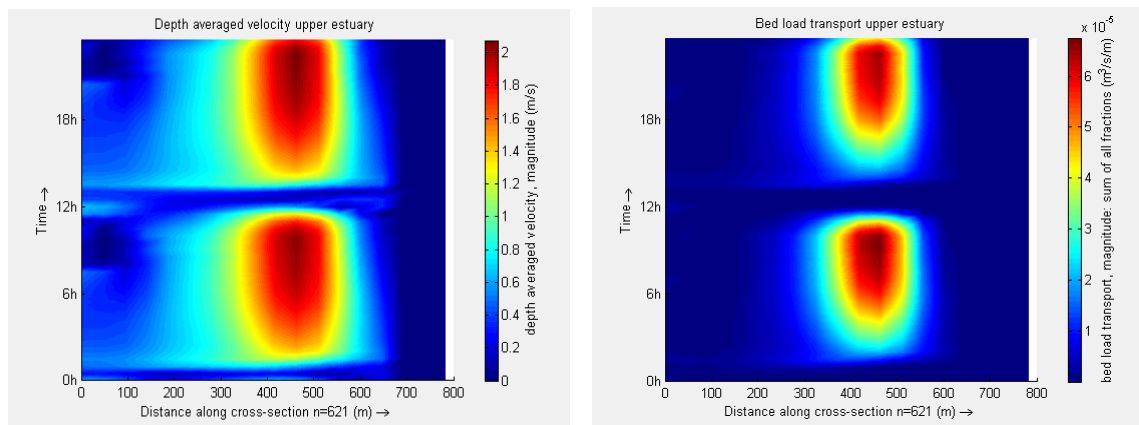


Figure 5.3: Upper estuary cross section plots of the velocity profile and the bed load transport of the wet season discharge configuration.

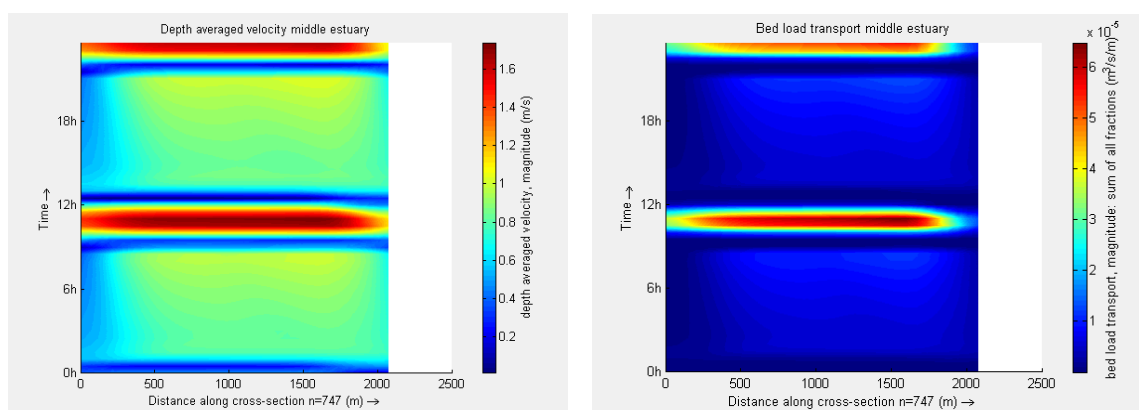


Figure 5.4: Middle estuary cross section plots of the velocity profile and the bed load transport of the wet season discharge configuration.

Dry season low river discharges

A different model has been created to simulate a dry season configuration with low river discharge which yields interesting results. In figures 5.5 and 5.6 the plots of the different cross sections can be seen. Because of less discharge the flow velocity in mainly the upper cross section has reduced significantly in relation to the wet season. Bed load transport at previous levels remained the same only during the period just before the arrival of the tidal bore.

In the middle of the estuary the flow velocity has been impacted by the reduced discharge as well. But the effect was present in a more dissipated way. The high water front seems to have arrived spread out over time more and continued to yield higher flow velocities for a longer period. Though the maximum flow velocity was lower, there was no obvious clarification at hand. What is evident from the transport profile is that the transport values were considerably higher than the orientation with the high river discharge. Not only with higher values but also occurring for a longer time during the high tide. This second features influence does not in itself have to command more erosion if one considers the transport capacity of the upper cross section which also has the same tendency.

A similar profile to the bed load transport profiles can be discerned from suspended transport of the cross sections. Shown in figure E.2 are the suspended sediment transport profiles for the wet season discharge. The same distribution was produced but with significantly higher values because of the way suspended sediments are transported and relating to the flow velocity.

5.2. Simulations of incidental large storm events

Incidental large storms can have a significant influence on estuary development and morphological trends, see section 1.6.2. As storm events have shown no influence on the bank erosion directly or

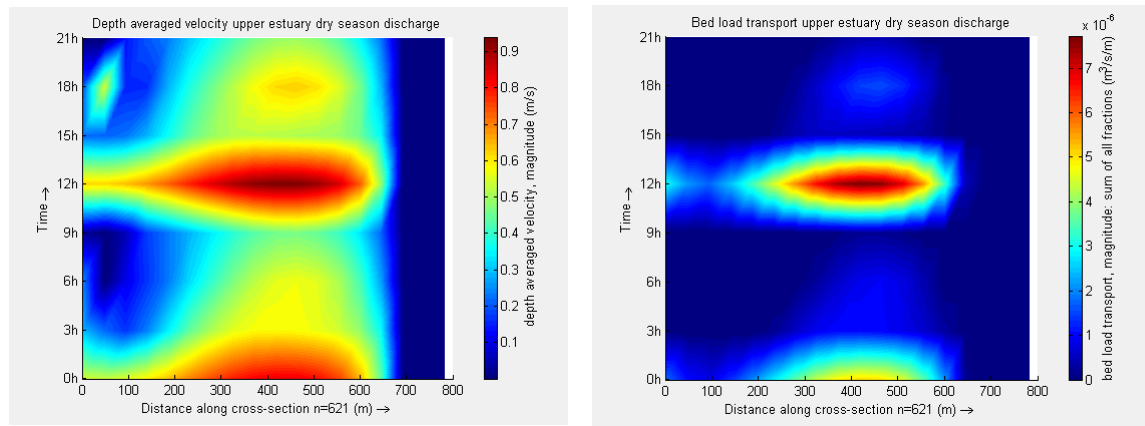


Figure 5.5: Upper estuary cross section plots of the velocity profile and the bed load transport of the dry season configuration.

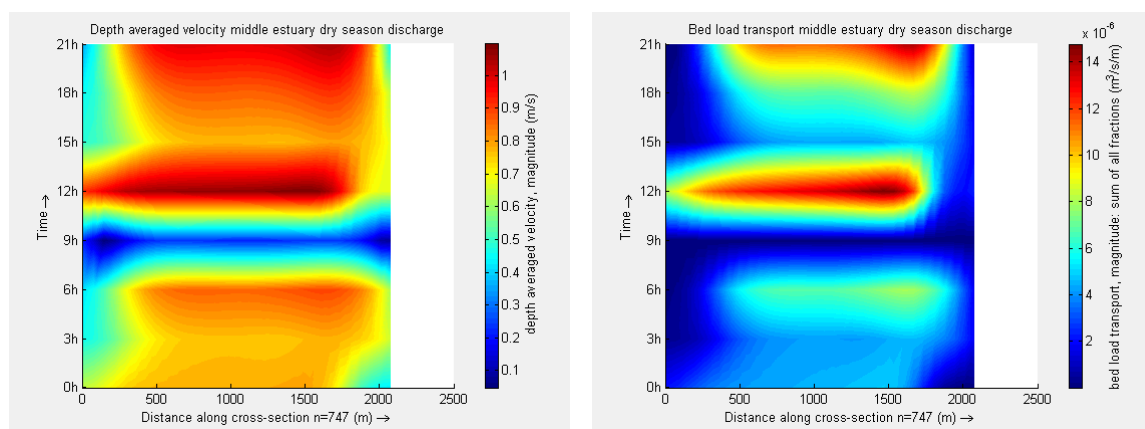


Figure 5.6: Middle estuary cross section plots of the velocity profile and the bed load transport of the dry season configuration.

the trend of the erosion. The simulations have tried to substantiate these observations. The satellite observations have shown that there is no clear increase in erosion rates from dry season to monsoon season, see section 4.3. It has been interesting to look at the differences in simulated orientations. The effect of the large storms could probably become an issue towards the end of a migration cycle. This is the period when the small channels on the mudflat connect, as seen in figure 4.5. The high water levels and discharge because of the heavy rain can speed up this process. Interesting to see was the difference in erosion caused by these heightened levels as opposed to general high water discharge. Besides the general increases of flow velocity the distribution of the flow over the entire width of the estuary was also of interest here. The model was altered to produce simulations that looked at the effects of the increase in discharge due to the massive precipitations increase during the large storm event. Gusts of wind can cause very high incidental local flow velocity which was not considered here. Data from the 2008 cyclone indicated a large increase in river discharge and water levels throughout the entire gulf. Three time average wet seasons levels have been employed in the simulations.

Figure 5.7 shows the velocity profile of the focused cross sections during a high storm discharge. In comparing these values with the images of 5.4 there were no large increases of values. In the main channels of the upper and middle estuary the maximum flow velocities did not increase. So there was no added transport and erosion capacity resulting from the increased discharges apparent from the simulations. What did result from the increased flows were the wet perimeter and effective cross section. The water reached onto the mudflats in large amounts, see figure E.5. This caused an increased flow and formation of the small channels which in turn promotes the eventual formation of a new tidal main channel.

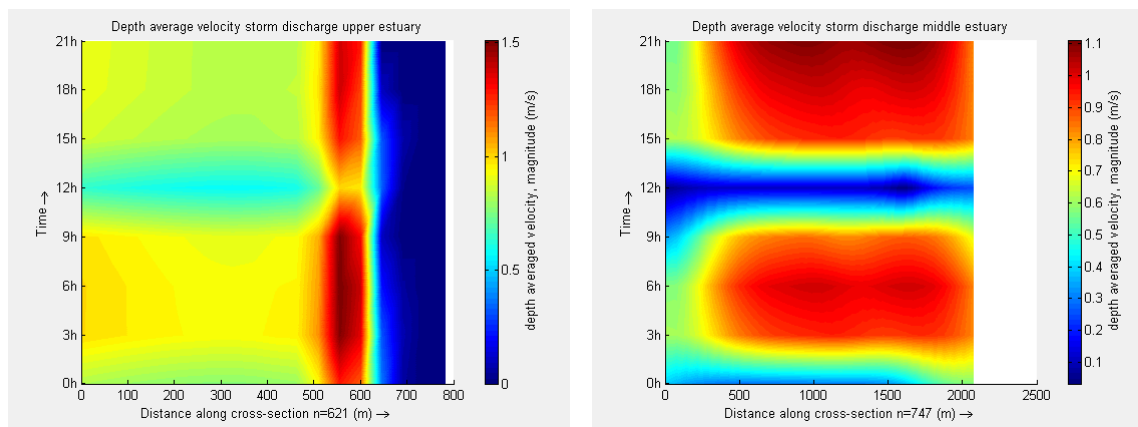


Figure 5.7: Upper and middle estuary cross section plots of the velocity profile during a large storm event discharge configuration.

5.3. Simulations of large-scale sediment transport

The changes in hydrodynamics effect morphological processes immediately, the actual changes in bed topography due to morphological effects take time. Sediment needs to be redistributed by the flowing water which takes time. There exists a lag in the morphological response to the hydrodynamic properties. Due to the dynamic properties of the hydrodynamics this may very well mean that the bed level topography and bank positions never reach an equilibrium. The resultant flow of the estuary is southward towards the sea, which is clear because there is no growing retention. Yet it could still be that the estuary is annually flood-dominated. This can be caused by the fact that the incoming tidal wave has a short duration coming with high flow velocities, while the ebb tide takes more time but has lower flow velocities and thus displaces sediment in a different manner.

5.3.1. Residual flow during spring tide

In order investigate the residual transport several main orientations have been simulated with the model. A full day was needed to calculate the residual flow with a small timescale of 10 minutes. Cases with a high and low river discharge were combined with a high and low incoming tide. Figure 5.8 shows the result of the residual flow for the spring tide situations with a high discharge and a low discharge. These produced mainly outbound residual flow in the main tidal channel for both cases but considerably lower outbound flow in the low discharge situation. Which is not surprising because if there is less water coming into the estuary through the tide the flow will be smaller.

The resulting flow in two directions caused the transport of large amounts of fines and sand throughout the estuary each tide. The difference between these sediment transports is called the residual sediment transport. Differences between these differently directed sediment transports resulted in a net import or export. The distribution of sediment will cause accretion and changes in the morphology. It was thus insightful to investigate the large-scale sediment import and export of the estuary.

5.3.2. Residual transport

What the plots of the simulations show, see figure 5.9, was that for high and low river discharge the residual transport of fine sediments was in the outward direction. The left of figure 5.9 is a plot of the calculated residual transport of fine sediments during the dry season. At locations where the discharge was less present, on the tidal flats for instance, upstream transport could occur. Parallel zones of downstream and upstream transport patterns were observed which indicated local sediment circulation areas. For fines a linear relation to the flow is applied resulting in m/s . For the sand fraction a third power relation has been applied, which resulted in a scale of m^3/s^3 . Denoted by the "n" in the model plots and figures.

While the fine sediments were shown to be transported outward the residual transport of sand was more influenced by river discharge. A residual bed load transport capacity was computed. For the low river discharge the result are shown in the left plot of figure 5.9. Striking was that almost the entire

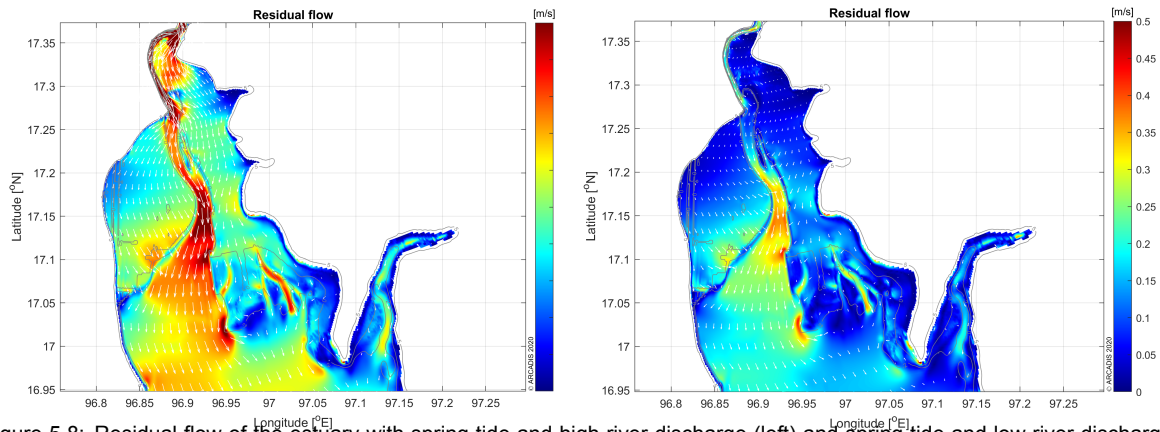


Figure 5.8: Residual flow of the estuary with spring tide and high river discharge (left) and spring tide and low river discharge (right). Mainly outbound residual flow in the main tidal channel for both cases but considerably lower outbound flow in the low discharge situation.

estuary experienced a northwards transport of the bedload sediment. This can cause an area where the sediment convergences in the upstream parts of the estuary. Such an phenomenon can occur in estuaries with sandy sediment profiles and is called a bedload convergence zone [14].

Figure 5.9 shows the residual transports of fines and sand for the case with a high river discharge and a spring tide. In this case there was even more export of fine sediments. Which is visible from the blue and dark blue shades of the figure and the outward arrows.

There were clear effects of the dry and wet season on the residual transports. The calculated residual transports points to large-scale and local redistribution of sediments. Erosion occurs at the main tidal channel and accretion on the mudflats. Which is consistent with the transport directions for sand and fine sediments that indicate that these areas display different morphological developments. The presence of adjacent upstream and downstream directed zones in the estuary indicates sediment circulation at the scale of the entire estuary, resulting in redistribution of sediment along the entire estuary.

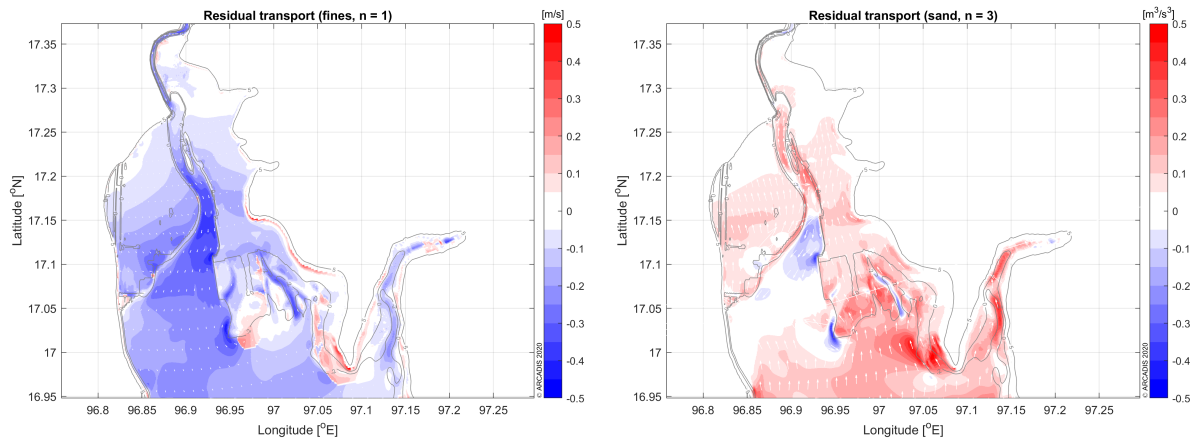


Figure 5.9: Residual transport of the estuary with spring tide and low river discharge. Determined for fines (left) and sand (right)

5.3.3. Main tidal channel contribution

It has been evident from examining the plotted results that the most transport has flown through the main tidal channel. This is also influenced most heavily by the distinction between high and low discharge cases because here the most flow occurred. A transect was examined at the height of the middle cross section in the previous simulations over the entire width of the estuary. Figure 5.10 and figure E.4 show the comparative results for the transect's bottom profile, the discharge and the potential transport. Here

the spring tide and high discharge situation were compared to the situations where there was the most difference. What was obvious was that the flow follows the bottom depth profile and that the transport was located at the position of the main tidal channel. There was a large increase of the low discharge situation in the potential transport, see the right plot of figure 5.10. Comparing this with the previous results it could be seen that at the location of the transect there was also an import of sediment. Over the mudflats, the area of the transect to the left of the main tidal channel, there was also an increase of the potential transport. Which can be ascribed to the increase in discharge over these areas from a small negative to around a neutral value. Having a total discharge of around zero while still showing an import potential transport indicates a mostly importing flow during the high incoming tide while flow is directed northward.

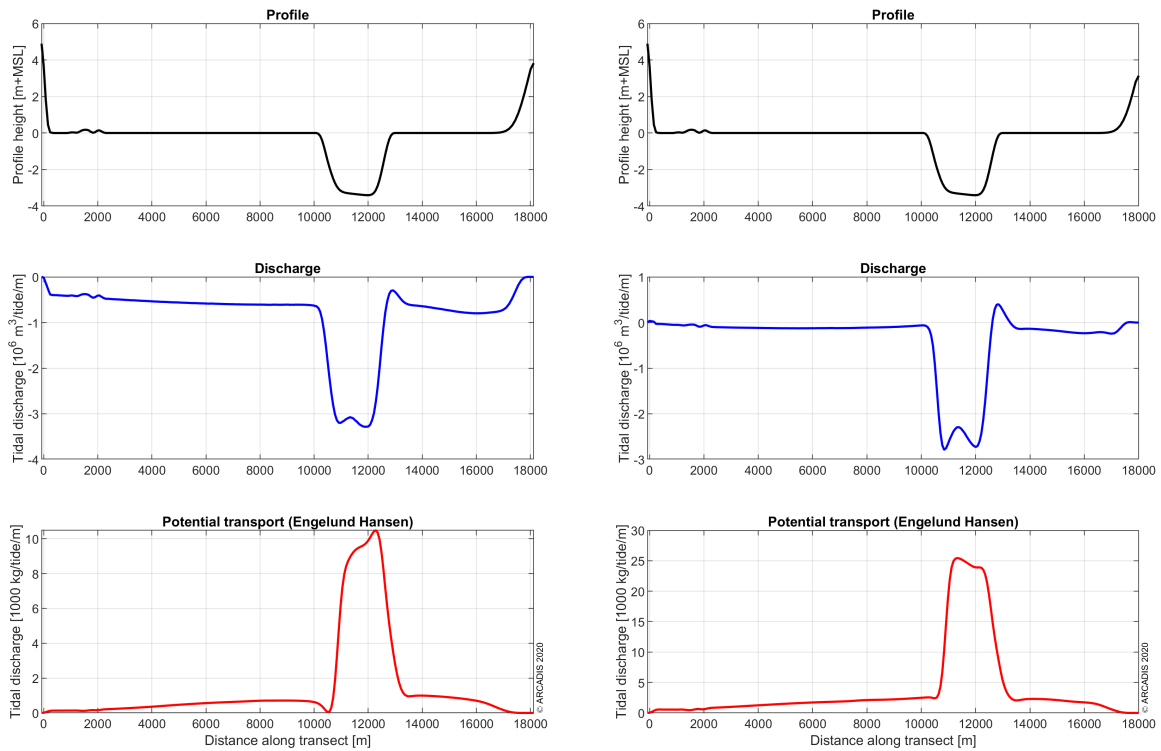


Figure 5.10: Cross section in the middle location of the estuary main tidal channel values for a high discharge spring tide orientation (left) and a low discharge spring tide (right). Above: profile height along transect. Middle: tidal discharge. Bottom: potential sand transport.

Modelling capabilities and limitations

Numerical modeling of long term channel formation in a submerged estuary environment has been researched in (Xie et al., 2009). While numerical modeling of a cross section bank erosion has been researched in (Stecca et al., 2017). Eventually, applying these numerical modeling approaches to a longitudinal stretch of estuary bank will further modelling potency. The orientation of the upstream channel and the effects on erosion have showed certain hindrances. But these have yielded interesting avenues of inquire with respect to the broader modeling capabilities which have been investigated in this chapter.

6.1. Simulations of cross section development

Initial model simulations showed a gentile move of the channel boundaries in the directions that were observed in the satellite analysis. Figure 6.2 shows the channels development in the direction that was expected based on the analyses. These runs were done with the improved settings for transverse bed slope factor and cohesive sediment fractions for an effective morphological period of 20 months. The qualitative representations were not near the correct values and also the bank at wet/dry interface did not necessarily show an eroded behaviour. Without attention to the channel incision effect the channels in the simulations would develop towards an unrealistic depth as can be seen in the results of figure 6.1. In order to check the response and evolution of the main tidal channel a long term simulation

has been designed. Figure 6.3 shows the result of an effective 25 year modelled period including a cohesive sediment fraction, a high transverse bed slope factor and a high morphological factor (50), for a high discharge situation. The results showed that this simulation has not produce a channel which continues to evolve towards the east. But rather a stop of the migration and a narrowing of the channel.

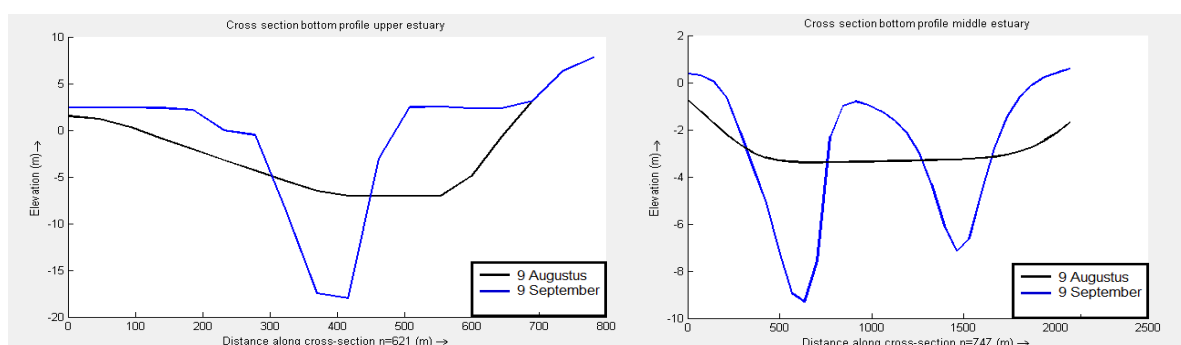


Figure 6.1: Development of the channel cross section at different estuary height with transverse bed slope factor 1.5

It was proposed to investigate how the model could be used to simulate long term bank erosion. This

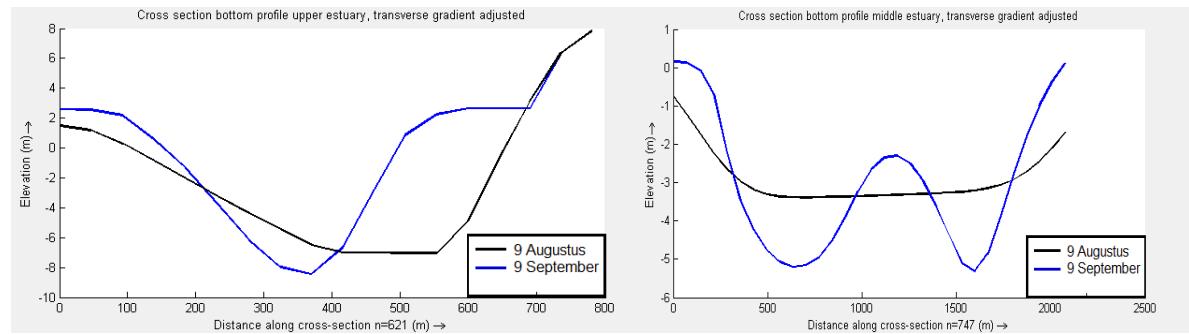


Figure 6.2: Effect on the channel cross section evolution's at different estuary height when increasing the transverse bed slope with a factor 100

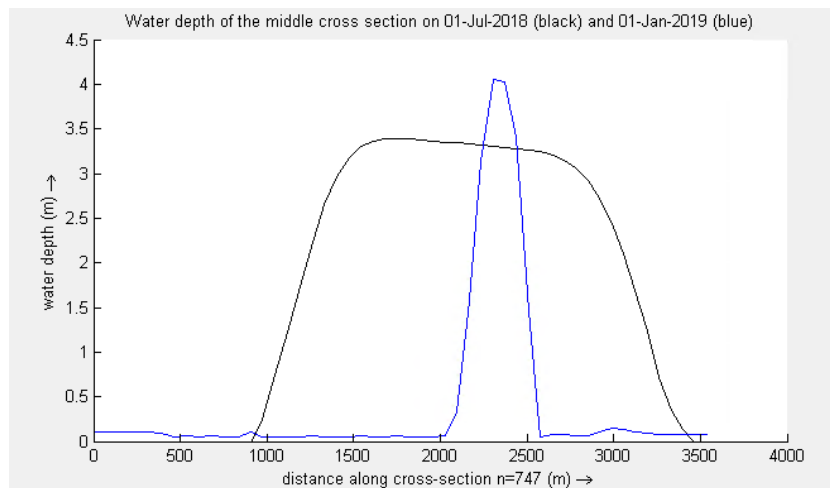


Figure 6.3: Water depth of the middle cross section on 01-Jul-2018 (black) and 01-Jan-2019 (blue). After a six month run time including a cohesive sediment fraction, a high transverse bed slope factor and a high morphological factor (50), for a high discharge situation. Producing an effective morphological time of 25 years.

has proven difficult to do achieve with the current model simulations. Because the exact representation of bank erosion in the model has been subject to some hindrances and it would require long term model simulations, in which particular mechanics might be under represented. It is found that the model simulations, even with all the advanced settings, had a difficult time representing the channel migration. The role of repeating high and low water level was expected to have a mitigating effect in this respect but it did not seem to do so. Steepness of the bank and more sedimentation at the mudflats were also important factors were reality was probably under represented in the simulations.

6.2. Chanel incision depth and transverse bed slope factor

Correct representation of the bed profile required extra attention. Channel incision levels occurred at to large a degree when left unattended, this can be seen in figure E.1. One way to stop the main tidal channel from cutting in to deep was to employ a dynamic depth into the model calculations. Another was to increase the transverse bed slope parameter to counter the incision effect. Starting with the introduction of a cohesive sediment fraction already had a significant impact on the incision capacity. Values that are presented in common literature are often to low for practical modeling. What can be seen when the transverse bed slope parameter was ascribed such values was that the channels formed at an increased rate. One way to alleviate this problem is to change the transport relation. Instead of the standard "van Rijn 93" relation, which is a bed and suspended load relation, the "Engelund-Hansen" relation, which is a total load relation, could be used. Models with the 'Van Rijn' transport predictor often have much steeper slopes and deeper channels than ones that use "Engelund-Hansen" (Baar, 2019). This has been investigated with model simulations but the differences remained small. The standard relation was considered the best applicable because it best corresponded to the processes

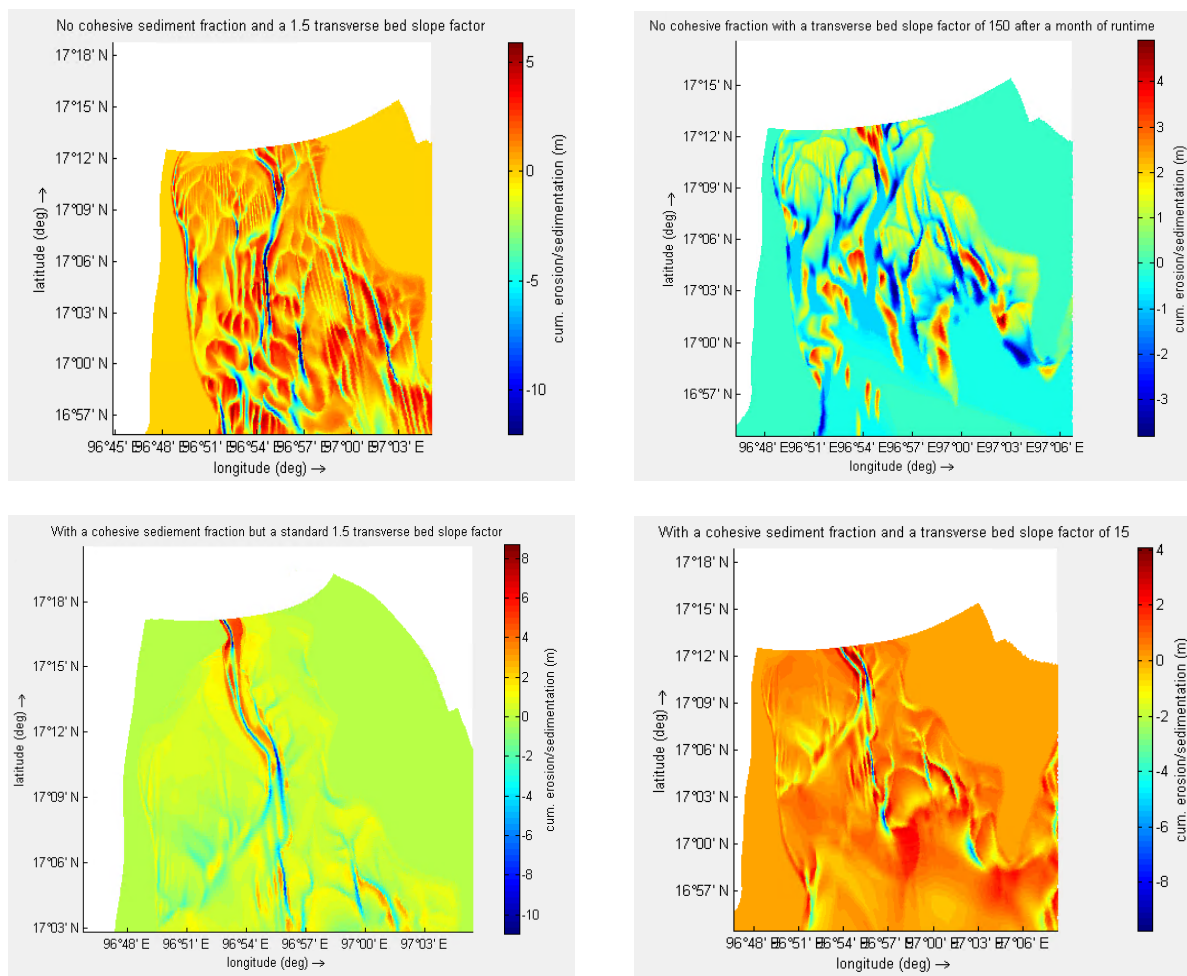


Figure 6.4: Plots of the high middle region of the estuary. Indicating the effect of different combinations of cohesive sediment fractions and values for the transverse bed slope factor. Plots indicating the effect on the channel incision rate and spread after a month run time with a morphological factor of 20.

that were happening in reality. But in this situation a simpler model is observed to occasionally yield better results (Braat et al., 2017). This has been discussed in conversations with K. van Hoof who is currently researching these phenomena. This has especially been the case in estuary environments which were rich in finer sediments. A numerical problem resulted in a miss representation of channel formation in the model simulations. Truncation errors from the longitudinal and transverse slope can become unstable and reinforce the incision behaviour.

In order to represent the channel depth formation in accordance with the field observed depths several configurations have been tested. Figure 6.4 shows the plots indicating the effect of different combinations of cohesive sediment fractions and values for the transverse bed slope factor. If there was no use of a cohesive sediment fraction there was an over formation of channels. Even a high transverse bed slope factor did not restrict this phenomenon. When a cohesive fraction was included it greatly improved this character, as it restricted to many channels from forming. Although the channel depths still did get to large. Figure E.8 shows the incision depth at middle estuary cross section for different configurations for the sediment fraction content and transverse bed slope factor. For both situations where a cohesive sediment was applied with a 1.5 and 15 transverse bed slope factor the channel developed towards a depth which is to large. This shows the current need for a combination of a cohesive sediment fraction of about 20% and a transverse bed slope factor of 150 to produce the observed channel depths, see figure 6.2.

There is no general consensus on why exactly these heightened levels of channel incision occur. There is however a good indication that the problems are caused by a fault in the numerical schematization.

Researcher B. van Prooijen of the TU Delft elaborated on these occurrences in a correspondence.

Most numerical schemes make use of an upwind method which adopts the flow velocity direction. Which is perfectly fine in one-dimensional cases. Because the velocity will increase for decreasing depth and decrease for increasing depth because of continuity. Therefore, in a one-dimensional case the bed celerity will be in the same direction as the velocity and the sediment transport. When considering a flow over a locally shallow area in a two-dimensional system, the relation between depth and velocity is not known up front. It is possible that the flow in the shallower part is weaker than in the deeper part as the flow can go around obstacles. This way the direction of the velocity can oppose the direction of the bed celerity, see figure 6.5. In such cases the wrong upwind direction is chosen and the system becomes unstable, because the bed evolution equation is actually solved with a (unstable) 'downwind' instead of upwind method (Volp et al., 2016).

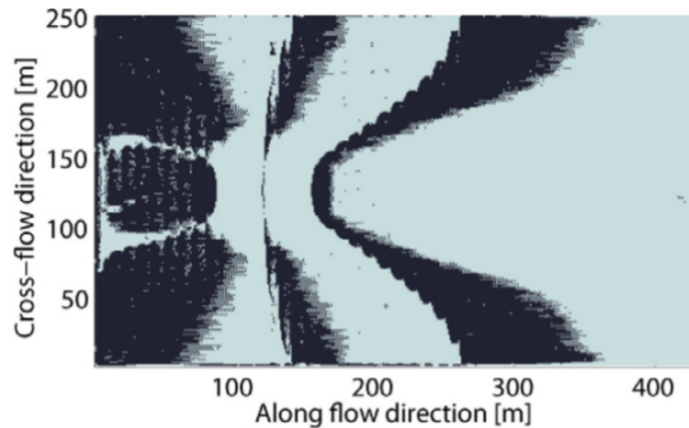


Figure 6.5: In 2D it is possible that the direction of the velocity is opposed to the direction of the bed celerity, shown in this figure from (Volp et al., 2016). Which can cause problems with the determination of the upwind scheme direction and stability. "The sign of the x-component of the bed celerity for the initial bathymetry, light is positive, black is negative." (Volp et al., 2016)

6.3. Limitations of accurate model representation

6.3.1. Bank detection and minimum erosion depth

What became clear from the model simulations was that the bank does not erode as much as it does in reality. The 'dry cell' feature allocates the erosion of the channels last wet cell to the next dry cell, constituting the bank in this case. But there was a hindrance in applying this technique. Since banks in natural channels can be very steep under certain cohesive conditions, such a description can be difficult and not produce results which have no direct physical meaning (Stecca et al., 2017). Part of the problem was the formation of a gradually declining bank slope, the minimum erosion depth and lower flow velocities in shallower depths. As the bank gradually erodes the slope becomes less steep. There is flow in these shallower parts of the channel but it might not be enough to exceed the minimum erosion depth. Which can be mitigated by lowering this threshold. But in doing so the flow velocity in these shallow section will not be sufficient for studies focusing on the erosion of river banks. In a sense the modeled 'erosion' of the bank stalled in such cases by not having large enough flow velocities to produce the required bed erosion.

High water levels contribute to upper bank erosion inducing mass failures through which it becomes more difficult for near bank flow to remove the failed material due to terrace elongation (Duró et al., 2020). Because of the fixed mesh of the model, bank shifts had to be represented by changes in the cell-averaged bed topography. Which in turn was enacted by transport of sediment from these cells (Stecca et al., 2017).

6.3.2. Small time output files velocity profile evaluation

The map output of the tidal simulations was set to 30 minutes to somewhat restrain the output size. This could potentially mean that the increased flow velocities of the incoming tide were missed in the results. Figure 6.6 shows the velocity profile of the map output when set to every 10 minutes. There were no large differences between the two settings. The maximum velocities did not increase. There

was a difference between the maximum flow velocities that were observed in field measurements, see for instance figure E.7, and the maximum flow velocities that were produced by the model. This could be because of the depth averaged approximation of the model versus the observed flow at the surface of the field data. This large difference indicates that the model could not investigate the entire extent of the tidal bore's effect on the erosion in its current shape.

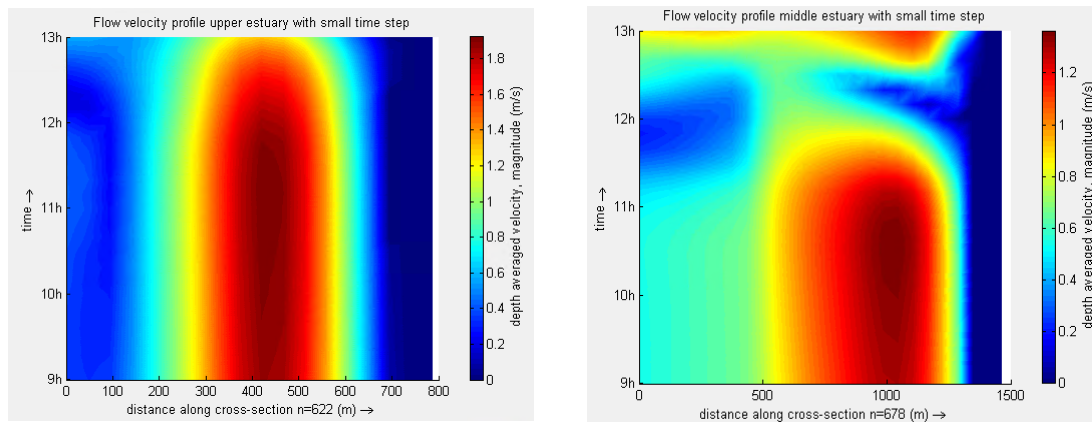


Figure 6.6: Cross sections upper and middle with small output time steps in order to evaluate the arrival of the bore front and the increase in flow velocity. Every 10 minutes the communication map files are stored and available for plotting.

6.3.3. Discharge frequency scaling

The combination of high river discharges or flood peak and a tidal motion required extra consideration when applying the MorFac option. When using this option in longer runs, the morphological changes would span multiple high-low discharge cycles. The duration of a cycle should have been scaled according to the MorFac value to have the correct forcing at the river discharge boundary. This was necessary if simulations over longer time spans were to be accurately represented. Entry of the high water front upstream and residence times of the higher water levels could have particular effects on the morphology. For the scope of this research these have proven to be too intricate to be of interest. Though in order to strive for accuracy and test applicability towards the future it has been attempted to scale the discharge in accordance with the MorFac value.

The high water entered the system as an “instantaneous” wave in the model as opposed to a gradual increase. The spin up time to adjust for the new hydrodynamic situation would be represented in a major way. Causing the morphological calculations to be based on incorrect situations. This can be seen in the accretion plot of figure E.9, where a MorFac of 20 and a normal wet season duration of 6 months had been applied. The duration of the seasons had been scaled to a duration of 9 days relative in the numerical model. Here the spin up caused inaccurate hydrodynamic situations for which the deposition of sediment was wrongfully high. Making adjustments to the code of the numerical model can in a way “skip” the spin up time and through the saved the map output continue with the correct conditions. Which was out of the scope of the current research.

7

Discussion

7.1. Discussion of the preceding state of research

The system analysis and examination of the previous studies has formed the basis around which the further research has been structured. Besides the more straight to the point data there were also aspects discovered which provided an important perspective. Given the extreme erosion rates, the evidence for large-scale dynamics and the lack of natural obstacles in the flat region, the entire coastal plain could be subject to erosion. This has been validated by examining historic charts of the region.

An overload of sediment had been alluded to as a potential cause for the dynamic activity. But there were no references to the origin or cause of the presence of the sediment. In bringing together the results of multiple studies there has been made a clear connection between three characteristics of the greater region which facilitate the sediment overload. A study by Ramaswamy et al. (Ramaswamy et al., 2004) has shown that fine sediment discharged by the Ayeyarwady Delta is transported mainly eastward towards the entry of the Gulf of Mottoma. Causing the Gulf of Mottoma to be one of the largest highly turbid areas of the world's oceans. The bathymetric map of the gulf of Mottoma showed that the depth in front of the entrance of the gulf is relatively shallow. This large area serves as a shelf where the fine sediment settles. Strong tidal currents cause drastic resuspension of sediment, increasing the sediment concentrations and flux during flood tide (Xie et al., 2018). This has also been observed to be occurring in the Sittaung estuary (Ahmed et al., 2018). A sediment overload of the estuary is thus facilitated by a combination seasonal fine sediment influx from the Ayeyarwady, shallow bathymetry and resuspension of sediments by strong tidal currents.

A field measurement campaign has been designed to investigate the other possible reason why the tidal channels have not developed any deeper. Which was the presence of an erosion-resistant layer in the subsoil of the estuary. The measurement campaign was designed and initiated to clarify these claims but has not yet been performed. The investigation would have focused on sediment cores of the top 10m of the subsoil.

7.2. Discussion of the satellite analysis

It has been concluded from the satellite analysis that the middle estuary region, where erosion has been most rapid, experienced erosion at an almost similar rate throughout the year. There has been little correlation between the wet season discharge increase and the bank erosion rate. The ten fold increase due to the monsoon season was expected to cause a stronger correlation. This lack of contribution to erosion has also been suggested by other studies. It was interesting to evaluate this finding as it would suggest even more dependency of the bank erosion rate on the incoming tide as opposed to the river discharge.

The direction with which the flow entered the estuary from the upstream point influenced the tidal channel formation visibly. In combination with the high discharges of the monsoon period this has been indicated as an important characteristic. Above the entry point there has been a stable point over the past 40 years. This point has been deemed to function as a hinge point. Downstream of this point the dynamic activity increased rapidly. The recent development of this point has been quite fascinating. There was a very real possibility that this hinge point would become dynamic over the course of this

research. The point has not yet been altered considerably but is still changing a-typically. As the direction that the discharged flow will be guided on at this location influence the development of the rest of the estuary. It would be sensible to monitor the development of this point during the research. It will likewise determine the period of the channel migration cycle.

What has been striking were the large difference of bank erosion between the upper and lower transects at relatively similar analysis locations. For instance occurring in the same bend of the tidal channel. This has been argued to be connected to the greater tendency of the bank to erode in a lower outer bend. This might be because the eroded bank material which has fallen at the toe of the bank is removed faster by the discharge directed towards the outer bend. Which makes it more prone to the erosive force of the next incoming tide.

Storm event contribution to the dynamic behaviour was found to be limited through examination of the effects of cyclone Nargis. As this was just one incidence of a large storm not all the aspects might have been present. If the storm would have come at a different moment in the tidal channel migration cycle the same forcing could have had a larger impact.

Tidal channel formation has taken place over a period of almost 2 years. River discharge has had a strong impact on the formation of of channel. This has been validated by the configuration of the tidal channel after the monsoon, when satellite data yield a sufficient view again. On the mudflats there had emerged flow paths and small channels because of the water that flows there during flood flows. Seemingly contributing to the channel formation. It has remained unclear when the conditions start to enable the forming of such channels over the mudflats. What has changed would be the distance that the main channel has moved into the bank. This distance has than increased the amplitude of the meander.

7.3. Discussion of the numerical modelling simulations

Interesting has been to see to what degree the tidal flows increased intensity could account for the differences in bank erosion. Even the the lack of evidence could something about the workings of unrepresented mechanisms. Comparing velocity profile results of the two investigated cross sections yields an entirely different, almost opposite, view. In the upper cross section there were high flow velocities for almost the entire time of the simulated cycle. Only when the tide arrived did the velocity decrease. The flows were much higher for a longer period of time than in the middle of the estuary. This was the case for all configurations. It could point to the underrepresented mechanisms of the tidal bore and the possible settling of the overloaded sediment.

In the middle of the estuary the flow velocity has been impacted by the reduced discharge. The high water front seems to have arrived spread out over time but the maximum flow velocity was lower. This was interesting but no obvious clarification was at hand. It could be that the wet season discharge compacted the tidal bore arrival and so increased the maximum velocity.

There has been an observed difference in relative importance between geomorphic processes. Extreme events or more frequent events with a smaller magnitude have been assessed by the amount of bank erosion they effectuate. In most rivers the bankfull stage seems to have most effect on the channel shape and dimensions (Wolman and Miller, 1960). This stage occurs generally more often. The relative importance of flows can be evaluated based on the quantity of sediment transported by each flow. When the quantity of sediment and frequency of flow are known, the percentage of total transported material for the significant flows is known (Wolman and Miller, 1960). Both the satellite analysis and the modelling simulations indicated that it was not the more catastrophic or large events that had a critical impact but rather the more frequently changing amplitudes of reasonably high water which had more geomorphic effect.

Simulations have shown that the large storm events have a limited effect on the the dynamic morphology of the system. This has been in accordance with the satellite analysis results. Main effect of the large storm was the increase of the river discharge due to the increased rainfall. It was concluded that there was little effect on the erosive capacity of this increase just as in the ordinary wet season discharge increase simulations. The dynamic character of this estuary might be to strong for such events to have an impact.

Zooming out and looking at the estuary-wide sediment transport shows a discrepancy between the observed import behaviour of fines and the two-dimensional modelled results. There was a strong

indication that the two-dimensional situation under-represents large-scale baroclinic sediment transport processes which are responsible for additional sediment streams.

While the fine sediments were shown to be transported outward the residual transport of sand was more influenced by river discharge. Striking was that almost the entire estuary experienced a northwards transport of bedload sediment. This could cause an area where the sediment convergences in the upstream parts of the estuary. Such an phenomenon can occur in estuaries with sandy sediment profiles and is called a bedload convergence zone (Dalrymple and Choi, 2007).

The model results showed a net export of fine sediments in all cases and an eventual import of coarse sediments. Field data shows that the estuary was comprised of a lot of fine sediments. So there seems to be a discrepancy here between the modeled domain and reality. This is an interesting proposition which can be ascribed to various causes. There could be processes active in the estuary which are not included in the current model representation like estuarine circulation. The current model is comprised of a two-dimensional grid which restricts the application of three-dimensional and baroclinic driven sediment transports in the estuary.

7.4. Discussion of the modelling capabilities and limitations

At the start of all the morphodynamic simulations the morphology is subject to some spin-up time. Before the actual changes of the morphology which are of interest occur it has to adjust to the hydrodynamic profile. Where the boundary lies between adjustment changes and morphological changes can not be known exactly so the results of the first period might better be dismissed. Instead, the results a bit further along the simulated period were investigated.

It has been investigated how the model could be used to simulate long term bank erosion. Initial model simulations showed a slight move of the channel boundaries in the directions that were observed in the satellite analysis. The channels developed in the direction that was expected based on the analyses. These runs were done with the improved settings for transverse bed slope factor and cohesive sediment fractions for an effective morphological period of 20 months. The qualitative representations were not near the correct values and also the bank at the wet/dry interface did not necessarily show an eroded behaviour. Without attention to the channel incision effect the channels in the simulations would develop towards an unrealistic depth which was evident from examining the longer runs where these factors were unattended to intentionally.

Long-term simulations with respect to the bank erosion result in several hindrances. These have been expounded on and researched with relation to the current objectives. The numerical difficulties with the channel incision were shown in their origination and possible work around. Why exactly the heightened levels of channel incision occur has been a difficult topic. There is however a good indication that the problems are caused by a fault in the numerical schematization. Most numerical schemes make use of an upwind method which adopts the flow velocity direction. In a one-dimensional case the bed celerity will be in the same direction as the velocity and the sediment transport. When considering a flow over a locally shallow area in a two-dimensional system, it is possible that the direction of the velocity can oppose the direction of the bed celerity. In such cases the wrong upwind direction is chosen the system becomes unstable (Volp et al., 2016). This issue can be resolved with a diligent dive into the code which determines the upwind direction in the advection bed profile update equation. Which has beyond the scope of the current research.

The impact of sediment transport predictors due to different choices of determining sediment motion and inclusion of suspended sediment has been covered. Most current morphodynamic model simulations opt generally for a single sediment fraction. While the application of multiple fractions better represents reality and produces channel depth reduction in long-term model simulations (Dastgheib et al., 2009).

Part of the the numerical difficulties was the fact that the model did not ascribe the erosion to the bank (dry) cells, even with the drycell feature of Delft3D enabled. This has probably been caused by the formation of a gradual bank slope, the minimum erosion depth and lower flow velocities in shallower depths. As the bank gradually erodes the slope becomes less steep. There is flow in these shallower parts of the channel but it might not be enough to exceed the minimum erosion depth. This process has been indicated as stalling by Stecca et al. (Stecca et al., 2017). This stalling can be mitigated by lowering the minimum erosion depth threshold. But in doing so the flow velocity in these shallow section will not be sufficient. A different approach focuses on the border between cells where transport

occurs and where it does not. This might be a more productive way to avoid the stalling effect of the erosion modelling.

Applying the numerical modelling approaches to a longitudinal stretch of estuary bank which resides on the wet/dry interface will eventually further modelling potency but has currently not been applicable.

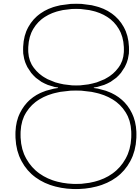
7.4.1. Discussion model input and starting conditions

In order to be able compare the different the cross sections and their respective erosion rates there were certain aspects to be noted. One had to do with the dimensions and geometry of the channels themselves. The high cross section had a deeper depth but was less wide. The middle cross section was much wider but also less deep. The depth of the channel was directly of effect on the erosion because there was less sediment that has to be eroded and transported. With a channel that was half as deep, the effective sediment that had to be transported would be half the volume per meter bank erosion.

There was a difference between the maximum flow velocities that were observed in field measurements and the maximum flow velocities that were produced by the model. This could have been because of the depth averaged approximation of the model versus the observed flow at the surface of the field data. These large differences indicated that the model could not investigate the entire extent of the tidal bores effect on the erosion in its current shape. Extra suspended sediment entering at the boundaries of the model has not been added. The choice was made not to focus on this aspect. One of the reasons was that there was virtually no existing data on suspended sediment concentrations in the estuary. Different transport relations were initially thought to have a strong impact on the morphology of the simulations. After altering the transport relations for several simulations the results showed little to no relevant differences. This is why there have been little further alterations of the transport relation during the modelling.

7.4.2. Application of the model for engineering purposes

It has been clear from the model simulations that the model cannot be used to predict the morphodynamics long-term. The complexity of factors affecting the erosion rates has made it difficult to isolate the effects of the processes due to their simultaneous occurrence and mutual interactions. Through this complexity a distance may arise between reality and the approached model situation. Keeping these developments in consideration has demanded an added level of caution when interpreting the results. Simulations have been performed to focus on a specific effect or difference between two configurations. The comparison between the satellite imagery and model results showed that the model is able to simulate relative differences between erosion and transport fluxes for different cross sections. The model cannot be used to determine what time and which locations erosion or deposition can be found, but it can be used to determine what what levels erosion or deposition is to be expected.



Conclusions and Recommendations

8.1. Conclusions

The satellite analysis has shown little to no correlation between the wet season and the bank erosion rates. The resulting heavy increase in discharge due to the monsoon is a factor that would have been suspected to be inductive to an increase in erosion. This points to an added importance of the tidal bore specific induced erosion. There has been examined a large difference between the erosion of the upper cross section of the estuary and the middle cross section of the estuary.

The large incidental storm events contribution to the dynamic behaviour of the estuary is found to be limited. Analysis of the recent cyclone arrival shows no additional implications. The development of the new main tidal channel could be altered marginally if impacted in a certain time window. The previous formation of the new tidal channel was triggered by the emergence of flow paths and small channels on the mudflats near the end of the cycle. Which formed into the new main tidal channel when large wet season discharges broke trough.

The indication of the velocity and transport profiles of different modelling configurations indicate a strong effect of the incoming tidal bore on the erosion. Comparing velocity profile results of the two investigated cross sections yields an entirely different, almost opposite, view. In the upper cross section there were high flow velocities for almost the entire time of the simulated cycle. Only when the tide arrived did the velocity decrease. The flows were much higher for a longer period of time than in the middle of the estuary. This was the case for all configurations. There has been an observed difference in relative importance between geomorphic processes. In the middle of the estuary the flow velocity has been impacted by the reduced discharge. The high water front seems to have arrived spread out over time but the maximum flow velocity was lower. Modelling results indicate a prominent role but cannot substantiate a quantitative impact of the tidal forcing and associated tidal bore.

Model simulations substantiated the satellite analysis that showed the large storm events have a limited effect on the the dynamic morphology of the system. Model simulations showed that there was little increased erosive force resulting from the storm configuration.

The large scale sediment analysis indicate a flood dominant system. There are clear effects of the dry and wet season on the residual transports. The calculated residual transports point to large-scale and local redistribution of sediments. The presence of adjacent upstream and downstream directed zones in the estuary indicates sediment circulation at the scale of the entire estuary, resulting in redistribution of sediment along the entire estuary. The two-dimensional model setup was unable to simulate baroclinic sediment transports. Fine sediments are transported out of the estuary according to the model simulations. But field observations clearly indicate the presence and even import of fine sediments into the estuary.

It has been investigated how the model could be used to simulate long term bank erosion. Initial model simulations showed a slight move of the channel boundaries in the correct direction. But the qualitative representations were not near the correct values.

Long-term simulations with respect to the bank erosion resulted in several hindrances. Heightened levels of channel incision occurred through a fault in the numerical schematization. The wrong upwind

direction could be chosen for the bed celerity and the system would than become unstable. The model also did not ascribe the erosion to the bank (dry) cells correctly, even with the drycell feature of Delft3D enabled. This caused stalling of the supposedly eroding bank.

There are several advancements which have been indicated but these require in-depth knowledge of source based model programming. Applying the numerical modelling approaches to a longitudinal stretch of estuary bank which resides on the wet/dry interface will eventually further modelling potency but has currently not been applicable.

A clear connection has been made between three characteristics of the greater estuary region which facilitate the sediment overload. Fine sediment discharged by the Ayeyarwady Delta is transported mainly eastward towards the entry of the Gulf of Mottoma. The bathymetric map of the gulf of Mottoma showed a large shallow shelf where the fine sediment settles. Strong tidal currents cause resuspension of sediment, increasing the sediment concentrations and flux during flood tide. Along with the strong incoming tide and tidal bore this makes the Sittaung estuary quite unique.

Hard engineering and conclusive solutions are not attainable in the existing context. Current attempts to mitigate the problems are standalone and lack general coordination. There is a knowledge gap and the causes of the erosion are only vaguely or erroneously known. Monitoring efforts of the shoreline and a managed retreat strategy are the most sensible approaches to mitigate the problems. Correctly transferring information to the beneficiaries is important, as are the level of interpretation that is required and the level of expertise connected to it. There remains a challenge of suitable dissemination of the information once obtained. The main characteristics, trends and drivers of the erosion mechanisms should be understood in order to direct the monitoring and convey coherent information.

8.2. Recommendations

The recommendations cover both suggestions for future research due to new findings and the way in which the results can best be interpreted and put to use.

In order to successfully manage the erosion problems of the Sittaung estuary, an integral consideration and agreement on what is actually transpiring is crucial. This is the first important step before policies or decisions can be made. With an excerpt of this research the information on morphological developments can be disseminated and agreed upon.

The modelling studies have fulfilled their role in the assessment of the dynamic morphology. But they do not have a practical future in the management of the system. So a focus should be applied on different methods. As hard technical solutions are not feasible, (autonomous) monitoring of the shoreline and managed retreat solutions are the best viable option.

Determining how to apply the depth-averaged two-dimensional model has to be done at the start of simulations. The modeled situation has been created to investigate certain hypotheses and in this sense serves a particular goal. Experts are well aware of these characteristics and handling. Counterparts or less initiated often seem to hold the possibilities of the model in a too high regard. Explaining the possibilities of the model from the start will create the correct expectations.

The current Sittaung estuary model is a very useful tool in enhancing the understanding of the hydrodynamic flows, sediment transport and morphological processes. The model should be calibrated and validated when new data is available or when the code is adjusted to serve the new features. A finer grid can be developed especially in the areas where the arrival of the bore head causes high flow velocities for a short period of time. Along with a small time and output step this can reproduce the complex flow in the shallow channels. With a more accurate model will come increased calculation times which will have to be weighed against the goal of the simulation and the longer run times.

Additional data can be of great help to better understand the estuary, if efforts focused on the correct aspects. These data inputs are of great importance for the estuary management as well as for the fundamental understanding of the specific erosion processes. The most important recommendations to collect data are for the sediment distributions as proposed in the measurement plan. The campaign, partly or in its entire proposed form, can be carried out as part of a new research or as part of the Yangon Technical University research activity. Suspended sediment concentrations at different locations for different specific times connected to the tide would be insightful to see to what degree these mechanisms are correlated. Furthermore, a detailed cross-sections of the main tidal channel and ve-

locity profile just after the passing of the tidal bore would be of great value. Especially when performed multiple times over a certain period with respect to the bank erosion.

Further research could benefit from the use a three dimensional model to investigate the baroclinic processes affecting the sediment balance of the estuary. Though this would require some hard work, especially due to the rapidly changing bed level profile, the three dimensional model setup can include a range of improvements to the model so the fine sediment dynamics are simulated much better. In seeing how impact full the fine sediment processes of the estuary are on the accretion and erosion trends, the insight into the complex dependent dynamic could be assessed in much more targeted manner. With the three dimensional grid also the flow profile at the critical bank regions at high tide will be describe in much more detail.

The results of this support the mitigation efforts of the social problems. In working with local professors, students and other staff the eagerness to get involved was omnipresent. From different directions people approached the project and wanted to offer their expertise to further the project. Building on this enthusiasm it would be wise to include these members of the wider community at an early stage in the governance and management of the region.

Bibliography

- [1] TS Ahmed, S Egashira, D Harada, A Yorozya, Y Kwak, BB Shrestha, D Kuribayashi, H Sawano, and T Koike. On bank erosion in estuary of sittaung river in myanmar. In *Scour and Erosion IX: Proceedings of the 9th International Conference on Scour and Erosion (ICSE 2018), November 5-8, 2018, Taipei, Taiwan*, page 161. CRC Press, 2018.
- [2] TS Ahmed, S Egashira, D Harada, and A Yorozya. Sediment transportation and sand bar deformation owing to tidal currents in sittaung river estuary, myanmar. *Journal of Japan, Society of Civil Engineer, Ser B1 Hydraulic Engineering*, 75, 2019.
- [3] Arcadis. Dealing with coastal erosion in the gulf of mottama, 2018.
- [4] Anne W Baar, Jaco de Smit, Wim SJ Uijtewaal, and Maarten G Kleinhans. Sediment transport of fine sand to fine gravel on transverse bed slopes in rotating annular flume experiments. *Water Resources Research*, 54(1):19–45, 2018.
- [5] Anne Wilhelmina Baar. *Impact of small-scale transverse bed slope effects on large-scale morphology: Experimental and modelling studies*. PhD thesis, Utrecht University, 2019.
- [6] P Bonneton, N Bonneton, J-P Parisot, and B Castelle. Tidal bore dynamics in funnel-shaped estuaries. *Journal of Geophysical Research: Oceans*, 120(2):923–941, 2015.
- [7] J Bosboom and MJ Stive. Coastal dynamics 1, 0.5 edn. *VSSD, Delft*, 2013.
- [8] Lianne Braat, Thijs van Kessel, Jasper RFW Leuven, and Maarten G Kleinhans. Effects of mud supply on large-scale estuary morphology and development over centuries to millennia. *Earth Surface Dynamics*, 5(4):617–652, 2017.
- [9] D Nathan Bradley and Gregory E Tucker. The storage time, age, and erosion hazard of laterally accreted sediment on the floodplain of a simulated meandering river. *Journal of Geophysical Research: Earth Surface*, 118(3):1308–1319, 2013.
- [10] Hubert Chanson. Undular tidal bores: basic theory and free-surface characteristics. *Journal of Hydraulic Engineering*, 136(11):940–944, 2010.
- [11] Hubert Chanson. Current knowledge in tidal bores and their environmental, ecological and cultural impacts. *Environmental Fluid Mechanics*, 11(1):77–98, 2011.
- [12] Alessandra Crosato and Erik Mosselman. An integrated review of river bars for engineering, management and transdisciplinary research. *Water*, 12(2):596, 2020.
- [13] Robert W Dalrymple. *Incised valleys in time and space: an introduction to the volume and an examination of the controls on valley formation and filling*. 2006.
- [14] Robert W Dalrymple and Kyungsik Choi. Morphologic and facies trends through the fluvial–marine transition in tide-dominated depositional systems: a schematic framework for environmental and sequence-stratigraphic interpretation. *Earth-Science Reviews*, 81(3-4):135–174, 2007.
- [15] Robert W Dalrymple, Brian A Zaitlin, and Ron Boyd. Estuarine facies models; conceptual basis and stratigraphic implications. *Journal of Sedimentary Research*, 62(6):1130–1146, 1992.
- [16] Richard Dame, Merryl Alber, Dennis Allen, Michael Mallin, Clay Montague, Alan Lewitus, Alice Chalmers, Robert Gardner, Craig Gilman, Björn Kjerfve, et al. Estuaries of the south atlantic coast of north america: their geographical signatures. *Estuaries*, 23(6):793–819, 2000.

- [17] Stephen E Darby and Colin R Thorne. Numerical simulation of widening and bed deformation of straight sand-bed rivers. i: Model development. *Journal of Hydraulic Engineering*, 122(4):184–193, 1996.
- [18] Ali Dastgheib, JA Roelvink, and Mick Van der Wegen. Effect of different sediment mixtures on the long term morphological simulation of tidal basins. In *2009. Proceedings of 6th IAHR Symposium on River, Coastal and Estuarine Morphodynamics: RCEM*, volume 2, page 913e918, 2009.
- [19] Gareth Davies and Colin D Woodroffe. Tidal estuary width convergence: Theory and form in north australian estuaries. *Earth Surface Processes and Landforms: The Journal of the British Geomorphological Research Group*, 35(7):737–749, 2010.
- [20] M.P. de Ridder. The tidal bore in the sittaung river; a sensitivity analyse of the propagation. *Additional thesis Master Hydraulic Engineering and Water Resource Management, Delft University of Technology*, 2017.
- [21] Deltares. *Validation Document Delft3D-FLOW, A software system for 3D flow simulations*, volume X0356. Deltares, 2008.
- [22] Deltares. *Delft3D-FLOW, Simulation of multi-dimensional hydrodynamic flows and transport phenomena, including sediments. User Manual*, volume 3.15. Deltares, 2014.
- [23] Andres Die Moran, Kamal El kadi Abderrezzak, Pablo Tassi, and Jean-Michel Herouvet. Modelling river bank erosion processes and mass failure mechanisms using 2-d depth averaged numerical model. In *EGU General Assembly Conference Abstracts*, volume 16, 2014.
- [24] Job Dronkers, MBAM Scheffers, F Gerritsen, Charitha Pattiaratchi, and W De Ruitjer. *Physics of estuaries and coastal seas*. CRC Press/Balkema, 1998.
- [25] G Duró, A Crosato, MG Kleinhans, D Roelvink, and WSJ Uijttewaal. Bank erosion processes in regulated navigable rivers. *Journal of Geophysical Research: Earth Surface*, 125(7): e2019JF005441, 2020.
- [26] Sediment Dynamics. Sediment dynamics course. *TU Delft*, CIE4308(Chapter 9), 2020.
- [27] M Eelkema, ZB Wang, and MJF Stive. Historical morphological development of the eastern scheldt tidal basin (the netherlands). In *Proceedings Of Coastal Dynamics 2009: Impacts of Human Activities on Dynamic Coastal Processes (With CD-ROM)*, pages 1–11. World Scientific, 2009.
- [28] Esther Eke, Gary Parker, and Yasuyuki Shimizu. Numerical modeling of erosional and depositional bank processes in migrating river bends with self-formed width: Morphodynamics of bar push and bank pull. *Journal of Geophysical Research: Earth Surface*, 119(7):1455–1483, 2014.
- [29] C Flokstra and FG Koch. Bed level computations for curved alluvial channels. IAHR Congress, 1980.
- [30] Carl T Friedrichs. Barotropic tides in channelized estuaries. *Contemporary issues in estuarine physics*, pages 27–61, 2010.
- [31] Miles O Hayes. Impact of hurricanes on sedimentation in estuaries, bays, and lagoons. In *Estuarine interactions*, pages 323–346. Elsevier, 1978.
- [32] Edward J Hickin and Gerald C Nanson. The character of channel migration on the beatton river, northeast british columbia, canada. *Geological Society of America Bulletin*, 86(4):487–494, 1975.
- [33] Edward J Hickin and Gerald C Nanson. Lateral migration rates of river bends. *Journal of Hydraulic Engineering*, 110(11):1557–1567, 1984.
- [34] Janet M Hooke. Magnitude and distribution of rates of river bank erosion. *Earth surface processes*, 5(2):143–157, 1980.
- [35] S Ikeda. Lateral bed-load transport on side slopes. *Journal of Hydraulic Engineering*, 1984.

- [36] Md Islam et al. River bank erosion and sustainable protection strategies. In *Proceedings 4th International Conference on Scour and Erosion (ICSE-4). November 5-7, 2008, Tokyo, Japan*, pages 316–323, 2008.
- [37] David A Jay and Jeffery D Musiak. Internal tidal asymmetry in channel flows: Origins and consequences. *Coastal and Estuarine Studies*, pages 211–249, 1996.
- [38] AB Klaven. Hydromorphological aspect of channel process modelling. In *Study of erosion, river bed deformation and sediment transport in river basins as related to natural and man-made changes*, pages 361–376, 1997.
- [39] Anke Knapen, Jean Poesen, Gerard Govers, Gwendolyn Gyssels, and Jeroen Nachtergaele. Resistance of soils to concentrated flow erosion: A review. *Earth-Science Reviews*, 80(1-2):75–109, 2007.
- [40] Stefano Lanzoni and Giovanni Seminara. On tide propagation in convergent estuaries. *Journal of Geophysical Research: Oceans*, 103(C13):30793–30812, 1998.
- [41] Giles R Lesser, JA v Roelvink, JATM Van Kester, and GS Stelling. Development and validation of a three-dimensional morphological model. *Coastal engineering*, 51(8-9):883–915, 2004.
- [42] Jasper RFW Leuven, Lisanne Braat, Wout M van Dijk, Tjalling de Haas, EP van Onselen, BG Ruessink, and Maarten G Kleinhans. Growing forced bars determine nonideal estuary planform. *Journal of Geophysical Research: Earth Surface*, 123(11):2971–2992, 2018.
- [43] Jasper RFW Leuven, Barend van Maanen, Bente R Lexmond, Bram V van der Hoek, Matthijs J Spruijt, and Maarten G Kleinhans. Dimensions of fluvial-tidal meanders: Are they disproportionately large? *Geology*, 46(10):923–926, 2018.
- [44] JRFW Leuven. Turning the tide: The effect of river discharge on estuary dynamics and equilibrium. Master's thesis, 2014.
- [45] AW Martinius and JH Van den Berg. *Atlas of sedimentary structures in estuarine and tidally-influenced river deposits of the Rhine-Meuse-Scheldt system*. EAGE Houten, 2011.
- [46] Wutt Yee Aung Yin Thuzar Tun May Thu Kyaw, Su Wutyi Aung and Wint Wah Oo. Study on the influences of sittaung river for the future port development near the gulf of martaban region, 2019.
- [47] E Mosselman. Mathematical modelling of morphological processes in rivers with erodible cohesive banks. 1993.
- [48] Gerald C Nanson and Edward J Hickin. Channel migration and incision on the beatton river. *Journal of Hydraulic Engineering*, 109(3):327–337, 1983.
- [49] Andrew P Nicholas. Modelling the continuum of river channel patterns. *Earth Surface Processes and Landforms*, 38(10):1187–1196, 2013.
- [50] Trimbak M Parchure and Ashish J Mehta. Erosion of soft cohesive sediment deposits. *Journal of Hydraulic Engineering*, 111(10):1308–1326, 1985.
- [51] Emmanuel Partheniades et al. Erosion and deposition of cohesive soils. *Journal of the Hydraulics Division*, 91(1):105–139, 1965.
- [52] V Ramaswamy, PS Rao, KH Rao, Swe Thwin, N Srinivasa Rao, and V Raiker. Tidal influence on suspended sediment distribution and dispersal in the northern andaman sea and gulf of martaban. *Marine Geology*, 208(1):33–42, 2004.
- [53] Massimo Rinaldi and Stephen E Darby. 9 modelling river-bank-erosion processes and mass failure mechanisms: progress towards fully coupled simulations. *Developments in Earth Surface Processes*, 11:213–239, 2007.
- [54] Hubert HG Savenije and Ed JM Veling. Relation between tidal damping and wave celerity in estuaries. *Journal of Geophysical Research: Oceans*, 110(C4), 2005.

- [55] Hubert HG Savenije, Marco Toffolon, Jennifer Haas, and Ed JM Veling. Analytical description of tidal dynamics in convergent estuaries. *Journal of Geophysical Research: Oceans*, 113(C10), 2008.
- [56] IUCN NAG Helvetas BANCA SDC, MONREC. First consultation workshop on developing a management plan for the wise use of the gulf of mottama (gom) at state/regional level., 2016.
- [57] T Shimozono, Y Tajima, S Akamatsu, Y Matsuba, and A Kawasaki. Large-scale channel migration in the sittang river estuary. *Scientific reports*, 9(1):1–9, 2019.
- [58] Andrew Simon and Stephen E Darby. Effectiveness of grade-control structures in reducing erosion along incised river channels: the case of hotophia creek, mississippi. *Geomorphology*, 42(3-4): 229–254, 2002.
- [59] JH Simpson, NR Fisher, and P Wiles. Reynolds stress and the production in an estuary with a tidal bore. *Estuarine, Coastal and Shelf Science*, 60(4):619–627, 2004.
- [60] G Stecca, R Measures, and DM Hicks. A framework for the analysis of noncohesive bank erosion algorithms in morphodynamic modeling. *Water Resources Research*, 53(8):6663–6686, 2017.
- [61] RC Steijn, J Cleveringa, JRFW Leuven, J van der Baan, and JJG van der Zanden. Extreme coastal dynamics of sittaung estuary (myanmar). In *International Conference on Asian and Pacific Coasts*, pages 1193–1200. Springer, 2019.
- [62] N Struiksma, KW Olesen, C Flokstra, and HJ De Vriend. Bed deformation in curved alluvial channels. *Journal of Hydraulic Research*, 23(1):57–79, 1985.
- [63] AM Talmon, N Struiksma, and MCLM Van Mierlo. Laboratory measurements of the direction of sediment transport on transverse alluvial-bed slopes. *Journal of hydraulic research*, 33(4):495–517, 1995.
- [64] Arnold Martien Talmon. Bed topography of river bends with suspended sediment transport. 1992.
- [65] CR Thome and AM Osman. Riverbank stability analysis. ii: Applications. *Journal of Hydraulic Engineering*, 114(2):151–172, 1988.
- [66] L Van Bendegom. Some considerations on river morphology and river improvement. *De Ingenieur*, 59(4):B1–B11, 1947.
- [67] Leo C Van Rijn. Sediment pick-up functions. *Journal of Hydraulic engineering*, 110(10):1494–1502, 1984.
- [68] ND Volp, BC Van Prooijen, JD Pietrzak, and GS Stelling. A subgrid based approach for morphodynamic modelling. *Advances in Water Resources*, 93:105–117, 2016.
- [69] M Gordon Wolman and John P Miller. Magnitude and frequency of forces in geomorphic processes. *The Journal of Geology*, 68(1):54–74, 1960.
- [70] Dongfeng Xie, Zhengbing Wang, Shu Gao, and HJ De Vriend. Modeling the tidal channel morphodynamics in a macro-tidal embayment, hangzhou bay, china. *Continental Shelf Research*, 29(15):1757–1767, 2009.
- [71] DongFeng Xie, Shu Gao, ZhengBing Wang, CunHong Pan, et al. Numerical modeling of tidal currents, sediment transport and morphological evolution in hangzhou bay, china. *International Journal of Sediment Research*, 28(3):316–328, 2013.
- [72] Dongfeng Xie, Cunhong Pan, Shu Gao, and Zheng Bing Wang. Morphodynamics of the qiantang estuary, china: Controls of river flood events and tidal bores. *Marine Geology*, 406:27–33, 2018.
- [73] Takao Yamashita and Htay Aung. Projection and historical analysis of hydrological circulation in sittaung river basin, myanmar. *Journal of Civil Engineering and Architecture*, 10:736–742, 2016.
- [74] Qian Yu, Yunwei Wang, Shu Gao, and Burg Flemming. Modeling the formation of a sand bar within a large funnel-shaped, tide-dominated estuary: Qiantangjiang estuary, china. *Marine Geology*, 299:63–76, 2012.

List of Figures

1.1	Overview of the region of the gulf of Mottoma and Sittaung estuary system from (Shimozono et al., 2019).	1
1.2	Rapid bank erosion and tidal channel formation of the Sittang estuary in the last decade (Shimozono et al.,2019).	2
1.3	Flow chart of the grouped report and research structure with indicated steps and parts.	3
1.4	Classification of morphological components in a filled estuary. As presented in (Leuven, 2014) from (Martinius and Van den Berg, 2011). Because energy dissipation plays an important role in sediment dynamics, the morphology can be related to the loss of hydraulic energy.	6
1.5	"Conceptual model for the development of self-formed estuaries. Interesting is phase II, where flow is diverted around the mid channel bar, causing high flow rates and extra bank erosion". From (Leuven et al., 2018).	7
1.6	Schematic representation of the funnel mechanism contribution to the tidal bore formation from (Savenije et al., 2008)	8
1.7	"Erosion of a cohesive river bank by lateral fluvial entrainment, Δn_s , and near-bank bed degradation, Δz_b , both inducing mass failure". A schematic representation from (Mosselman, 1993, p38).	9
2.1	Current bathymetric profile of the created Gulf of Mottoma model. Main channel in the middle of the estuary (Arcadis,2018).	14
2.2	"Visualization of the computational grid (blue) (Source background imagery: Google Earth)" from (Arcadis,2018) Appendix C, p2.	17
2.3	Overview of the of bed level profiles of the estuary with 2018 configuration (a) and updated 2020 configuration (b).	18
2.4	Water level cycle of an observation point near the estuary south boundary tidal forcing. With a visible amplitude of nearly 6 meters at the maximum moment just after full and new moons.	18
2.5	Hydrodynamic verification of the morphodynamic model after altering boundary conditions. Water level responses of the observation point at Sat Pu Na in the upper estuary.	20
3.1	Historic estuary locations extracted from old maps of the region (a,b,c) and the mapped outline superpositions of the estuary around 100 years apart (d). Supplementary figures from (Shimozono et al., 2019).	23
3.2	Overview of the Sittaung estuary. The circles indicate the areas with differing levels of dynamic activity (Arcadis, 2018).	24
3.3	"Relationship between the local channel width and the meander amplitude from (Leuven et al., 2018)". From the study of Arcadis (Arcadis, 2018) based on fluvial-tidal meanders worldwide.	25
3.4	Daily discharge comparison between observations and simulations upstream in the Sittaung river. (Yamashita and Aung, 2016)	26
3.5	Suspended sediment concentrations data by satellite analysis from (Ramaswamy et al., 2004). Showing the eastward transport toward the gulf of Mottoma.	27
3.6	"Bathymetric map of the northern Andaman Sea and Gulf of Martaban. Contour values are in meters. Stippled area (a) denotes area occupied by modern mud's (sand <20%)." (Ramaswamy et al., 2004)	28
3.7	Particle diameter distribution for bed and bank samples in the estuary. From a field survey by (Ahmed et al., 2018). It shows the particle size distributions of sediment collected in beds and banks, in which sediment sizes of the estuary's sediment are shown. Silt and clay particles are dominant in the upper bank material according to the results illustrated	28

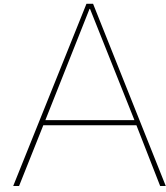
4.1	Bank position lines over the past years indicating a gradual erosion trend towards the west, gathered from (Arcadis, 2018)	31
4.2	Cross section erosion data of the bank position lines through the years. Cross section 3 indicated at 4.1, gathered from (Arcadis, 2018)	31
4.3	Map of the Sittaung estuary showing the erosion of the middle west bank. The lines indicate the position of the channel bank from 2012 till 2017. A clear erosion trend can be discerned. The upper transect showed a lot less erosion than the lower transect. The rates have been calculated and presented in table 4.1.	32
4.4	Map of the recent shoreline position changes and transect erosion rates in the region of the estuary indicated as area 2. The distances between the lines that have been measured at the transects can be read in table 4.2 and ??	33
4.5	Formation of the tidal channel overview. Sequential satellite imagery showing the emergence and evolution of the tidal channel in the new middle main tidal channel in the upper part of the estuary. Red area indicating the channel position and the orange area is the upstream region of influence on the direction of the flow	34
4.6	A map indicating the present changes that have happened at the upper part of the estuary. In previous years the outer bend was directed to the west. Recent development has seen the main flow direction shift to the east. This has possible implications for the erosion of the bank and subsequently the tidal channel further downstream of the estuary.	35
4.7	Overview of the estuary and development trends in the years before cyclone Nargis and the years after. There has been no obvious change visible in the direction of the migration or the location of the erosion. Trends that have been initiated before the storm remain present after.	36
4.8	Map of the Sittaung estuary situation pre and post the cyclone Nargis Event in 2008. The imagery of April 2008 is from a low tide, this makes the channel positions well visible. The November imagery is during high tide. There is no large redistribution of channels or bank positions. But the migration trend present at the time is continued.	37
5.1	Observation cross sections for erosion capability analysis of different hydrodynamic modifications.	40
5.2	Amplitude difference between the cross section in the middle of the estuary and higher up towards the river. The figure has been created from the 29th of August of the model simulation where the largest amplitude of the tidal signal is active.	40
5.3	Upper estuary cross section plots of the velocity profile and the bed load transport of the wet season discharge configuration.	41
5.4	Middle estuary cross section plots of the velocity profile and the bed load transport of the wet season discharge configuration.	41
5.5	Upper estuary cross section plots of the velocity profile and the bed load transport of the dry season configuration.	42
5.6	Middle estuary cross section plots of the velocity profile and the bed load transport of the dry season configuration.	42
5.7	Upper and middle estuary cross section plots of the velocity profile during a large storm event discharge configuration.	43
5.8	Residual flow of the estuary with spring tide and high river discharge (left) and spring tide and low river discharge (right). Mainly outbound residual flow in the main tidal channel for both cases but considerably lower outbound flow in the low discharge situation.	44
5.9	Residual transport of the estuary with spring tide and low river discharge. Determined for fines (left) and sand (right)	44
5.10	Cross section in the middle location of the estuary main tidal channel values for a high discharge spring tide orientation (left) and a low discharge spring tide (right). Above: profile height along transect. Middle: tidal discharge. Bottom: potential sand transport.	45
6.1	Development of the channel cross section at different estuary height with transverse bed slope factor 1.5	47
6.2	Effect on the channel cross section evolution's at different estuary height when increasing the transverse bed slope with a factor 100	48

6.3	Water depth of the middle cross section on 01-Jul-2018 (black) and 01-Jan-2019 (blue). After a six month run time including a cohesive sediment fraction, a high transverse bed slope factor and a high morphological factor (50), for a high discharge situation. Producing an effective morphological time of 25 years.	48
6.4	Plots of the high middle region of the estuary. Indicating the effect of different combinations of cohesive sediment fractions and values for the transverse bed slope factor. Plots indicating the effect on the channel incision rate and spread after a month run time with a morphological factor of 20.	49
6.5	In 2D it is possible that the direction of the velocity is opposed to the direction of the bed celerity, shown in this figure from (Volp et al., 2016). Which can cause problems with the determination of the upwind scheme direction and stability. "The sign of the x-component of the bed celerity for the initial bathymetry, light is positive, black is negative." (Volp et al., 2016)	50
6.6	Cross sections upper and middle with small output time steps in order to evaluate the arrival of the bore front and the increase in flow velocity. Every 10 minutes the communication map files are stored and available for plotting.	51

List of Tables

1.1	Tabular overview of the costs and benefits of the several avenues of mitigation of the problem. The hard engineering solutions are opposed to the more softer managerial solutions.	4
2.1	Physical parameters Delft3D	21
2.2	Numerical parameters Delft3D	21
4.1	Erosion rates of the middle west side of the estuary from 2012 to 2017 for two transects. The lower transact has seen considerably more erosion than the upper transect.	32
4.2	Erosion rates of the middle of the estuary east bank after the formation of the new middle tidal channel from 2018 to the start of 2020 for three transects. The west bank of the estuary clearly shows a stop in the erosion trend. The erosive behaviour has been transferred to the east bank.	34

Appendices



Research context

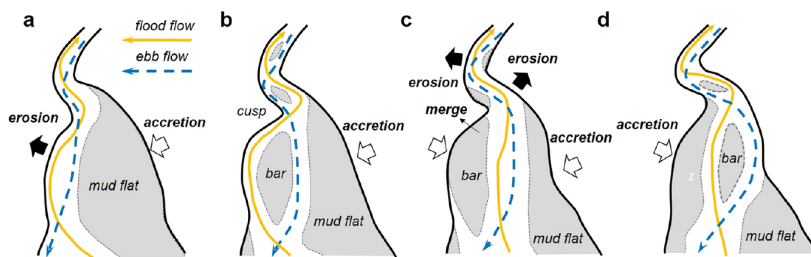


Figure A.1: Schematization of large-scale channel migration (Shimozono et al., 2019)



Figure A.2: QR-code linking to a short clip with introductory footage of the Sittaung estuary erosion.

- | | |
|---|--|
| Bago and Mon State regions <ul style="list-style-type: none">- Vulnerable communities assisted- Guidance in effective resources management | Student involvement <ul style="list-style-type: none">- Guidance and assistance in the project- Professional experience in relevant environment- Local engagement in a growing sector |
| Helvetas <ul style="list-style-type: none">- Initial need addressed- Monitoring of critical region available- Academic and professional approach | Company involvement <ul style="list-style-type: none">- Better entrenchment in Myanmar- Positioning as key player- Appealing river and coastal project |
| Communities <ul style="list-style-type: none">- Informed, heard and assisted- Guidance in problem mitigation- Clear contact point | University involvement <ul style="list-style-type: none">- Showcasing expertise- Student activity- Applied knowledge in an international and social setting |

Figure A.3: Benefits of involvement for different stakeholders

B

Processing of satellite data

This appendix describes which satellite data is used and how this data is processed in this research.

Data

Qualitative data about the system and hypothesis properties is needed to design test. Data on the historic development and erosion trends of the hinge point and configuration of the entrance point is needed. As well as data on the bank regression and erosion rates at several locations along the estuary banks. Also the channel locations and formation of the tidal channel in temporal scale are important. Besides these data requirements any information gained that will contribute to the understanding of the system will be reported.

Period	4 - '18 / 12 - '18	12 - '18 / 2 - '19	4 - '19 / 12 - '19	12 - '19 / 5 - '20
Upper transect western bank erosion (m)	0	0	0	-200
Middle transect western bank erosion (m)	250	0	0	0
Lower transect western bank erosion (m)	50	50	0	50

Table B.1: Erosion rates of the middle of the estuary west bank after the formation of the new middle tidal channel from 2018 to the start of 2020 for three transects. The west bank of the estuary clearly shows a stop in the erosion trend. The erosive behaviour is now transferred to the east bank.

Tools

Satellite remote sensing could be done in a variety of fashions. Allowing for added accuracy and certainty. This is beyond the scope of the current study, as this study is concerned with the longer term rates and evolution's. For this study the USGS landlook satellite services is being used to examine and retrieve high quality data. The 'world time timelapse' service is used to quickly estimate behaviour and trends. A customized code for the 'google earth engine' specifically looking at the changes of water and land is used to locate changes in the water stream. In order to combine and analyse data the Qgis environment is employed where distances can be determined and maps created.

B.1. Bank and channel positions

B.1.1. Incidental large storm

What is needed to analyze the effect of a large storm event is a satellite analysis of the tidal channel development and migration direction prior to storm and after the storm. Relating these observations with the numerical modeling can help determine the effects of the storm on the dynamic morphology. Figure 4.8 shows a map of the Sittaung estuary situation pre and post the cyclone Nargis Event in 2008. The imagery of April 2008 is from a low tide, this makes the channel positions well visible. When comparing the two situations this has to be taken into account. The November imagery is during high tide. There is no large redistribution of channels or bank positions. But the migration trend present at the time is continued.

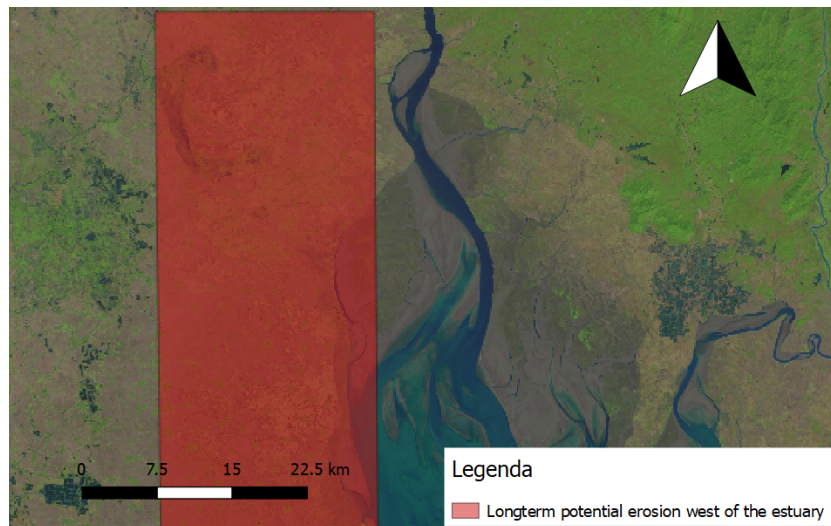


Figure B.1: Overview of the estuary system configuration of May 2020 with the indicated region that is potentially prone to erosion. Determined by examining historic charts of the region.

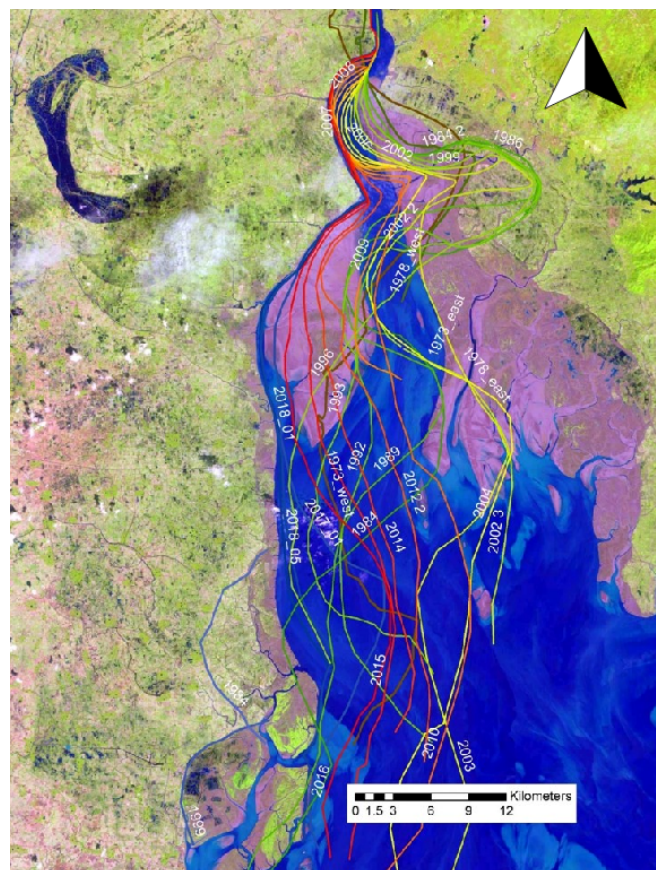


Figure B.2: Overview of the centre lines for the tidal channel evolution from 1983 to 2018 as determined in a study by Arcadis (Arcadis, 2018)

B.1.2. River entry

What is especially interesting is the development of the lower west part of the bank. If the bank will continue to erode at the current rate of tens of meters per week it can have severe effects. The configuration of the meander can change as a result of which the “hinge point” will disappear and so the area further south is subject to strong dynamic unpredictable behaviour.

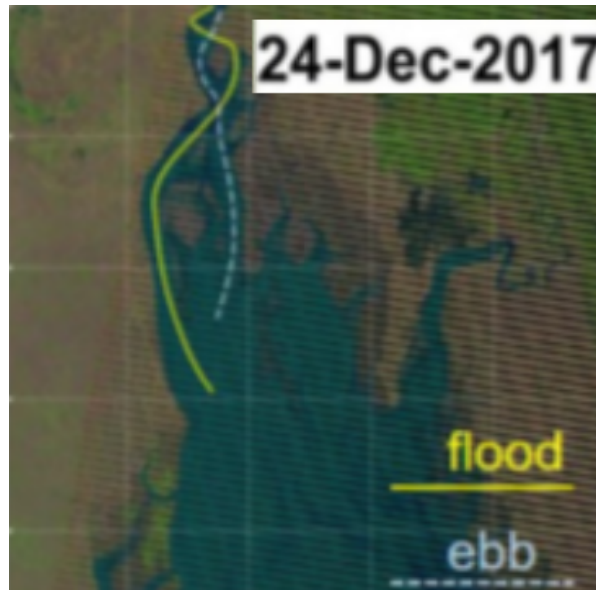


Figure B.3: "Yellow and light-blue lines highlight dominant flood and ebb flow courses in main channel, respectively. Sinuous channel migrated laterally with its end fixed in upper channel. Channel migration caused erosion on two sides of central basin alternately. Landsat imagery courtesy of NASA Goddard Space Flight Center and U.S. Geological Survey." Shimozono et al. [57]

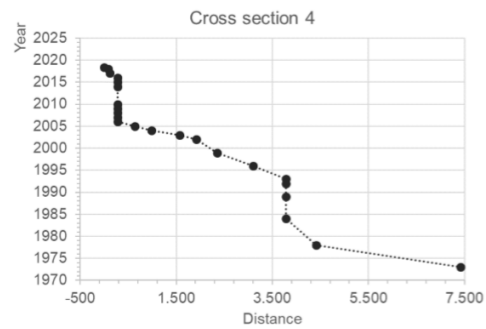
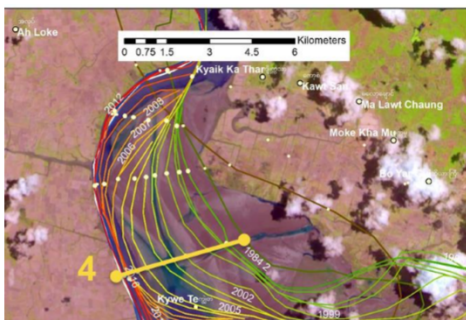


Figure B.4: Bank position lines over the past years for transect 4 indicating a gradual erosion trend towards the west, gathered from (Arcadis, 2018)

Figure B.5: Cross section erosion data of the bank position lines 4 indicated at B.4, gathered from (Arcadis, 2018)

Figure B.10 shows the position and direction of the main channel bends. Indicating an ongoing development and slight change in the extent of the bends. Which is influenced directly by changes in the hinge point. Alternations of channel bends will cause re-positioning of erosive force in the estuary.

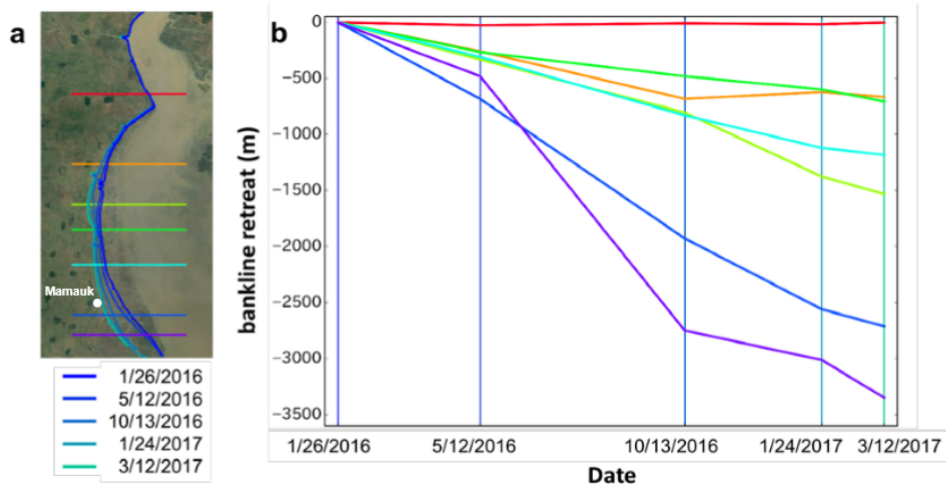


Figure B.6: Annual changes of west coastline from January 2016 to March 2017. " a, Coastlines on west side of Sittang River estuary extracted from Synthetic Aperture Radar (SAR) ... at five different timings. b, Bank retreat plotted against time for seven transects shown with same line colours as in a." Supplementary Figure S5 from (Shimozono et al., 2019)

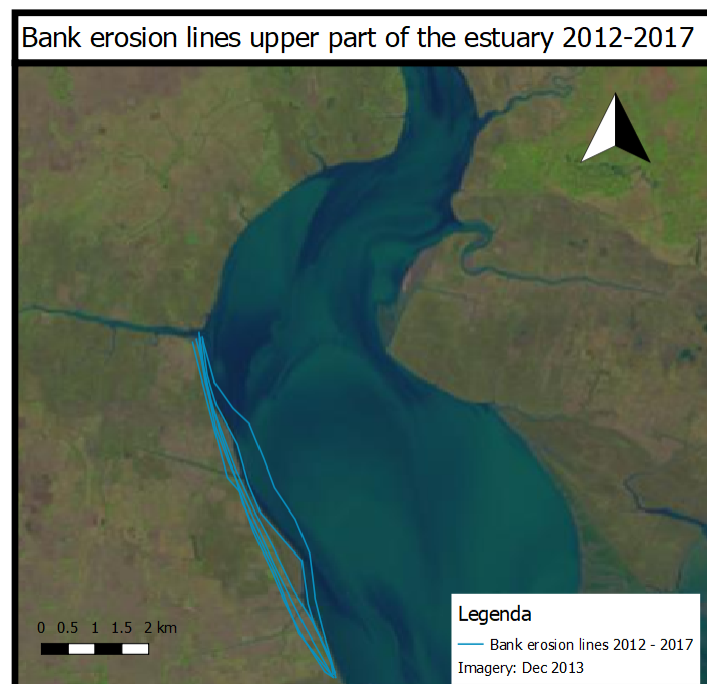


Figure B.7: Satellite imagery map from 2013 showing the bank position lines from 2012 till 2017. A slight erosion can be seen to occur in this part of the estuary. Mainly in the first two years, in the later part of the period the bank is quite stable.

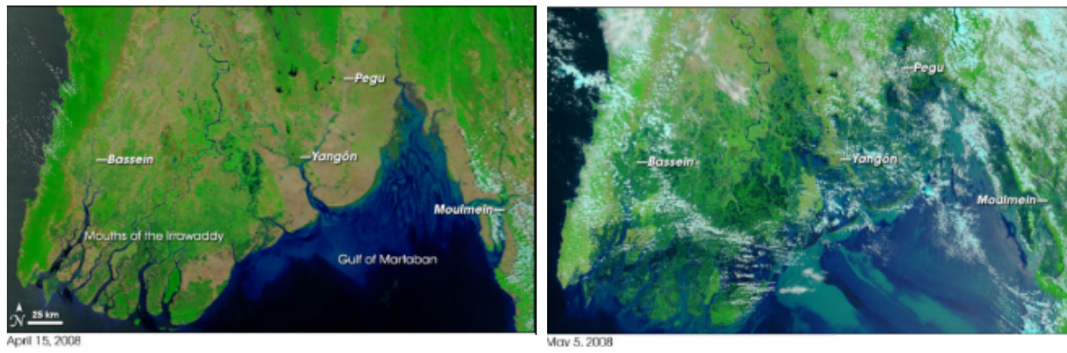


Figure B.8: "Satellite photos from NASA's Terra satellite, showing part of Myanmar on April 15, 2008 (top) and May 5, 2008 (bottom), resulting in before-and-after comparisons of the impact from Cyclone Nargis." (www.nasa.gov/topics/earth/features/nargisfloods.html)



Figure B.9: Satellite images from May 2002 (left) and November 2002 (right) with the location of the meander cut-off indicated with arrows. As presented in (Arcadis, 2018). It indicates the volatile and dynamic behaviour starting downstream of the estuary entry point.

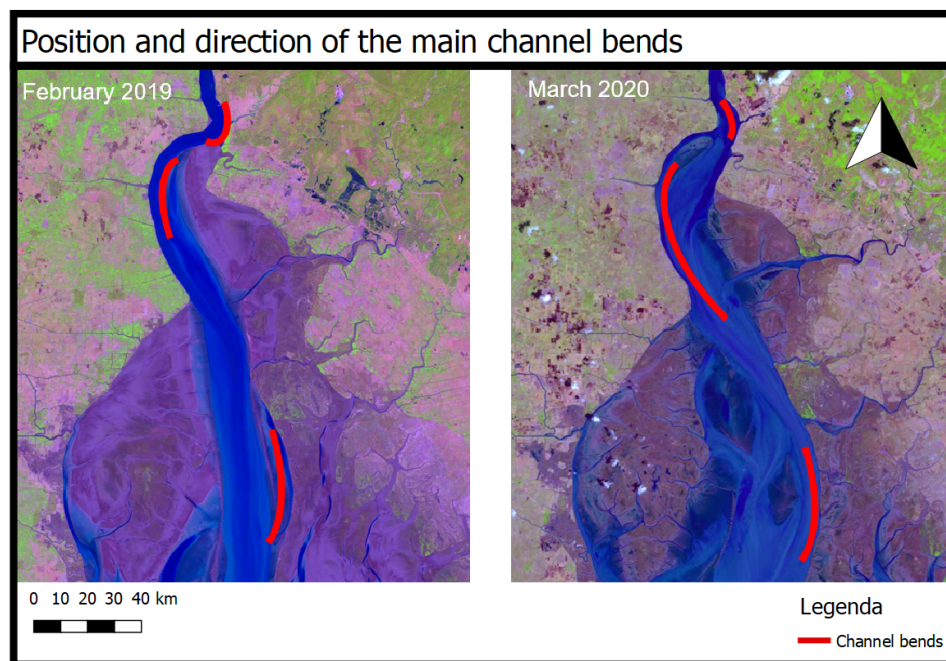
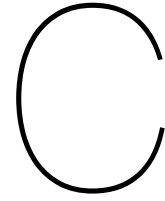


Figure B.10: Position and direction of the main channel bends. Showing an ongoing development and slight change in the extent of the bend. Which is influenced directly by changes in the hinge point. Alternations of channel bends will cause re-positioning of erosive force in the estuary.



Delft3D general

C.1. General

Deltares has developed an unique, fully integrated computer software suite for 3D computations of coastal, river and estuarine areas. It is capable of flow, sediment transport, wave, water quality, morphological development and ecology simulations. It consists of several modules that are capable of interacting with one another. Delft3D-FLOW is a multi-dimensional hydrodynamic and transport simulation program which calculates non-steady flow and transport phenomena that result from specific forcing on a rectilinear or a curvilinear grid. It solves the two-dimensional shallow water equations for depth averaged velocities, hydrostatic pressures that are derived from the Navier-Stokes equations for incompressible free surface flow. The equations are shown below with the mass conservation (C.1), the conservation of momentum in x direction (C.2) and the conservation of momentum in y direction (C.3). The momentum equation in the z direction reduces to the hydrostatic pressure. (Deltares, 2014). Turbulence modelling would require very small time steps and spatial scales to resemble the processes. To circumvent this the fluid viscosity is increased to account for the effects instead (Deltares, 2014). The software version used in this study is "Delft3D 4"

The discretised equations describe the relations between the flow values in the points of the grid and between one time step and the next. A time stepping scheme is applied to determine the evolution of the grid values in time. In Delft3D-FLOW a stable combination of second order central and third order upwind spatial discretisation is used, plus a so-called ADI-type time stepping scheme to solve the discretised equations in time. This offers a combination of accuracy, stability and acceptable computation times.

$$\frac{\partial h}{\partial t} + \frac{\partial Uh}{\partial x} + \frac{\partial Vh}{\partial y} = Q \quad (C.1)$$

$$\frac{\partial u}{\partial t} + u \frac{\partial u}{\partial x} + v \frac{\partial u}{\partial y} + w \frac{\partial u}{\partial z} - fv = -\frac{1}{\rho_0} \frac{\partial P}{\partial x} + Fx + \frac{\partial}{\partial z} \left(v_v \frac{\partial u}{\partial z} \right) + M_x \quad (C.2)$$

$$\frac{\partial v}{\partial t} + u \frac{\partial v}{\partial x} + v \frac{\partial v}{\partial y} + w \frac{\partial v}{\partial z} - fu = -\frac{1}{\rho_0} \frac{\partial P}{\partial y} + Fy + \frac{\partial}{\partial z} \left(v_v \frac{\partial v}{\partial z} \right) + M_y \quad (C.3)$$

Here:

- U Depth averaged velocity in x direction
- V Depth averaged velocity in y direction
- h Water depth

u	Velocity in x direction
v	Velocity in y direction
w	Velocity in z direction
Q	Sink or source term (discharge)
f_u, f_v	Coriolis forces
F_x, F_y	Horizontal Reynolds stresses
ν_v	Vertical eddy viscosity coefficient
M_x, M_y	Contributions due to external sources or sinks of momentum (external forces).
$\frac{\partial P}{\partial y}, \frac{\partial P}{\partial x}$	Pressure gradients

The D-Morphology module computes sediment transport (both suspended and bed total load) and morphological changes for an arbitrary number of cohesive and non-cohesive fractions. It is designed to simulate the morphodynamic behaviour of rivers, estuaries and coasts on time-scales of days to years. Problems to be studied using the morphological module are typically complex interactions between waves, currents, sediment transport and bed topography. Sediment can be cohesive or non-cohesive. For the suspended load this module connects to the 2D or 3D advection-diffusion solver of the D-Flow module. An essential feature of this module is the dynamic feedback with the D-Flow module, which allows the flows to adjust to the local bed topography and enables simulations on any time scale.

For simulating the morphodynamic changes "Van Rijn (1993)" transport formulations are default for calculating the suspended and bed load sediment transports. The numerical implementation is undertaken by means of the finite volume solver, where the continuity equation is solved implicitly in time and the advection term in the momentum equation explicitly in time. More extensive explanation of the implemented processes and numerical aspects can be found in the manual (Deltares, 2014). Some of the relevant processes and utilities are listed below:

Features:

- Tidal forcing.
- Density driven flows (pressure gradients terms in the momentum equations).
- Advanced turbulence models to account for the vertical turbulent viscosity and diffusivity based on the eddy viscosity concept.
- Time varying sources and sinks (e.g. river discharges).
- Various options for the co-ordinate system (rectilinear, curvilinear or spherical).
- Optional facility to calculate the intensity of the spiral motion phenomenon in the flow (e.g. in river bends) which is especially important in sedimentation and erosion studies (for depth averaged — 2DH — computations only).
- Optional facility for tidal analysis of output parameters.
- Optional facility for user-defined functions.
- Domain decomposition.

Utilities:

- RGFRID;
For generating curvilinear grids

- QUICKIN;
For preparing and manipulating grid oriented data, such as bed topography or initial conditions for water levels, salinity or concentrations of constituents.
- Delft3D-QUICKPLOT;
For visualisation and animation of simulation results

C.2. Model setup

C.2.1. Time frame

The Courant–Friedrichs–Lewy, CFL, condition is a condition for the stability of unstable numerical methods that model convection. It expresses that the distance that information travels during the time step length within the grid must be lower than the distance between grid elements. So the information from a given cell can only propagate to its neighbors in a single time step.

C.2.2. Sediment transport

To understand the implementation of the morphological functions and how they interacts with the sediment transport predictor, the calculation of sediment transports is examined. The amount of sediment in a cell holds can only change if the in- and outfluxes are unequal. A gradient in the sediment transport can cause the the bed level to change, which in turn influences the hydrodynamics. For simulating the morphodynamic changes "Van Rijn" is default for calculating the suspended and bed load sediment transports. The numerical implementation is undertaken by means of the finite volume solver, where the continuity equation is solved implicitly in time and the advection term in the momentum equation explicitly in time. More extensive explanation of the implemented processes and numerical aspects can be found in the manual (Deltares, 2014).

C.2.3. Transverse bed slope

Downslope sediment transport, affected by a transverse bed slope gradient, can be calculated by a predictor that deflects the sediment transport vector. Delft3d offers a range of options to calculate transverse slope and implement a change in direction. The two most commonly used methods are the Ikeda (1984) and Koch and Flokstra (1981). These methods differ slightly in the way the alteration of direction is calculated and implemented.

The Ikeda (1984) method uses the transverse slope predictor (eq. D.9) to calculate an additional vector in transverse direction. It has αI as an input parameter. This vector is added to the vector in streamwise direction to determine the resulting direction and magnitude of the transport vector.

$$\alpha_s = 1 + \alpha_{bs} \left(\frac{\tan(\phi)}{\cos(\tan^{-1}(\frac{\partial z}{\partial s}))(\tan(\phi) - \frac{\partial z}{\partial s})} - 1 \right) \quad (C.4)$$

In contrast, for the method of Koch and Flokstra (1981) the direction of sediment transport is corrected for transverse gradients by enforcing a rotation. It uses the transverse slope predictor (eq. C.5) with input parameter αK to determine the amount of deflection. The method of calculating the sediment transport vector in both slope options therefore has major implications for calibrating models with the transverse slope parameter.

$$\tan(\alpha) = \frac{\sin(\delta) - 1 \frac{1}{f(\theta)} \frac{\partial z_b}{\partial y}}{\cos(\delta) - \frac{1}{f(\theta)} \frac{\partial z_b}{\partial x}} \quad (C.5)$$

As a result of the differences, Ikeda amplifys the direction and **magnitude** of the transport when a transverse slope is present. Which increases the total sediment transport significantly. Contrary, Koch Flokstra only alters the direction of the sediment transport. The sediment transport predictor of Van Rijn makes a distinction between bed load and suspended sediment, and only the bed load part is used to calculate downslope sediment transport. In contrast, the predictor of Engelund Hansen is a total load predictor, and therefore suspended load is treated as bed load and the bed slope effect acts

on all sediment in transport. The effects on the morphology of using different slope predictors can be analyzed by requiring either the magnitude or the direction of to be equal and comparing the differences.

C.2.4. Morphological spin-up interval

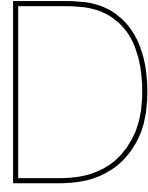
In most cases a hydrodynamic simulation will require some spin-up time from the initial conditions to the active boundary conditions. During this stabilisation period the patterns of erosion and accretion that are reported do not accurately reflect the true morphological development. These reported values should be omitted from the morphological analysis. This is made possible by use of a morphological spin-up interval. Which makes it possible to specify a time interval after which the morphological bottom updating will begin. During the specified time interval all other calculations are performed as they would, however the effect of the sediment fluxes on the available bottom sediments is left out.

It is important yet often arbitrary where to draw the line for the morphological spin up. The morphological profile will adjust to the initial configuration and forcing of the system by changing rapidly at the start. But this will continue without a apparent sign into the morphological changes that are naturally occurring and are the objective of the simulation.

C.2.5. Morphological scale factor

The morphological scale factor is a very convenient option when examining the morphological evolution of a system. It should be employed carefully and requires additional validation. The increase of the sedimentation and accretion fluxes might yield unreasonable results over longer time spans when the factor becomes to high. The maximum value of the factor that can be included in a morphodynamic model without affecting the accuracy will depend on the particular situation modeled. This can be validated with a computational run where the morphological factor is decreased and the run time increased to reach a similar morphological evolution time. If these changes do not affect the overall simulation results the application of the morphological factor is permitted.

For applications with tidal motion the MorFac option is particularly relevant. From a hydrodynamical point of view this increase in morphological development rate is allowed if the hydrodynamics is not significantly influenced. The combination of high river discharges or flood peak and a tidal motion require extra consideration when applying the MorFac option. The effect of the morphological factor is different for bed and suspended load. Only the transports are increased by the morphological factor used for the time step considered. **The erosion and deposition fluxes are increased by the morphological factor, but the suspended concentrations are not.** Changes in the morphological factor can lead to a mass-balance error in the order of the suspended sediment volume times the change in morphological factor.



System analysis and data

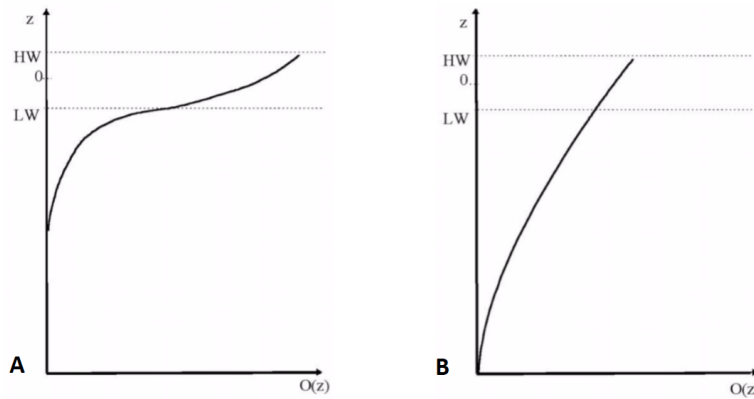


Figure D.1: Hypsometric curves. A) represents a basin with a large intertidal storage area and shallow channels, B) represents a basin with small intertidal storage area and deep channels. From (Bosboom and Stive, 2013).

Tidal bore

$$Encb_s = constant \rightarrow \hat{\eta}\sqrt{ghb_s} \quad (D.1) \quad \frac{\hat{\eta}_2}{\hat{\eta}_1} = \frac{h_1^{1/4} b_{s1}^{1/2}}{h_2 h_{s2}} \quad (D.2)$$

Here E is the energy, nc is the group velocity and b_s the width, η the amplitude, h the water depth. Showing the higher order impact of width reduction over depth reduction on the amplitude (Bosboom and Stive, 2013). Identifying the contribution of the funnel shape to the tidal bore formation. If the tidal bore does not change over time the following equation can be used to derive the propagation speed of the bore, derived from the hydraulic jump equation.

$$c = -v_1 - \frac{\sqrt{gd_2 - d_1}}{2d_1} \quad (D.3)$$

Bank erosion

$$\Delta w = \frac{R(\tau - \tau_c)\Delta t}{v\tau_c} \frac{du}{dy} \quad (D.4)$$

in which Δw = bank erosion distance (m) in one bank; τ_c = critical shear stress (dynes/cm²) for cohesive soils; ν = soil unit weight (kN/m³) ; τ = average shear stress (dynes/cm²) and Δt = computational time interval in minutes.

Transverse bed slope

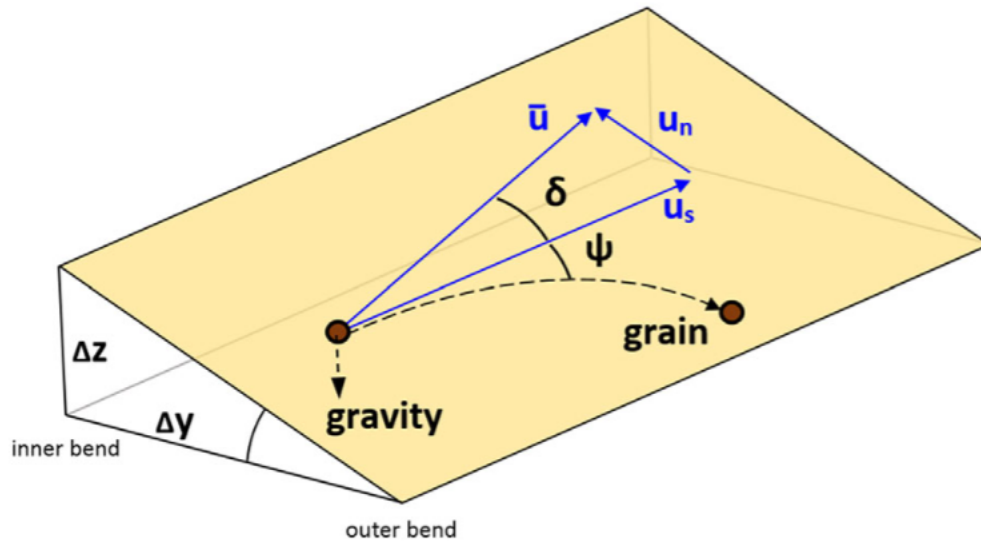


Figure D.2: "Definition of the main variables that determine the transverse bed slope effect. Grains on a slope transverse to the main flow direction (u_s) are deflected downslope due to gravity. When a secondary current is present, e.g., in bends, the inward and upslope directed shear stress drags particles upslope. In this case the equilibrium slope that develops (Δz , Δy) is a balance between the angle of deflection due to gravity (w) and the angle between the local flow velocity vector (ψ) and the main flow direction (δ) near the bed, which represents the secondary flow intensity." from (Baar, 2019)

Van Bendegom (Van Bendegom, 1947) formulated the earliest relation between downslope sediment transport and secondary flow. It is a linear relation between the secondary flow intensity and the transverse bed slope:

$$\frac{\partial z_b}{\partial y} = B \frac{u_n}{u_s} \quad (D.5)$$

$$\frac{\partial z_b}{\partial y} = Af(\theta) \frac{h}{R} \quad (D.6)$$

With $\frac{\partial z_b}{\partial y}$ = transverse bed slope, u = magnitude of the flow velocity [m/s] in transverse direction (n) and streamwise direction (s) and B = a dimensionless slope factor. Slope factor B relates the secondary flow intensity to the transverse slope. The secondary flow intensity in this case is determined by the ratio between the magnitude of the normal flow and secondary flow (Baar, 2019).

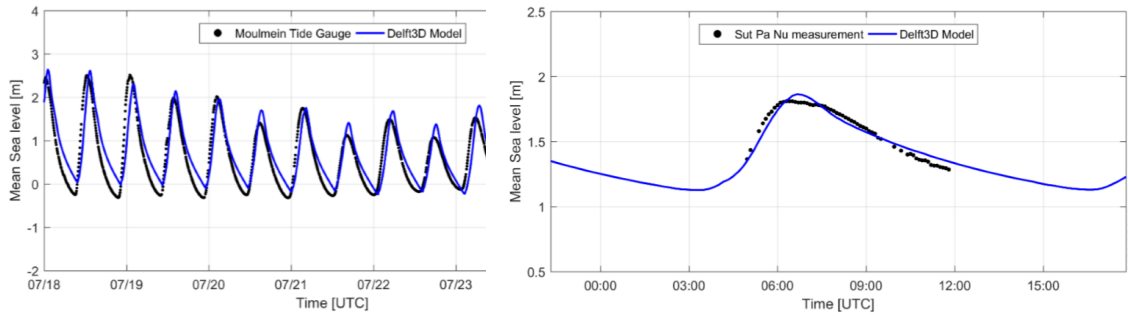
There are formulations with similar goals, to determine the cross-subsectional shape of river bends (Crosato and Mosselman, 2020). Also balancing the inward gravity gradient effect and the outward spiral flow effect, equation D.6 (Struiksmas et al., 1985). Here A is a coefficient weighing the intensity of spiral flow, $f(\theta)$ is a function of local Shields parameter representing gravity pull along the slope, h is the local water depth and R is the radius of depth-averaged streamline curvature. The function for the effect of gravity pull, $f(\theta)$, here E is a calibration coefficient (Talmon et al., 1995), can be expressed as:

$$f(\theta) = \frac{0.85}{E} \sqrt{\theta} \quad (D.7)$$

Most theoretical models aiming to adjust the direction of the sediment transport when divergent from the bed shear stress consist of a balance of forces. These forces are acting on a sediment particle moving along the transverse inclined bed. Equation D.8 shows an adaption of the direction of the sediment movement due to the transverse effects according to the Koch-Flokstra relation (Flokstra and Koch, 1980). Equation D.9 follows the relation according to Ikeda (Ikeda, 1984).

$$\tan(\alpha) = \frac{\sin(\delta) - 1 \frac{1}{f_s(\theta)} \frac{\partial z_b}{\partial y}}{\cos(\delta) - \frac{1}{f_s(\theta)} \frac{\partial z_b}{\partial x}} \tag{D.8}$$

$$\alpha_s = 1 + \alpha_{bs} \left(\frac{\tan(\phi)}{\cos(\tan^{-1}(\frac{\partial z}{\partial s}))(\tan(\phi) - \frac{\partial z}{\partial s})} - 1 \right) \tag{D.9}$$



(a) Measured and modelled Water levels at Moulmein

(b) Measured and modelled water levels at Sut Pa Nu

Figure D.3: a: Comparison between measured tidal signal and simulated tidal signal at Moulmein tide gauge as validation of the model. b: Comparison between measured tidal signal and simulated tidal signal at Sut Pa Nu as validation of the model. Reported in (Arcadis, 2018)

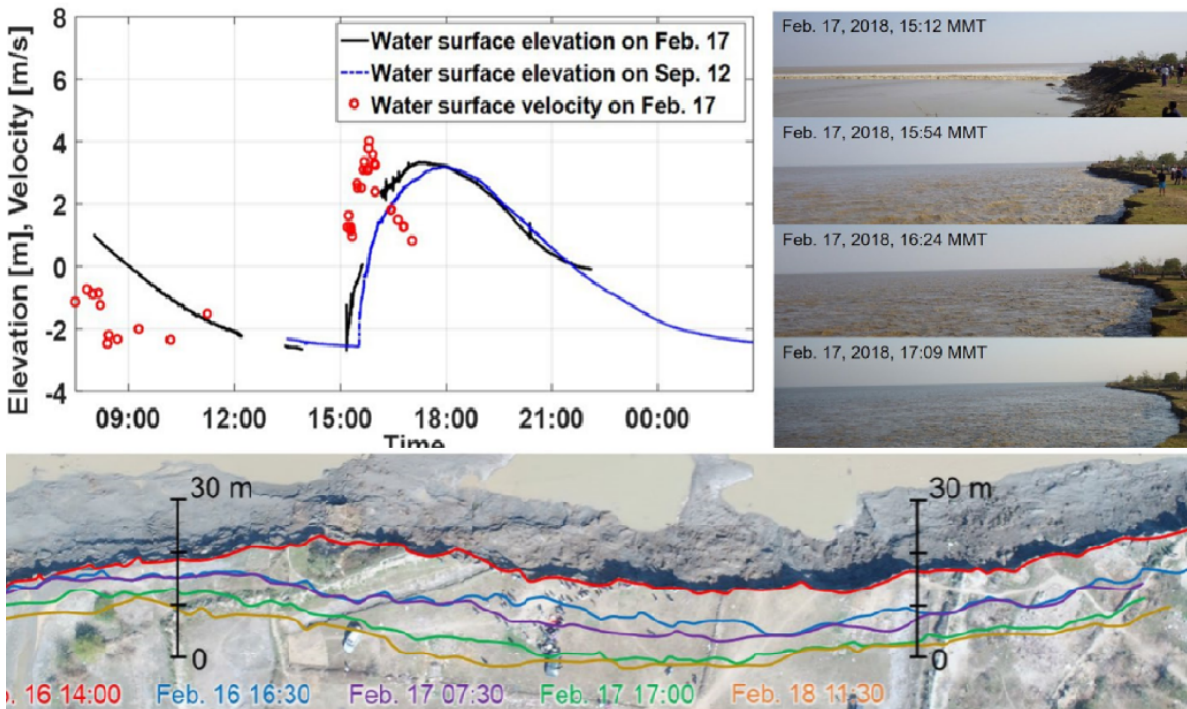


Figure D.4: "Observed water-level and flow-velocity changes over spring tidal cycle in dry and rainy seasons (Water-level profile in dry season has some data breaks (left). Bank erosion process during flood phase from dry-season survey (right). Bank line retreating 10–20 m over four tidal cycles. (down)" (Shimozono et al., 2019, p.4)

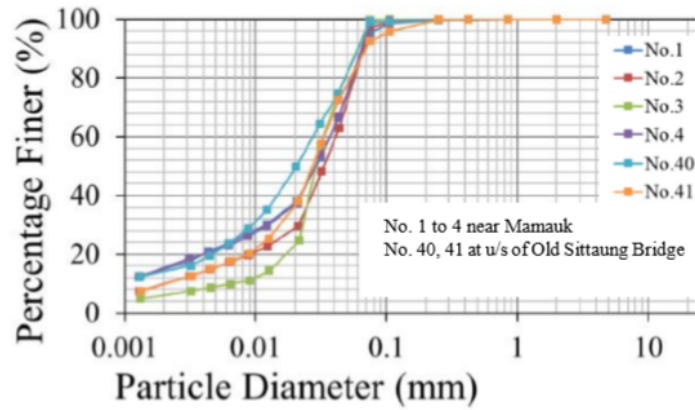


Figure D.5: Grain size distribution curves of river and estuary bank locations. Form a field study in 2019 by (Ahmed et al., 2019)



Location (Fig 3)	Sand [%]	Silt [%]	Clay [%]	Organic material	d50 [μm]	d90 /d10	Additional remark
003	90	10			100	5	Very fine sand, well graded
008	50	50			90		bit sticky
123	80	20			100	4	Very fine sand, well graded
170			100	X			consolidated clay, easy erodible, no smell, obtained below MSL
425	20		80	X			non consolidated clay, small fraction organic material (grass), obtained above MSL



Figure D.6: Information on the sediment characteristics at different locations in the estuary. From a fieldwork in 2018 by Arcadis staff (Arcadis, 2018).



Figure D.7: "Bank-cut surface exposes thin layers indicating that high land was created by mud accumulation over neap-spring tide cycles." (Ahmed et al., 2018)

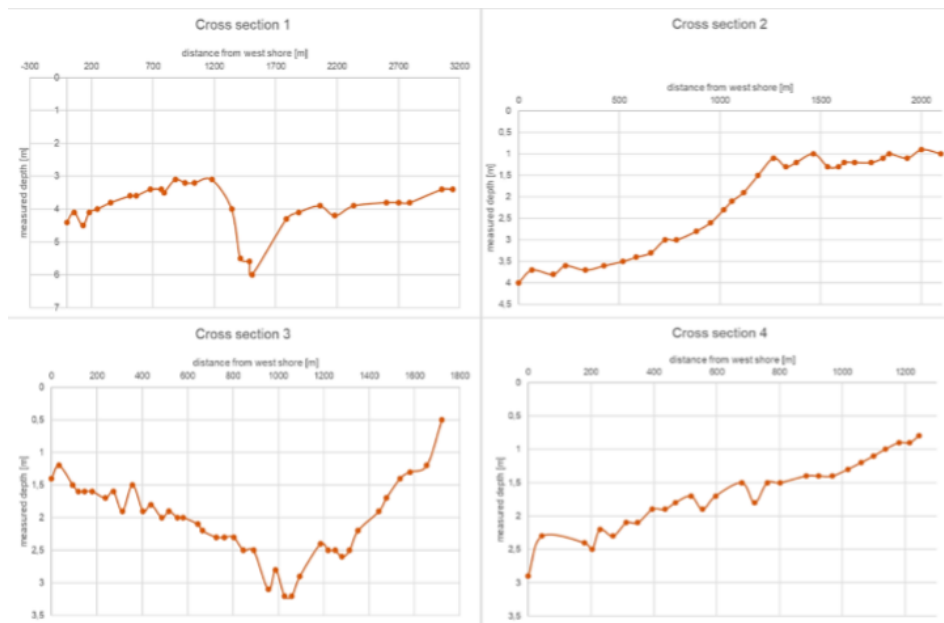


Figure D.8

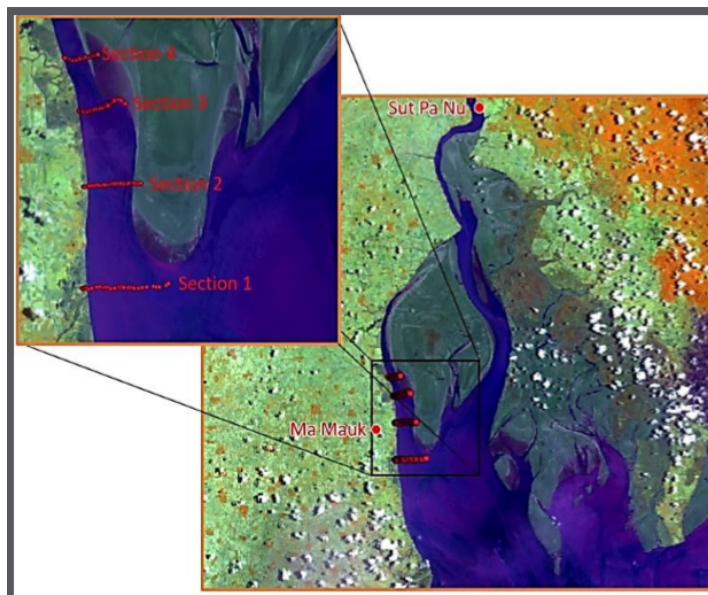
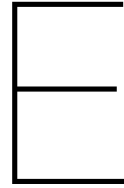


Figure D.9



Numerical modelling simulations

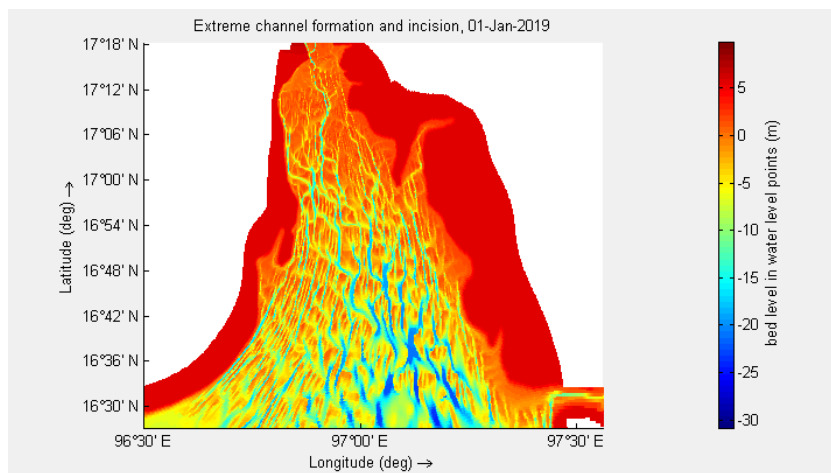


Figure E.1: Extreme channel formation and incision with unsuitable model parameters for transverse bedslope effect. After 6 months run time with a morphological scaling factor of 20. Effectively subjecting the estuary to a morphological change of 10 years.

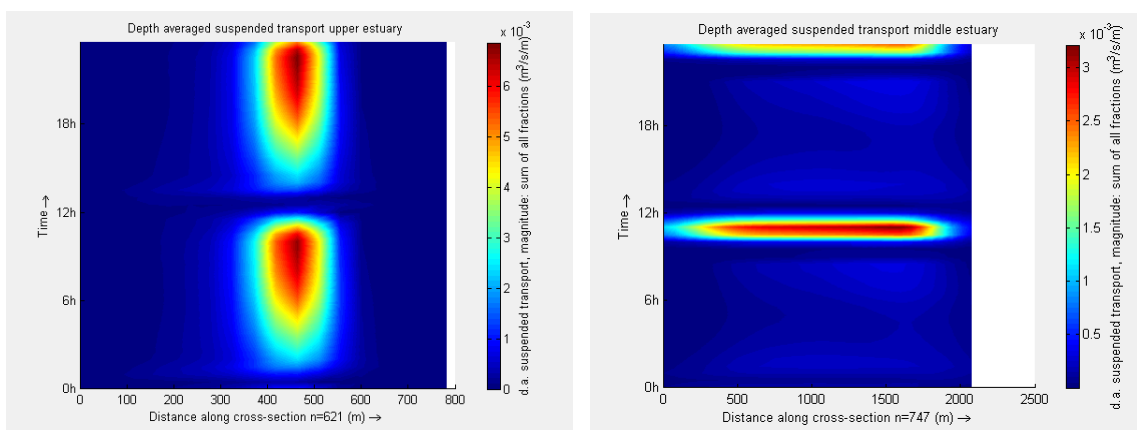


Figure E.2: Wet season suspended transport upper (left) and middle (right) cross section. Showing a similar profile to the bedload transport profiles of the same configuration only with a significantly higher value.

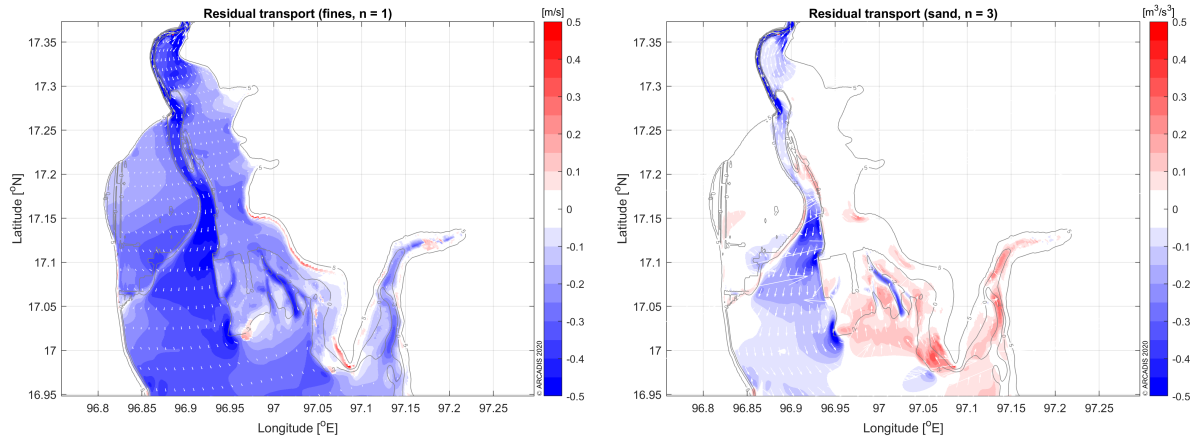


Figure E.3: Residual transport of the estuary with spring tide and high river discharge. Determined for fines (left) and sand (right)

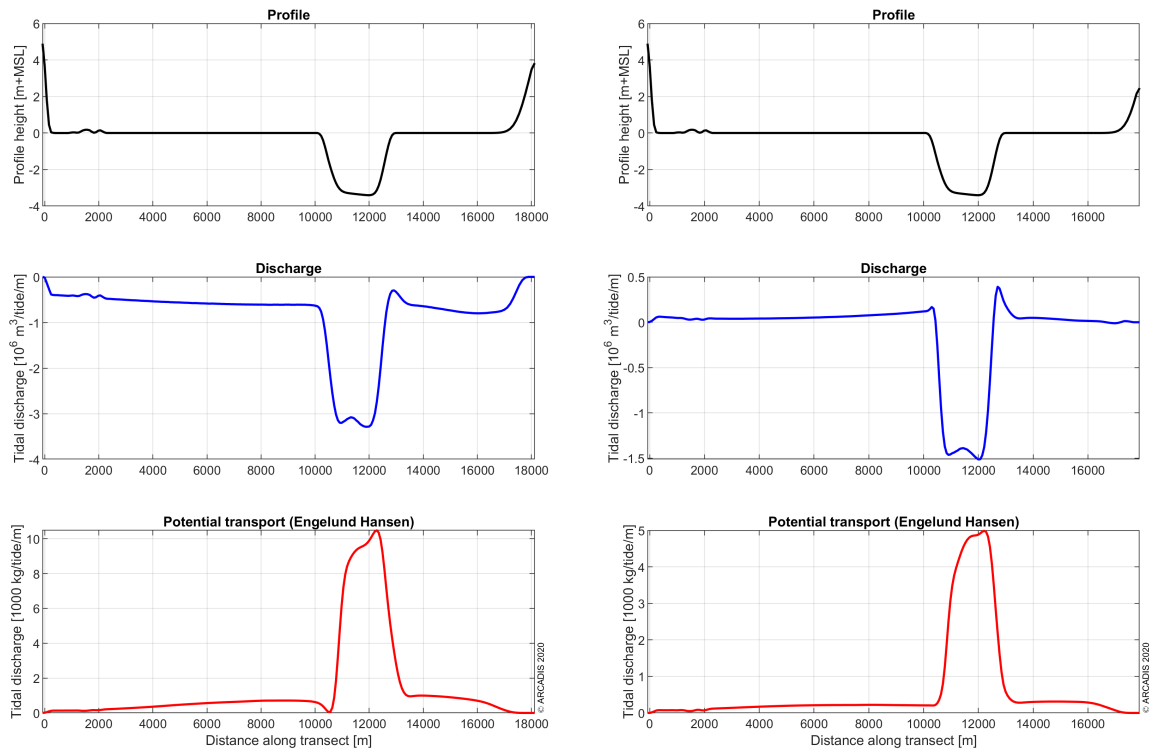


Figure E.4: Cross section in the middle location of the estuary main tidal channel values for a high discharge spring tide orientation (left) and a low discharge neap tide (right). Above: profile height along transect. Middle: tidal discharge. Bottom: potential sand transport.

Estuarine circulation refers to the residual flow induced by density differences. It can occur due to both horizontal and vertical stratification. Gravitational circulation is caused by horizontal stratification. Estuarine circulation due to vertical stratification is called tidal straining. Gravitational circulation is the circulation of water within the estuary, caused by the density differences along the length of the estuary. Because salt water has a higher density, the pressure of the water column on the sea side is larger than that of the river. This results in a slightly sloping water level. The freshwater flow is lighter and

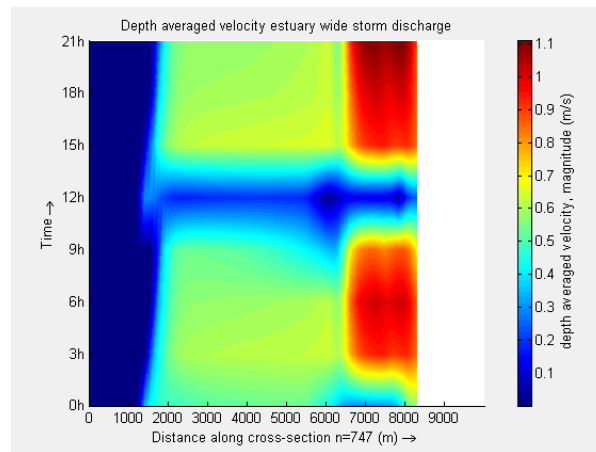


Figure E.5: Middle estuary cross section over the entire width of the estuary, mudflat included. Plot of the velocity profile during a large storm event discharge configuration.

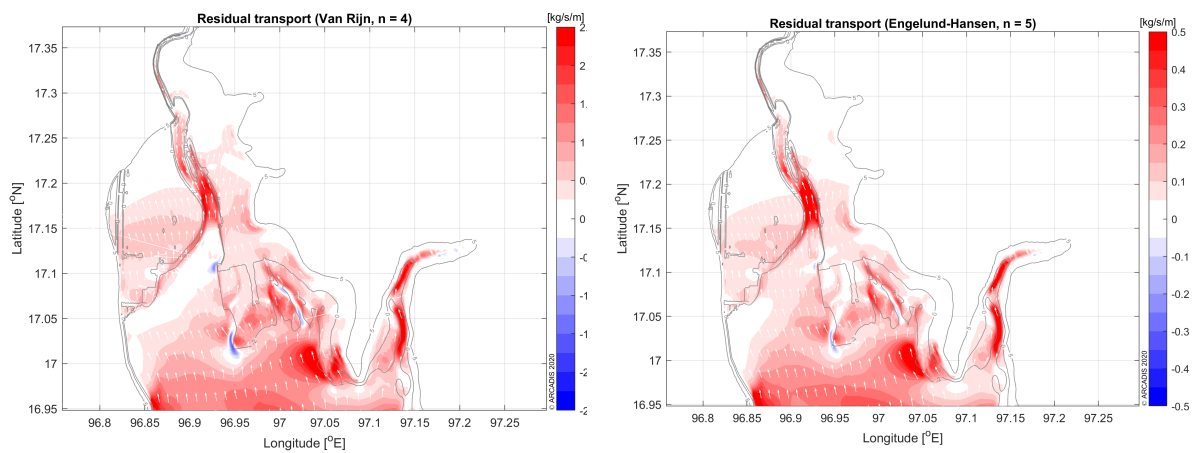


Figure E.6: Residual transport differences between a Van Rijn transport (left) relation and Engelund-Hansen relation (right). Van Rijn having a considerably higher value which can be ascribed to the inclusion of fine sediments as opposed to Engelund-Hansen.

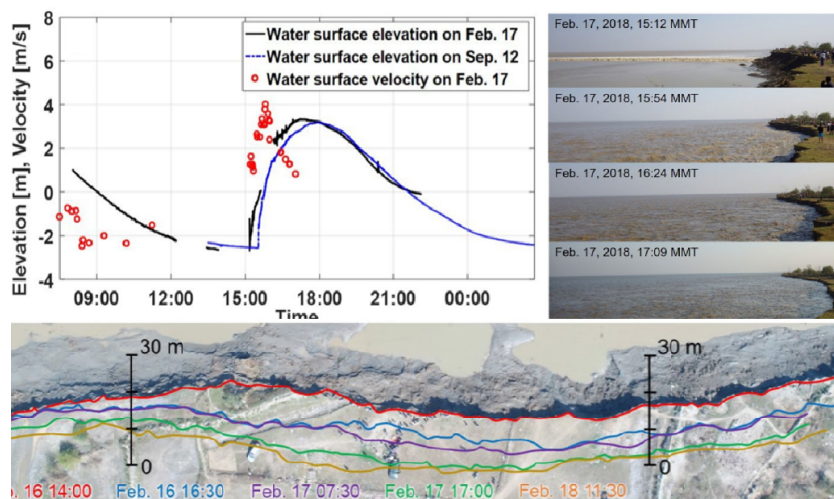


Figure E.7: "Observed water-level and flow-velocity changes over spring tidal cycle in dry and rainy seasons (Water-level profile in dry season has some data breaks (left). Bank erosion process during flood phase from dry-season survey (right). Bank line retreating 10–20 m over four tidal cycles. (down)" (Shimozono et al., 2019, p.4)

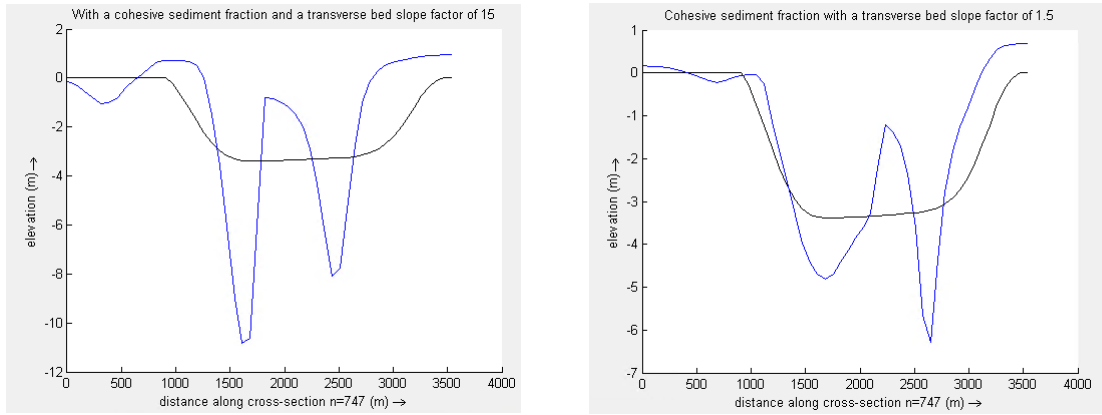


Figure E.8: Middle estuary cross section plots of the channel incision depth at different configurations for the sediment fraction content and transverse bed slope factor.

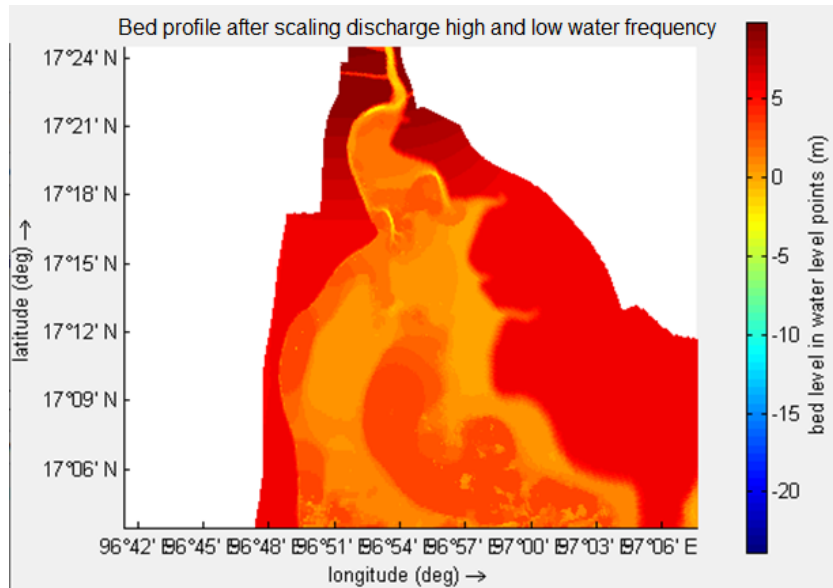


Figure E.9: Bed profile after a one month run time with scaled discharge frequency for high and low water.

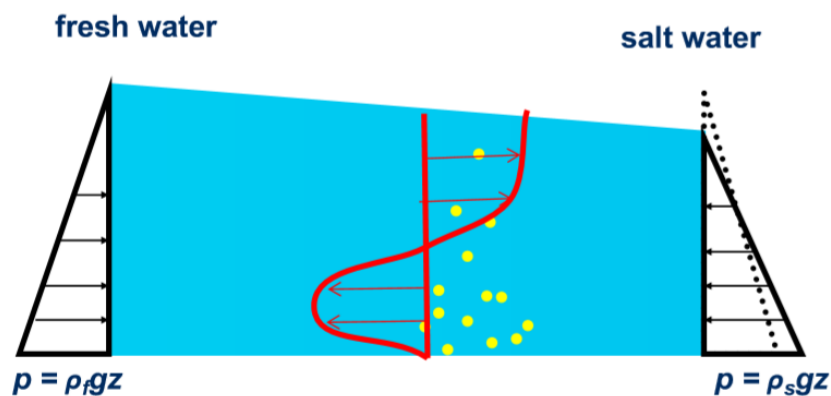


Figure E.10: Schematized estuarine circulation between fresh and salt water. Effecting horizontal flow and sediment transports through salinity gradients. (Dynamics, 2020)

therefore closer to the surface than the denser salt water flow. Resulting in a density gradient driven flow to balance the fluxes (Dynamics, 2020), see figure E.10. Gravitational circulation is enhanced for

a larger water depth because the vertical distance between the net fresh water flow and the net saline water flow is larger. Tidal straining, mostly active in well-mixed estuaries, is defined as the stratified flow that occurs when fresh water is flowing on top of the saline water due to the density effect. Tidal straining of the density fields causes the stratification to be greater during ebb than flood (Jay and Musiak, 1996). The resulting asymmetric mixing and velocity profile produces a residual flow of the same character as the density-driven circulation: downstream flow near the surface and upstream flow near the bottom.

F

Designed field measurement campaign

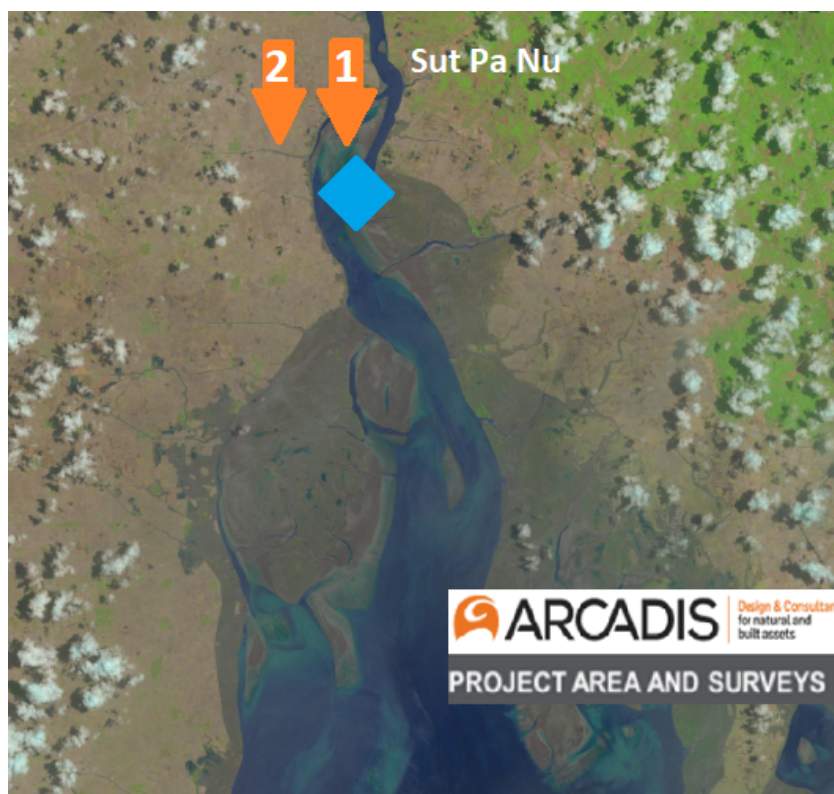


Figure F.1: Figure with the planned measurement locations of the field campaign in the new configuration. The orange arrows indicate the drilling sites for sediment measurements. The blue diamond indicates the location for the WaveDroid installation.

Introduction

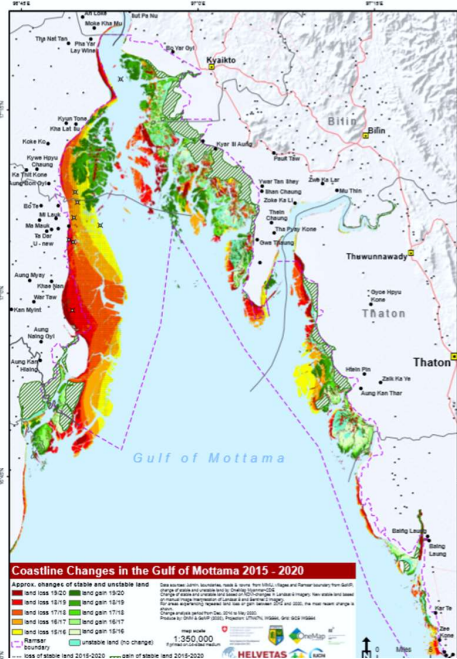


Figure 2: Recent erosion and sedimentation in the gulf of Mottama (Helvetas, 2020).

The dynamics of the tidal channels in the Sittaung estuary result in ongoing severe coastline regression. Erosion in the Bago Region has forced entire villages to retreat and to abandon the area. Changes in erosion and sedimentation patterns are frequent, see with anecdotal evidence reporting the erosion cycle repeats each 10 to 15 years. Understanding of the erosion processes, rates and future extent is needed to take adequate measures to protect the inhabitants in the region against future flooding and erosion.

In a preceding project investigating the region Helvetas Myanmar acted as partner in a consortium with IUCN, NAG and BANCA to improve the livelihood security and to build resilience of communities in the Gulf of Mottama. Resulting from this project there originated follow up questions. A research in collaboration with the TU Delft is now being performed.

A key element is the understanding of the coastal dynamics, through the analysis of existing datasets, with the use of numerical modeling and by performing field measurements. The field measurements will be used to calibrate the model. The field measurements also allow to check on assumptions for the model, for instance on the erodibility of the sediments. The field measurements focus on the key parameters for the understanding and modelling of the estuary and encompasses sediment-bed composition and incoming tide characteristics.

The dynamics of channels and bars is so large in this estuary, that it makes it unique in the world. A comparison of field measurements and data from other estuaries worldwide showed that the channels in this estuary are too small for the amount of water flowing through. The small size of the channels may be caused by the presence of a hard layer in the subsurface that prevents channels from becoming deeper.

Survey

This document describes the planning and locations, measurements and instruments connected with the field activities performed for the survey campaign during the 'wet' season. The aim of the measurements is to gather numerical model calibration data for the hydraulic model of the greater Yangon region.

Wavedroid

Intro

Because of the dynamic position of the tidal channel and force of the incoming tidal wave. The options to measure the wave profile or water level are limited. The Wavedroid offers a very apt solution. Originally data collection on waves is often expensive, difficult and laboursome. WaveDroid offers an accurate, lightweight and low-cost solution: with a small motion sensor it measures wave speed, height and frequency. It is easy to install, provides real-time data and has GPS tracking to limit the risk of theft.

Wavedroid 1.0 was tested at Ngapali beach to understand local beach erosion issues and WaveDroid 2.0 has been tested by the Myanmar Port Authority for an off-shore LNG loading point at Yangon Port. Testing results were excellent, WaveDroid provided accurate real-life data under all circumstances.



Figure 3: Source <https://www.tudelft.nl/myanmar/innovations/wavedroid/>

Hypotheses

1 The contribution of the wave profile to the erosion is insubstantial

- Test: Examine the wave profile with the help of the WaveDroid
- Expected: Wind driven wave profile is low and has no influence on the erosion.

2 In the wake of the tidal wave arrival the wave profile will increase for a limited time.

- Test: Examine the wave profile with the help of the wavedroid around the tidal wave arrival
- Expected: The waves will increase substantially for a short period.

Technical

In a short measurement time some more incidental events will be missed. To what extent do the waves contribute to the erosion? Wave height, amplitude swell and tidal range. Wind driven swell will probably be comparatively small because of the shallow shelf. Compare and see where the wave profile is positioned for the macro-mesotidal characteristics of the estuary. The tidal wave is most potent in the days after the full moon.

Security

The WaveDroid will have to be protected against theft.

Installation procedure

Wave data are stored to the SD card after every burst.

Hand drill sediment measurements

Introduction

The relatively shallow channels in the Gulf of Mottama can either result from an overload in sediment caused by constant reworking of soil stored temporarily in land, or from the presence of erosion-resistant layers in the subsurface (like clay). The latter hypothesis can be investigated with a geological investigation of the top 10 meters of sediments by use of hand coring. The cores can be collected from land-sites (or the tidal flats) where in the recent past a tidal channel was located. The analysis of the cores should focus on the presence of erosion resistant materials in the deeper segments (Arcadis report 2018). To obtain an estimate of how fast the tidal channels migrate over longer time-scales, it is recommended to do at least one coring in the large former tidal meander located west of the estuary. This former meander is shown in **Error! Reference source not found.** with orange dots indicating the possible locations to obtain cores

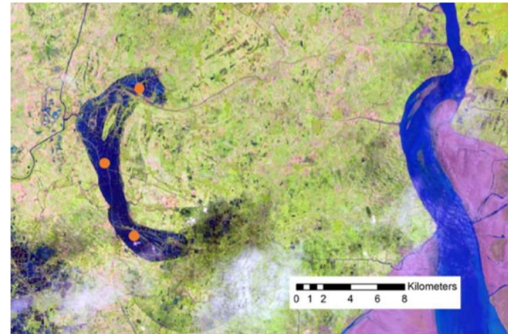


Figure 4: Historic meander location, disconnected from the estuary in a previous channel avulsion (Arcadis, 2018).

The interesting research objective here would be to date the sediment deposits. This is quite laborious and requires expert knowledge, like optical luminescence techniques, beyond the means of the current campaign. What can be achieved and also is of interest for the purpose of the research is the possible presence of an erosion resistant layer, like clay, below the relatively new deposited sediment layers. Here the tidal channel has flown in the recent past and has not been able to penetrate deeper. Also the sediment distribution of the newly deposited sediments can be analyzed and compared to the sediment that has been deposited some years previous. This to compare the distributions which can hold information on the source. As well as validate the choice of sediment fractions used in the model simulations.

Hypotheses

1 The subsoil of estuary of comprised of a erosion resistant layer.

- Test: Examining the subsoil of the abandoned bank to see if there is a erosion resistant layer. sediment samples and core drilling into the subsoil
- Expected: around and below 8 meters an erosion resistant layer is expected / sediment with a lot of clay.

2 The source of the deposited soils is constant and similar of the deposit periods.

- Test: Gather sediment samples at different depths of the bank soil and newly deposited material. Compare the newly deposited sediment with sediment of the bank.
- Expected: If the soil is comprised of layers of successive deposits of sediment important through the tidal forcing these distributions should be relatively similar. Depth can have an influence on the distribution because of flow and settling velocity.

3 Sediment distribution of the newly deposited material.

- Analyze the composition of the sediment that is actively accreting in the estuary to validate the model choices.

How to classify clay? Including fine fractions.

How to compare the two location and the sand. Silt concentration and added contents (sand yes or no).

Equipment

The hand drill set consists, among other things, of the drill head, an upper part with detachable grip, extension rods, push/pull handle, a utility probe and various accessories, see Figure 6. To connect these parts a conical screw thread connection is used. The complete set is contained in a canvas bag for easy transport.